

ON THE STEREOCHEMISTRY AND KINETICS OF CONFORMATIONAL
CHANGE INVOLVED IN RESTRICTED INTERNAL ROTATION

HOWEL GWYNNE GILES

A THESIS
in
The Department
of
Chemistry

Presented in Partial Fulfillment of the Requirements for
the Degree of Doctor of Philosophy at
Sir George Williams University
Montreal, Canada

April, 1973

ABSTRACT

ON THE STEREOCHEMISTRY AND KINETICS OF CONFORMATIONAL CHANGE
INVOLVED IN RESTRICTED INTERNAL ROTATION.

Howel Gwynne Giles, Ph.D.

Sir George Williams University, 1973

Supervisor: Dr. L. D. Colebrook

Restricted internal rotation has been examined in a number of compounds by high resolution nuclear magnetic resonance spectroscopy. The results are discussed in terms of the stereochemistry of the molecules.

Part I

Rotation about the aryl C-N bond in a series of 2-benzyl-3-aryl-4(3H)-quinazolinones was found to be highly restricted. High rotational stabilities were observed even in the absence of bulky ortho substituents on the aryl ring as a consequence of the bulk and geometry of the hetero ring.

Part II

The barriers to rotation about the aryl C-N bond of some 3-aryl-5-methyl-2-thiohydantoins have been examined. In cases where the rotational stability is very high, the rotation was followed by the equilibration of diastereomers,

whereas in the compounds with lower rotational stabilities the rotational barriers were determined by n.m.r. line shape analysis. A high barrier to rotation was found in a thiohydantoin that lacks a bulky ortho aryl substituent.

In this series of compounds, an ortho methyl group is less effective than an ortho chloro group in restricting rotation about the aryl C-N bond. This is inconsistent with the normally accepted sizes of the moieties. The observation is attributed to repulsion between the chlorine atom and the carbonyl oxygen atom in the torsional transition state.

A strong conformational preference was observed, in solution, between the diastereomeric rotational isomers of the thiohydantoins that have very high rotational stabilities. The results of an X-ray crystallographic study of the thermodynamically less stable diastereomer of 3-o-bromophenyl-5-methyl-2-thiohydantoin suggest that this preference is a consequence of the steric effect of the C₅-methyl group being transmitted to the aryl group via an unsymmetrical solvent shell around the carbonyl group.

Part III

The very high rotational stability (about the aryl C-C bond) of 2,2'-bis-(bromomethyl)-3,3'-dichlorobiphenyl is attributed, in part, to the buttressing effect of the chlorine atom. The high rotational stability of 1-(β -naphthyl)-1,2-dihydro-2,2-dimethyl-4,6-diamino-s-triazine is attributed to the bulk and geometry of the heterocyclic ring.

ACKNOWLEDGEMENTS

The author would like to express his appreciation to

Dr. L. D. Colebrook who directed this work with patience and good humour despite the crushing defeats suffered by New Zealand at the hands of the 1971 British Lions.

Dr. Andre Rosowsky of the Children's Cancer Research Foundation, Inc., Boston, for a sample of the triazine.

Prof. D. E. Pearson of Vanderbilt University for a sample of the biphenyl.

Mr. A. R. Fraser who gave, and suffered, several months of non-stop abuse during the crystal structure determination.

Dr. P. H. Bird contributed over tea.

Dr. R. Rye for running a mass spectrum.

His wife, Suzette, who made the sandwiches.

TABLE OF CONTENTS

	Page
TITLE PAGE	i
ABSTRACT	iii
ACKNOWLEDGEMENTS	v
TABLE OF CONTENTS	vi
LIST OF TABLES	viii
LIST OF FIGURES	xi
VITAE	xv
INTRODUCTION	1
Calculation of Thermodynamic Parameters	11
Notes on the Activation Parameters	28
PART I, Studies on the Kinetics of Rotation about the Aryl C-N Bond of 2-Benzyl-3-aryl-4(3H)- Quinazolinones	30
Causes of Non-Equivalence and Spectra Observed	31
Results and Discussion	34
Summary	46
Suggestions for Future Work	47
PART II, Studies on the Stereochemistry and Kinetics of Rotation about the Aryl C-N Bond of 3-Aryl-5-methyl-2-thiohydantoins	49
Causes of Non-Equivalence and Spectra Observed	50
Results	53
Discussion	100

Summary	137
Suggestions for Future Work	138
PART III, Miscellaneous Compounds	139
EXPERIMENTAL	144
General	144
Synthetic	151
REFERENCES	209
APPENDIX	215

LIST OF TABLES

	Page
1. Lifetimes, Temperatures and Corresponding Free Energies of Activation	14
2. N.m.r. Data and Minimum Free Energies of Activation for Quinazolinones Having Bulky <u>ortho</u> Substituents	36
3. N.m.r. Data, Coalescence Temperatures and Free Energies of Activation for Quinazolinones Lacking Bulky <u>ortho</u> Substituents (Nitrobenzene Solution)	40
4. Chemical Shifts of the Diastereotopic Benzylic Methylene Protons of the Quinazolinones in Nitrobenzene Solution	44
5. Infrared Carbonyl Stretching Frequencies of the Quinazolinones	45
6. Comparison of Integration with Curve Resolving in the Determination of the Equilibrium Constant between the Diastereomers of 3- α -Naphthyl-5-methyl-2-thiohydantoin	56
7. Chemical Shifts and Coupling Constants of the Methyl Groups of Some 3-Aryl-5-methyl-2-thiohydantoins	58
8. Equilibrium Constants of the Diastereomeric Rotational Isomers of some 3-Aryl-5-methyl-2-thiohydantoins	60
9. The Equilibration of the Thermodynamically Less Stable Diastereomer of 3- <u>o</u> -Bromophenyl-5-methyl-2-thiohydantoin in Pyridine at 88.5°C	61
10. The Equilibration of the Thermodynamically Less Stable Diastereomer of 3- <u>o</u> -Bromophenyl-5-methyl-2-thiohydantoin in Pyridine at 78.5°C	62
11. The Equilibration of the Thermodynamically Less Stable Diastereomer of 3- <u>o</u> -Bromophenyl-5-methyl-2-thiohydantoin in Pyridine at 67.5°C	63
12. The Equilibration of the Thermodynamically Less Stable Diastereomer of 3- <u>o</u> -Bromophenyl-5-methyl-2-thiohydantoin in Pyridine at 58°C	64

13. The Equilibration of the Thermodynamically Less Stable Diastereomer of 3- <i>o</i> -Bromophenyl-5-methyl-2-thiohydantoin in Pyridine at 49°C	65
14. The Equilibration of the Thermodynamically Less Stable Diastereomer of 3- <i>o</i> -Bromophenyl-5-methyl-2-thiohydantoin in Pyridine at 23.5°C	67
15. Rotational Lifetimes from the Equilibration of 3- <i>o</i> -Bromophenyl-5-methyl-2-thiohydantoin in Pyridine at Various Temperatures	71
16. Arrhenius and Eyring Activation Parameters for the Restricted Internal Process of the Thermodynamically Less Stable Diastereomer of 3- <i>o</i> -Bromophenyl-5-methyl-2-thiohydantoin	73
17. The Equilibration of the Thermodynamically Less Stable Diastereomer of 3- <i>o</i> -Tolyl-5-methyl-2-thiohydantoin in Pyridine at 57.5°C	76
18. The Equilibration of the Thermodynamically Less Stable Diastereomer of 3- <i>o</i> -Chlorophenyl-5-methyl-2-thiohydantoin in Pyridine at 58.5°C	78
19. The Equilibration of the Thermodynamically Less Stable Diastereomer of 3- <i>o</i> -Methoxyphenyl-5-methyl-2-thiohydantoin in Pyridine at 28.5°C	81
20. Free Energies of Activation for Rotation about the Aryl C-N Bond in Some 3-Aryl-5-methyl-2-thiohydantoins	82
21. Infrared Carbonyl Stretching Frequencies of some 3-Aryl-5-methyl-2-thiohydantoins	88
22. The Observed and Calculated Structure Factors	94
23. Final Positions and Thermal Parameters with ESD'S	96
24. Selected Interatomic Distances	98
25. Bond Angles	99
26. Equilibrium Constants and Corresponding Ground State Free Energy Differences of the Rotational Isomers	106
27. Free Energies of Activation for 1-Aryl Hydantoins	125

28. Free Energies of Activation for 3-Aryl Hydantoins
and 3-Aryl 2-thiohydantoins 127
29. Free Energies of Activation for Rotation About the
Aryl C-N Bond in Some 1-Aryl Substituted Triazines 143

LIST OF FIGURES

	Page
1. Simulated Spectra of a Typical AB System at Various Temperatures	13
2. Variation in the Ratio of Diastereomers with Time	17
3. Simulated Time Dependent Spectra	18
4. Various Projections of a 2-Benzyl-3-aryl-4(3H)-quinazolinone	32
5. Various Projections of a 3-Aryl-5-methyl-2-thiohydantoin	51
6. The Equilibration of the Thermodynamically Less Stable Diastereomer of 3-o-Bromophenyl-5-methyl-2-thiohydantoin in Pyridine at Various Temperatures	68
7. 100 MHz NMR Spectrum of the Methyl Region of the Diastereomeric Rotational Isomers of 3-o-Bromophenyl-5-methyl-2-thiohydantoin in Pyridine soon after the start of Equilibration (50 Hz scan)	69
8. 100 MHz NMR Spectrum of the Methyl Region of the Equilibrium Mixture of the Diastereomeric Rotational Isomers of 3-o-Bromophenyl-5-methyl-2-thiohydantoin in Pyridine (50 Hz scan)	70
9. Arrhenius Plot and Weighted Least Squares Line for the Thermodynamically Less Stable Diastereomer of 3-o-Bromophenyl-5-methyl-2-thiohydantoin in Pyridine	72
10. 100 MHz NMR Spectrum of the Methyl Region of the Equilibrium Mixture of the Diastereomeric Rotational Isomers of 3-o-Tolyl-5-methyl-2-thiohydantoin in Pyridine (50 Hz scan)	75
11. 100 MHz NMR Spectrum of the Methyl Region of the Equilibrium Mixture of the Diastereomeric Rotational Isomers of 3-o-Chlorophenyl-5-methyl-2-thiohydantoin in Pyridine (50 Hz scan)	77
12. 100 MHz NMR Spectrum of the Methyl Region of the Equilibrium Mixture of the Diastereomeric Rotational Isomers of 3-o-Methoxyphenyl-5-methyl-2-thiohydantoin in Pyridine (50 Hz scan)	80

13. Simulated Spectrum of the Methine Region of the Diastereomeric Rotational Isomers of 3- β -Naphthyl-5-methyl-2-thiohydantoin with both Rotamers having Lifetimes of 5.00 sec.	85
14. Simulated Spectrum of the Methine Region of the Diastereomeric Rotational Isomers of 3- β -Naphthyl-5-methyl-2-thiohydantoin with both Rotamers having Lifetimes of 0.85 sec.	86
15. Simulated Spectrum of the Methine Region of the Diastereomeric Rotational Isomers of 3- β -Naphthyl-5-methyl-2-thiohydantoin with both Rotamers having Lifetimes of 0.55 sec.	87
16. The Structure of the Thermodynamically Less Stable Diastereomer of 3- <u>o</u> -Bromophenyl-5-methyl-2-thiohydantoin	109
17. A Sketch of the Thermodynamically Less Stable Diastereomer of 3- <u>o</u> -Bromophenyl-5-methyl-2-thiohydantoin Viewed Along the Aryl C-N Bond From a Position Midway Between N(1) and C(5)	110
18. The Two Possible Rotational Transition States for 3- <u>o</u> -Bromophenyl-5-methyl-2-thiohydantoin	117
19. Infrared Spectrum of N-Phenylacetyl anthranilic acid	155
20. Infrared spectrum of 2-Benzyl-3-(2-chloro-6-methylphenyl)-4(3H)-quinazolinone	157
21. 100 MHz NMR spectrum of 2-Benzyl-3-(2-chloro-6-methylphenyl)-4(3H)-quinazolinone in deuteriochloroform solution (1000 Hz scan)	158
22. Infrared spectrum of 2-Benzyl-3- <u>o</u> -bromophenyl-4(3H)-quinazolinone	160
23. 100 MHz NMR spectrum of 2-Benzyl-3- <u>o</u> -bromophenyl-4(3H)-quinazolinone in deuteriochloroform solution (1000 Hz scan)	161
24. Infrared spectrum of 2-Benzyl-3- <u>o</u> -tolyl-4(3H)-quinazolinone	163
25. 100 MHz NMR spectrum of 2-Benzyl-3- <u>o</u> -tolyl-4(3H)-quinazolinone in deuteriochloroform solution (1000 Hz scan)	164

26.	Infrared spectrum of 2-Benzyl-3- <u>o</u> -chlorophenyl-4(3H)-quinazolinone	167
27.	100 MHz NMR spectrum of 2-Benzyl-3- <u>o</u> -chlorophenyl-4(3H)-quinazolinone in deuteriochloroform solution (1000 Hz scan)	168
28.	Infrared spectrum of 2-Benzyl-3- <u>o</u> -fluorophenyl-4(3H)-quinazolinone	170
29.	100 MHz NMR spectrum of 2-Benzyl-3- <u>o</u> -fluorophenyl-4(3H)-quinazolinone in deuteriochloroform solution (1000 Hz scan)	171
30.	Infrared spectrum of 2-Benzyl-3- β -naphthyl-4(3H)-quinazolinone	174
31.	100 MHz NMR spectrum of 2-Benzyl-3- β -naphthyl-4(3H)-quinazolinone in deuteriochloroform solution (1000 Hz scan)	175
32.	Infrared spectrum of 2-Benzyl-3- <u>m</u> -acetylphenyl-4(3H)-quinazolinone	177
33.	100 MHz NMR spectrum of 2-Benzyl-3- <u>m</u> -acetylphenyl-4(3H)-quinazolinone in deuteriochloroform solution (1000 Hz scan)	179
34.	Infrared spectrum of 2-Benzyl-3- <u>m</u> -bromophenyl-4(3H)-quinazolinone	181
35.	100 MHz NMR spectrum of 2-Benzyl-3- <u>m</u> -bromophenyl-4(3H)-quinazolinone in deuteriochloroform solution (1000 Hz scan)	182
36.	Infrared spectrum of <u>o</u> -Bromophenyl isothiocyanate	184
37.	Infrared spectrum of <u>o</u> -Chlorophenyl isothiocyanate	186
38.	Infrared spectrum of <u>o</u> -Methoxyphenyl isothiocyanate	188
39.	Infrared spectrum of 3- <u>o</u> -Bromophenyl-5-methyl-2-thiohydantoin	190
40.	100 MHz NMR spectrum of 3- <u>o</u> -Bromophenyl-5-methyl-2-thiohydantoin in DMSO- d_6 solution (1000 Hz scan)	191
41.	Infrared spectrum of 3- <u>o</u> -Tolyl-5-methyl-2-thiohydantoin	194
42.	100 MHz NMR spectrum of 3- <u>o</u> -Tolyl-5-methyl-2-thiohydantoin in DMSO- d_6 solution (1000 Hz scan)	195

43.	Infrared spectrum of 3- <u>o</u> -Chlorophenyl-5-methyl-2-thiohydantoin	197
44.	Infrared spectrum of 3- <u>o</u> -Methoxyphenyl-5-methyl-2-thiohydantoin	200
45.	100 MHz NMR spectrum of 3- <u>o</u> -Methoxyphenyl-5-methyl-2-thiohydantoin in DMSO-d ₆ solution (1000 Hz scan)	201
46.	Infrared spectrum of 3- <u>o</u> -Fluorophenyl-5-methyl-2-thiohydantoin	203
47.	100 MHz NMR spectrum of 3- <u>o</u> -Fluorophenyl-5-methyl-2-thiohydantoin in DMSO-d ₆ solution (1000 Hz scan)	204
48.	Infrared spectrum of 3- β -Naphthyl-5-methyl-2-thiohydantoin	206
49.	100 MHz NMR spectrum of 3- β -Naphthyl-5-methyl-2-thiohydantoin in DMSO-d ₆ solution (1000 Hz scan)	208

VITAE

The author was born on the 4th July, 1945 in Paddock Wood, U.K. He received his General Certificates of Education from the Grammar-Technical School, Brecon, in June 1964, his B.Sc. in Chemistry and Geology from University College, Swansea, in June 1968, and his M.Sc. in Chemistry, under the supervision of Dr. J. A. Kampmeier, from the University of Rochester, New York, in June 1971. In September 1970, the author undertook a graduate programme leading to the Degree of Doctor of Philosophy at Sir George Williams University under the supervision of Dr. L. D. Colebrook.

INTRODUCTION

This thesis represents part of the continuing studies, performed in these laboratories, in the areas of stereochemistry and kinetics of conformational change¹⁻³. Fehlner⁴, Bentz⁵, Hund⁶, Williams⁷, Granata⁸, and Icli⁹ have made recent contributions.

Over the last twenty years, there has been a rapid development in the understanding of the process of restricted internal rotation. In his review, Millen¹⁰ has listed several methods that have been applied to determine the heights of barriers in simple molecules: microwave, infrared, and Raman spectroscopy are included. Unfortunately, these methods may not be applied to more complex molecules.

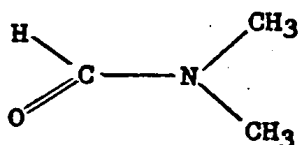
Most early efforts to determine the 'barriers to internal rotation in complex molecules were restricted to molecules in which the workers were able to isolate an optically active rotamer. The process of internal rotation is then observed as racemisation in a polarimeter. The technique has been applied to many systems, particularly 2,2'-disubstituted biphenyls where Harris¹¹⁻¹⁵ has recently contributed much to the field following the pioneering work of Adams¹⁶. Hall and Harris¹¹ have reported many systems in which the rotational stability, as indicated by

the rotational free energy of activation, is greater than 20 kcal mole⁻¹.

Most modern efforts to determine the barriers to rotation in complex molecules involve nuclear magnetic resonance (n.m.r.) spectroscopy.

There are two methods by which the kinetic and thermodynamic parameters of the process of restricted internal rotation may be determined by n.m.r. spectroscopy. First considered will be n.m.r. line shape analysis. This method is most useful in cases where the lifetimes of the rotamers are in the region 10¹ to 10⁻⁵ sec. This range of lifetimes has become known as the "n.m.r. time scale"¹⁷, and the method used to study the processes has become known as "dynamic nuclear magnetic resonance"¹⁷. If two interconvertible species have long lifetimes on the n.m.r. time scale, the spectrum is the sum of the spectra of the individual species. When the lifetimes are short, however, the spectrum is a time averaged spectrum of the two species. Partial collapse from the individual spectra to the time averaged spectrum may be observed at intermediate lifetimes.

In a review of nuclear magnetic resonance and stereochemistry, Gillespie and White¹⁸ include the temperature dependent n.m.r. spectrum of N,N-dimethylformamide as the classic example of the above method

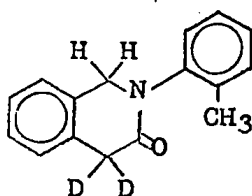


At room temperature, there are two methyl peaks in the n.m.r. spectrum. Increasing the temperature, however, causes an increase in the frequency of rotation about the C-N bond, and the average environment of the two methyl groups becomes more similar. In consequence, the two signals gradually merge into a single peak. It should be noted, however, that the review¹⁸ of the study of intramolecular rate processes by dynamic nuclear magnetic resonance indicates that the Arrhenius activation energy of this compound appears to be author dependent. Several other systems that this method has been applied to, with more reproducible results, have been listed in the two reviews cited above, and many other examples are in the current literature.

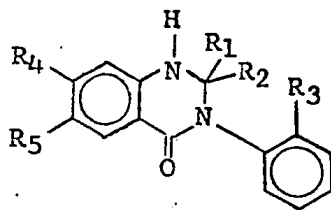
The other n.m.r. method of determining kinetic and thermodynamic parameters of the process of restricted internal rotation is the equilibration method. There are, among others, two important requirements for the application of this method. First, the rotamers must be diastereomers, and secondly, the rotation must be highly hindered. The method involves the isolation of one diastereomer and the following of the equilibration, at constant temperature, to the equilibrium mixture of diastereomers. If the rotamers are enantiomers there is nothing to observe since two enantiomers have the same n.m.r. spectrum in non-dissymmetric media. The degree of rotational stability is important since rotational barriers with a free energy of activation substantially greater than about 20 kcal mole⁻¹ are required to allow a

worker reasonable time in which to follow the equilibration. The method clearly has similarities to the method employing the racemisation of optically active rotamers.

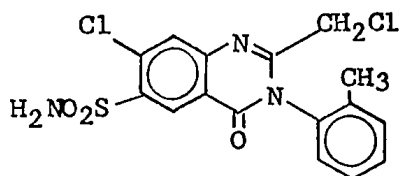
With the exception of studies in these laboratories, there is only one report, by Mislow and his co-workers¹⁹, on hindered rotation about the aryl C-N bond in N-aryl cyclic amides. These workers determined a free energy of activation of $17.3 \text{ kcal mole}^{-1}$, at 73°C for the following compound



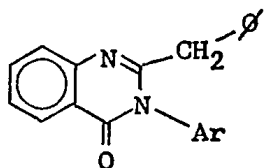
Fehlner⁴, examined a series of 3-aryl substituted quinazolinones with the hope that the study would lead to a



better insight into the mechanism of rotation in such systems. Interpretation of the results was hampered, however, by the flipping of the non-planar heterocyclic ring caused by the pyramidal nitrogen. In an attempt to overcome this problem, he examined the following compound

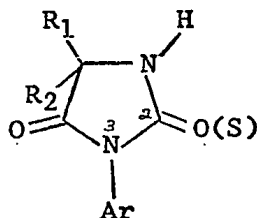


Unfortunately, there was no observable chemical shift difference between the potentially non-equivalent methylene protons at the lowest temperature obtainable in DMSO- d_6 , and no thermodynamic data were obtained. Thus Part I of this thesis, in which a series of quinazolinones with the following type of structure was studied, may be taken to represent an



attempt to observe restricted rotation in these systems.

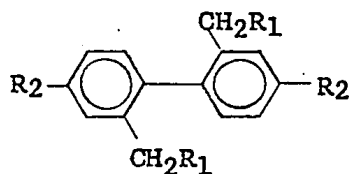
Fehlner also observed high rotational stabilities in 3-aryl hydantoins and 3-aryl-2-thiohydantoins



Among his observations, he noted that there is a slight

conformational preference between the diastereomeric rotational isomers in both series of compounds, and that an ortho chloro substituent on the aryl ring is more effective than an ortho methyl group in restricting the rotation in the hydantoin series although the van der Waals radius of chlorine is less than that of methyl²⁰. Since it is hard to see the origin of any conformational preference in these molecules, it was decided to investigate the observation more rigorously. In addition, it was decided to see if an ortho chloro substituent is effectively larger than an ortho methyl substituent in hindered rotation in the 3-aryl-2-thiohydantoin series. It was also desired to obtain more data on the thiohydantoin series such that it may be compared with the hydantoin series.

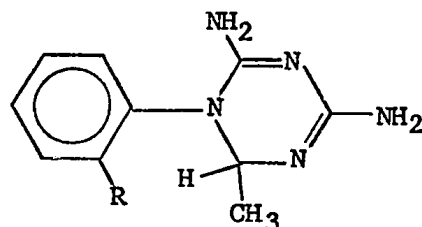
Bentz⁵ has examined hindered rotation about the phenyl-phenyl bond of several pairs of 2,2'-disubstituted biphenyls by means of complete line shape analysis of their temperature dependent n.m.r. spectra.



Both members of each pair had the same R₁ substituent, but R₂ = NO₂ in one while R₂ = H in the other. He found that the relative rotational stability of the 4,4'-dihydro compound

compared to the 4,4'-dinitro compound in each pair was found to be temperature dependent. In addition, the enthalpies of activation for the members of each pair were found to differ. This observation prevented attributing changes in rotational stability, due to the addition of the 4,4'-dinitro groups, to entropy effects alone, in contrast to the results of Harris¹¹.

Bentz also examined hindered rotation about the central C-N bond of two triazines.



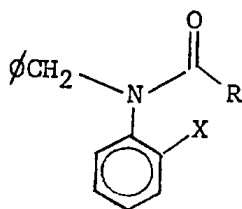
R = CH₃
and R = Cl

The barrier to rotation in the first compound (R = CH₃) was examined by following the thermodynamic equilibration of the two diastereomers, while the barrier to rotation in the second compound (R = Cl) was examined by means of complete line shape analysis.

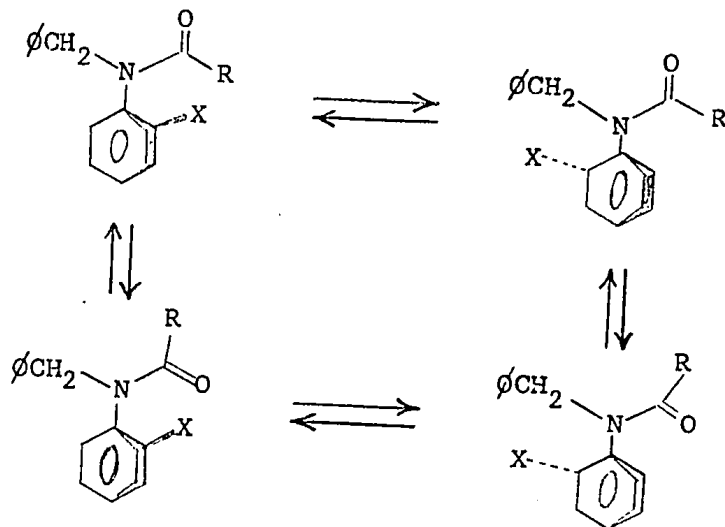
The 2'-methyl compound was found to have a greater rotational stability than the 2'-chloro compound. The enthalpies of activation were greater for both diastereomers of the former compared with the latter, while the entropies of activation were about equal for the two compounds. This suggested that the barrier to rotation in these compounds was primarily a function of the steric requirements of the 2'-substituent. That is, in this series, an ortho methyl group

is effectively larger than an ortho chloro group in restricting the internal rotation process.

Another example of the complexities that may be involved in the study of restricted internal rotation in amides has been presented by Hund⁶. He examined a series of *N*-benzyl-*N*-ortho substituted amides and noted the effect of structural



changes on the kinetic parameters. The parameters were evaluated through complete line shape analysis of the temperature dependent AB portion of the n.m.r. spectra. He concluded that the process which interchanges the magnetic environments of the methylene protons is not simply rotation about the aryl C-N bond but also involves rotation about the C-N bond of the amide function. He also concluded that the



extent of involvement of the latter process depends on the identity of the ortho and amide substituents and on solvent polarity. Fortunately, rotation about the C-N bond of the amide function is not possible in the cyclic amides prepared for discussion in this thesis.

Williams⁷, who also worked in these laboratories, studied the ¹³C n.m.r. spectra of some 3-aryl hydantoins. In particular, he studied the change in the carbon chemical shift values with the number of methyl groups in the C₅ position and the change in the carbon chemical shift values with various ortho substituents on the aryl ring. Most dramatically, he found that there is a downfield shift of the C₂ and C₄ carbonyl carbon atoms with a decreasing effective size of the ortho aryl substituent. This result will be referred to again in the Discussion section concerning the dihedral angle between the heterocyclic and aryl rings.

The work of Granata⁸ included an investigation into the electronic effects involved in rotation about the aryl C-N bond of 3-aryl substituted hydantoins. He found that an ortho chloro group is effectively larger than an ortho methyl group in restricting the internal rotation process. He also studied the effect on rotation of a chlorine atom in the para position of an ortho substituted aryl ring. His data are presented in the Discussion section.

Icli⁹ has investigated the stereochemistry and

kinetics of conformational change involved in restricted internal rotation about the aryl C-N bond of 1-aryl substituted hydantoins, using ^1H n.m.r. line shape analysis, ^{13}C n.m.r. spectroscopy, and n.m.r. studies employing an optically active solvent. His kinetic studies include the larger effective size of methyl than chlorine in restricting rotation about the aryl C-N of these compounds. The results are referred to in the Discussion section.

There is a considerable amount of interest in the physiological effects of derivatives of the compounds prepared for this study. Quinazolinones are diuretics^{21,22}, triazines have many medical uses and the size of the aryl moiety has been found to influence the effect²³, hydantoins are anticonvulsants²⁴, and biphenyl containing compounds have several pharmacological uses²⁵.

Calculation of Thermodynamic Parameters

The key to the calculation of the thermodynamic parameters lies in the determination of the rate constant (1/lifetime) for the rotation process at known temperatures. Some of the compounds give rise to temperature dependent spectra, some give rise to time dependent spectra, while others may give both.

Temperature Dependent Spectra

There are various methods of determining the rate constant at each temperature ¹⁷. Of these methods, complete line shape analysis has met with the most success. The spectra are digitized and a computer gives the best values of the chemical shift difference between the two moieties, the line width and the rate constant after an iterative procedure. There are two important criteria for a study of this type: first, the spectrum must collapse at elevated temperatures and secondly, the chemical shift difference between the two moieties must be reasonably large. Unfortunately, neither of these criteria was met in any of the compounds studied.

Collapse of an AB system

The temperature dependence of a typical AB system

is simulated in Fig. 1 .

When an AB system does not collapse at the highest temperature attainable, it is possible to calculate the minimum value of the lifetime at this temperature by employing the following formulae ²⁶.

$$(1) \quad 1/\tau = \pi((\delta^2 + 6J^2)/2)^{1/2}$$

$$(2) \quad \tau_A = \tau_B = 2 \tau$$

where τ_A = lifetime in one of the two possible conformations
 δ = chemical shift difference between the two protons
 and J = coupling constant.

In the derivation of equation (1), the authors assumed a zero line width. Clearly, this is not possible and as a consequence the lifetimes thus obtained should be regarded as being approximate. However, it is not the lifetime that is used in the calculation of the free energy of activation, it is the benevolent logarithmic form of the quantity ²⁷.

$$(3) \quad \Delta G_T^\ddagger = 2.303 R T (10.319 + \log_{10} T + \log_{10} \tau_A)$$

where ΔG_T^\ddagger = free energy of activation at the specified temperature
 R = gas constant
 T = temperature of the observation, °K.
 and τ_A = lifetime, seconds.

Thus, the error in the minimum free energy of activation is quite small (Table 1).

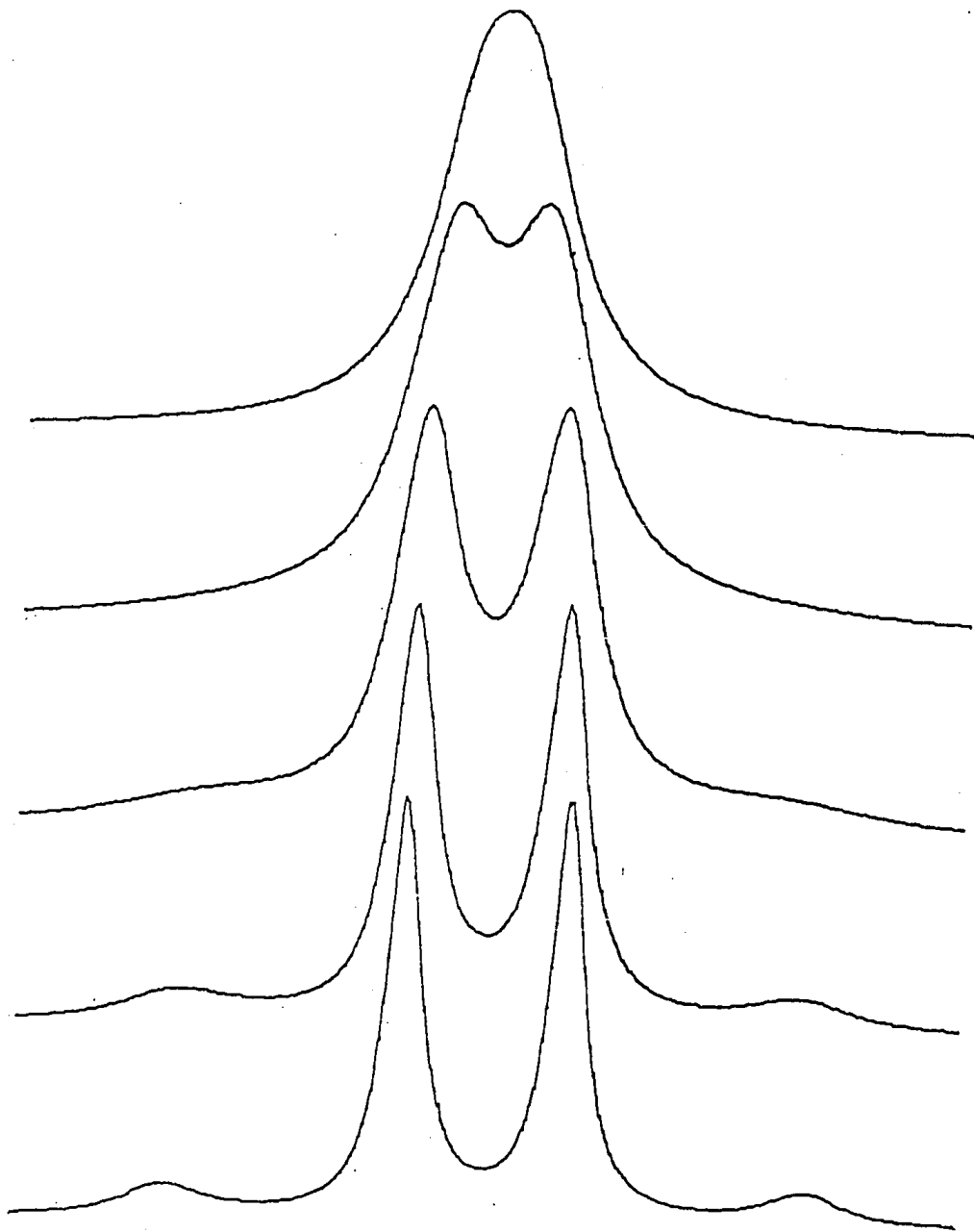


Fig. 1 . . Simulated Spectra of a Typical
AB System at Various Temperatures

Table 1

Lifetimes, Temperatures and Corresponding Free Energies
of Activation

Lifetime ^a	Temperature ^b	$\Delta G^{\ddagger c}$
0.08	100	20.1
0.09	100	20.2
0.10	100	20.3
0.11	100	20.4
0.12	100	20.4
0.13	100	20.5
0.10	97	20.1
0.10	98	20.2
0.10	99	20.2
0.10	101	20.4
0.10	102	20.4
0.10	103	20.5

(a) Seconds. (b) Degrees C. (c) Free energy of activation, kcal/mole.

In the case where there is a small chemical shift difference between the protons and in which collapse of the AB system may be observed, equation (1) may be used to calculate the lifetime at coalescence. A better method is available, however. Computer generated spectra can be compared visually with the experimental spectra to obtain the lifetime. The advantage of the method is that it does not assume a zero line width. The disadvantage is that the determination of the coalescence point is somewhat subjective.

Collapse of a pair of singlets to a single peak

The method used was similar to that used for the collapse of an AB system, i.e. computer generated spectra were compared visually with the experimental spectra to obtain the lifetime at coalescence. The free energy of activation at the coalescence point was then obtained using equation (3).

Collapse of a pair of quartets to a single quartet

The computer generated spectra are shown in the Results section of the work on 3- β -naphthyl-5-methyl-2-thiohydantoin.

Collapse of a pair of doublets to a single doublet

The lifetime at the coalescence temperature was

calculated from the following equation ²⁸ .

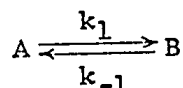
$$\tau = 2^{1/2} / 2 \pi \delta$$

and equation (2).

Time Dependent Spectra

In compounds where the rotamers are diastereomers, the rotational lifetimes may be calculated by "traditional" methods if the rotational barrier is sufficiently high.

One diastereomer may be isolated in close to 100% isomeric purity by careful crystallisation of a mixture of the two diastereomers. Consider two diastereomeric rotational isomers, A and B, in solution at equilibrium.

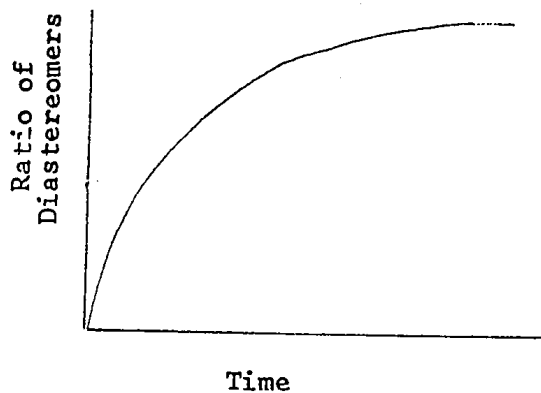


Because A and B are diastereomers, they have different chemical properties. In particular, their solubilities will be slightly different. Now, in the simplest case of equilibrium where A and B are present in equal concentration, i.e. when $k_1 = k_{-1}$, it is easy to see that one of the diastereomers, say A, will crystallise before the other. The equilibrium, however, has been disturbed by this process and some B will be converted to A to maintain it. The process will continue if crystallisation is slow, until a small concentration of

A and B is left in solution and crystals of pure A are isolated. The process is an asymmetric transformation.²⁹

After the isolation of a pure diastereomer, rotation about the aryl C-N bond may be observed as equilibration of one diastereomer to the equilibrium mixture. The process is observed in the n.m.r. spectrometer as the increase in concentration of one diastereomer with time and the decrease in concentration of the other. The C5 methyl peaks of the 2-thiohydantoins were used as a probe. Fig. 3 simulates the process. The area under the peaks may be determined by use of a curve resolver (see Experimental section). The ratio of the areas is equal to the ratio of the concentrations of the diastereomers. The variation of this ratio with time is shown in Fig. 2.

Fig. 2



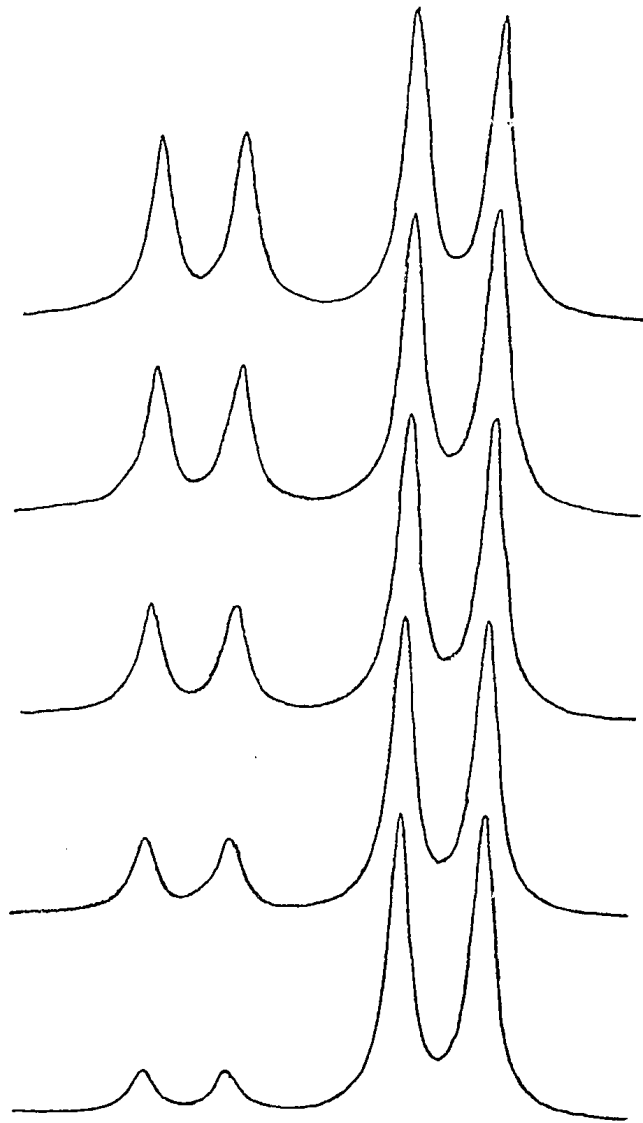
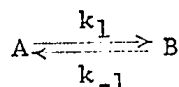


Fig. 3 . Simulated Time Dependent Spectra

The problem then is the determination of rate constants for a reversible first order reaction. Consider the reaction



and let the concentration of A be a mol/l and B be b mol/l at time $t = 0$. If after a time t , x mol/l of A have been transformed into B, A is present at a concentration of $a-x$ while the concentration of B is $b+x$. The differential rate equation will then be

$$dx/dt = k_1(a-x) - k_{-1}(b+x)$$

and since the equilibrium constant, $K = k_1/k_{-1}$

$$dx/dt = k_1(a-x) - (k_1/K)(b+x)$$

The above expression can be integrated and solved for the ratio $(b+x)/(a-x)$ at any time, t :³⁰

$$\frac{b+x}{a-x} = \frac{1 - \exp(-k_1(1+1/K)(t+t_0))}{1/K + \exp(-k_1(1+1/K)(t+t_0))}$$

The time, t_0 , is the time at which only pure A exists. It is not necessary to start at t_0 , i.e. with pure A, but it is

necessary to start with a sample substantially enriched with one diastereomer. t_0 may then be obtained by extrapolation of the equilibration curve.

By using the three parameters K , k_1 and t_0 , a non-linear least squares programme (EQUAB) will fit, by an iterative procedure, a calculated curve to the experimental plot of the ratio of diastereomers versus time. The equilibrium constant, K , is held constant in the calculation.* However, K is an experimentally derived quantity and has an associated error. Thus, the calculation is repeated using a K with the maximum error (90% confidence limits). The rate constant, k_1 , thus derived, allows the calculation of the free energy of activation at the temperature of the equilibration.

The complete set of Arrhenius and Eyring activation parameters may be obtained from the results of equilibrations at several temperatures.

The Arrhenius activation energy, E_a , and frequency factor, A , are defined by the Arrhenius equation ³¹

$$(4) \quad k_r = A \exp(-E_a/RT)$$

k_r is the rate constant for the rotation process, R is the gas constant and T is the temperature in degrees Kelvin. A plot of $\log_e k_r$ versus $1/T$ has a slope of $(-E_a/R)$ and an intercept of $\log_e A$. The first part of a computer programme, WAYTPA, calculates E_a and $\log_e A$ at 90% confidence limits after a weighted least squares analysis of the plot.

* The value of K can be found by the computer if the equilibration is followed to equilibrium.

There are two methods available to calculate the Eyring activation parameters. The results of the two methods are, however, not significantly different.

Method 1

The free energy of activation, ΔG^\ddagger , the enthalpy of activation, ΔH^\ddagger , and the entropy of activation, ΔS^\ddagger , are defined by the Eyring equation²⁷, equation (5) or (6).

$$(5) \quad k_r = KkT/h \exp(-\Delta G^\ddagger/RT)$$

$$(6) \quad k_r = KkT/h \exp(-\Delta H^\ddagger/RT) \exp(\Delta S^\ddagger/R)$$

K is the transmission coefficient (assumed to be unity²⁷), k is the Boltzmann constant and h is Planck's constant. When K is equated to unity and logarithms are taken, Eq (6) becomes

$$\log_e k_r = \log_e (kT/h) - \Delta H^\ddagger/RT + \Delta S^\ddagger/R$$

Differentiation gives

$$d(\log_e k_r)/dT = (h/kT)(k/h) + \Delta H^\ddagger/RT^2$$

which may be written as

$$(7) \quad d(\log_e k_r)/dT = RT/RT^2 + \Delta H^\ddagger/RT^2$$

Now in logarithmic form, the Arrhenius equation, equation (4), may be written as

$$\log_e k_r = \log_e A - E_a/RT$$

Differentiation gives

$$d(\log_e k_r)/dT = E_a/RT^2$$

Equating equations (7) and (8) gives

$$(9) \quad \Delta H^\ddagger = E_a - RT$$

Equation (5) may be written as

$$(10) \quad \Delta G^\ddagger = 2.303 RT (10.319 + \log_{10} T + \log_{10} (1/k_r))$$

In addition, the following equality has been derived ²⁷

$$(11) \quad \Delta S^\ddagger = (\Delta H^\ddagger - \Delta G^\ddagger)/T$$

Thus, from equations (9), (10) and (11) the Eyring activation parameters may be determined. The second part of the computer programme, WAYTPA, calculates these quantities, at any specified temperature, at 90% confidence limits. The principal objection to this method is that it imposes a slight temperature dependence on ΔH^\ddagger and ΔS^\ddagger ¹⁷.

Method 2

This method was not used. Consider equation (6). A plot of $\log_e (k_r/T)$ versus $1/T$ has a slope of $-\Delta H^\ddagger/R$ and an intercept of $\log_e (Kk/h) + \Delta S^\ddagger/R$. Thus ΔH^\ddagger and ΔS^\ddagger may be determined as temperature independent parameters. ΔG^\ddagger may be determined at any temperature using equation (5).

Weighted Least Squares Analysis and Programme WAYTPA

In the analysis of an Arrhenius plot, it has been common practice to determine the slope and intercept by a "simple" least squares analysis. The method assumes that there is no error associated with the various temperatures measured in the experiment and that each rate constant has the same associated error.

In most experiments the determination of temperature presents few problems and the assumption of error-free temperatures is reasonable. The assumption of constant error in the rate constant, however, is most unreasonable. Both chemically and mathematically the assumption is unjustified.

Every experimentalist recognises that it is usually impossible to monitor with the same precision processes whose rates may differ by several orders of magnitude. Thus, those rate constants that have small associated errors should be more important in the analysis of the plot. In a "simple" least squares analysis they are not.

The mathematical argument is as follows. Consider an equation of the form

$$y = mx + c$$

The variance in y , V_y , is related to the variance in x , V_x , by

$$V_y = (\delta y / \delta x)^2 V_x$$

but

$$(\delta y / \delta x)^2 = m^2 = \text{a constant}$$

i.e. the variance in y is linearly related to the variance in x . Now consider a logarithmic equation

$$y = \log_e x$$

$$(\delta y / \delta x)^2 = (1/x)^2$$

therefore
$$V_y = (1/x)^2 V_x$$

i.e. the variance in y is not linearly related to the variance in x . Stated more simply, the error in y depends on x . Thus, a "simple" least squares analysis is unsatisfactory when logarithmic functions are involved.

The problem then is to attach a different importance to each point. This is achieved by giving each point a weighting factor, w_i , defined by $w_i = x^2/V_x$, or in the case of the Arrhenius equation, $w_i = k_i^2/V_{k_i}$, where k is the rate constant. The variance in this expression may be replaced by the square of the standard deviation

thus
$$w_i = k_i^2/\sigma_{k_i}^2$$

and to a good approximation, we may write

$$w_i = k_i^2/s_{k_i}^2$$

where s_{k_i} is the standard error in k_i . The weighting factors are normalised to the number of data points. The expression has been presented by Bamford and Tipper ³². From the

expression, it is seen that the importance of each point is given by the magnitude of the weighting factor. In the equilibration method it is clear that the rate constants determined at the higher temperatures will have large associated errors and count for very little. The key point is that it is not necessarily desirable to have a large range of data for a logarithmic plot. It is more important to obtain data in the region where the errors are reasonably small.

In practice, we have found the above expression too extreme. The weighting factors associated with the rate constants determined at high temperatures are too small to make sense chemically. In consequence we have used the expression *

$$w_i = k_i/s_k i$$

with more satisfactory results. Thus, E_a and $\log_e A$ were calculated from

$$E_a/R = \frac{\sum_{i=1}^{i=N} w_i x_i \sum_{i=1}^{i=N} w_i y_i - \left(\sum_{i=1}^{i=N} w_i \right) \left(\sum_{i=1}^{i=N} w_i x_i y_i \right)}{D}$$

$$\log_e A = \frac{\sum_{i=1}^{i=N} w_i y_i \sum_{i=1}^{i=N} w_i x_i^2 - \left(\sum_{i=1}^{i=N} w_i x_i \right) \left(\sum_{i=1}^{i=N} w_i x_i y_i \right)}{D}$$

* There is precedence for this, Ref. 33.

where

$$D = \left(\sum_{i=1}^{i=N} w_i \right) \left(\sum_{i=1}^{i=N} w_i x_i^2 \right) - \left(\sum_{i=1}^{i=N} w_i x_i \right)^2,$$

N = number of data points,
 $x_i = 1/T_i$
 and $y_i = \log_e k_i$

The standard errors in E_a and $\log_e A$ may be estimated from the sum of the squares of the residuals, δ_s , defined by

$$\delta_s = y_s - (\log_e A - E_a/RT)$$

Thus

$$s(E_a) = R \left[\frac{g \sum_{i=1}^{i=N} w_i}{(N-2)D} \right]^{1/2}$$

and

$$s(\log_e A) = \left[\frac{g \sum_{i=1}^{i=N} w_i x_i^2}{(N-2)D} \right]^{1/2}$$

where

$$g = \sum_{i=1}^{i=N} w_i \delta_s^2$$

The errors at 90% confidence limits may then be calculated using a student's t test of significance. ³⁴

The Eyring parameters are determined at the same level of confidence at each temperature employed in the experiment and at any temperature specified by the user (usually 25°C.).

The output also includes the calculated best fit values of the rate constants in a form that is suitable for

the construction of a graphic Arrhenius plot.

Notes on the Activation Parameters

Experimental Activation Energy, E_a

The parameter is known to show a small temperature dependence ³². When the range of temperatures employed is not large, however, this fact is usually ignored.

The activation energy does not give a good measure of the rate of rotation. It can easily be shown that

$$E_a = \Delta G^\ddagger + T(\Delta S^\ddagger + R)$$

i.e., E_a is a function not only of the rate dependent thermodynamic function ΔG^\ddagger and the temperature but also depends on the entropy of activation, ΔS^\ddagger .

Frequency Factor, A

The parameter is not significant in modern kinetic theory. It is related to the entropy of activation.

Free Energy of Activation, ΔG^\ddagger

In the context of this type of work, the free energy of activation is the most important kinetic parameter. It is a rate dependent thermodynamic function and may be determined with a high degree of precision. The greater the value of ΔG^\ddagger , the more hindered is the rotation process.

Entropy of Activation, ΔS^\ddagger

The entropy of a state represents the randomness of that state. Thus, the entropy of activation represents the difference in degree of order between the ground state and the transition state. A negative ΔS^\ddagger therefore implies that the transition state is more ordered than the ground state.

Enthalpy of Activation, ΔH^\ddagger

By examination of the equation

$$\Delta G^\ddagger = \Delta H^\ddagger - T\Delta S^\ddagger$$

it is seen that the enthalpy of activation contributes to the overall stability of the molecule as given by ΔG^\ddagger . The enthalpy of activation is the best estimate of the steric factors involved in the rotation process.

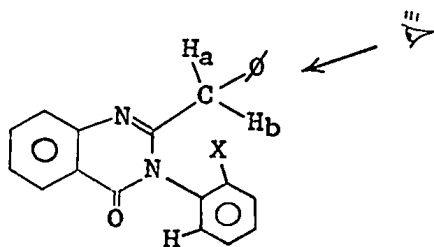
PART I

STUDIES ON THE KINETICS OF ROTATION ABOUT
THE ARYL C-N BOND OF 2-BENZYL-3-ARYL
4(3H)-QUINAZOLINONES

Causes of Nonequivalence and Spectra Observed

In the following discussion, the two benzyl protons of 2-benzyl-3-aryl-4(3H)-quinazolinones will be shown to be chemically nonequivalent provided that rotation of the aryl group is slow on the n.m.r. time scale. The structures mentioned refer to Fig. 4. The diagrams have been drawn for the stated purpose only, no actual conformation is implied.

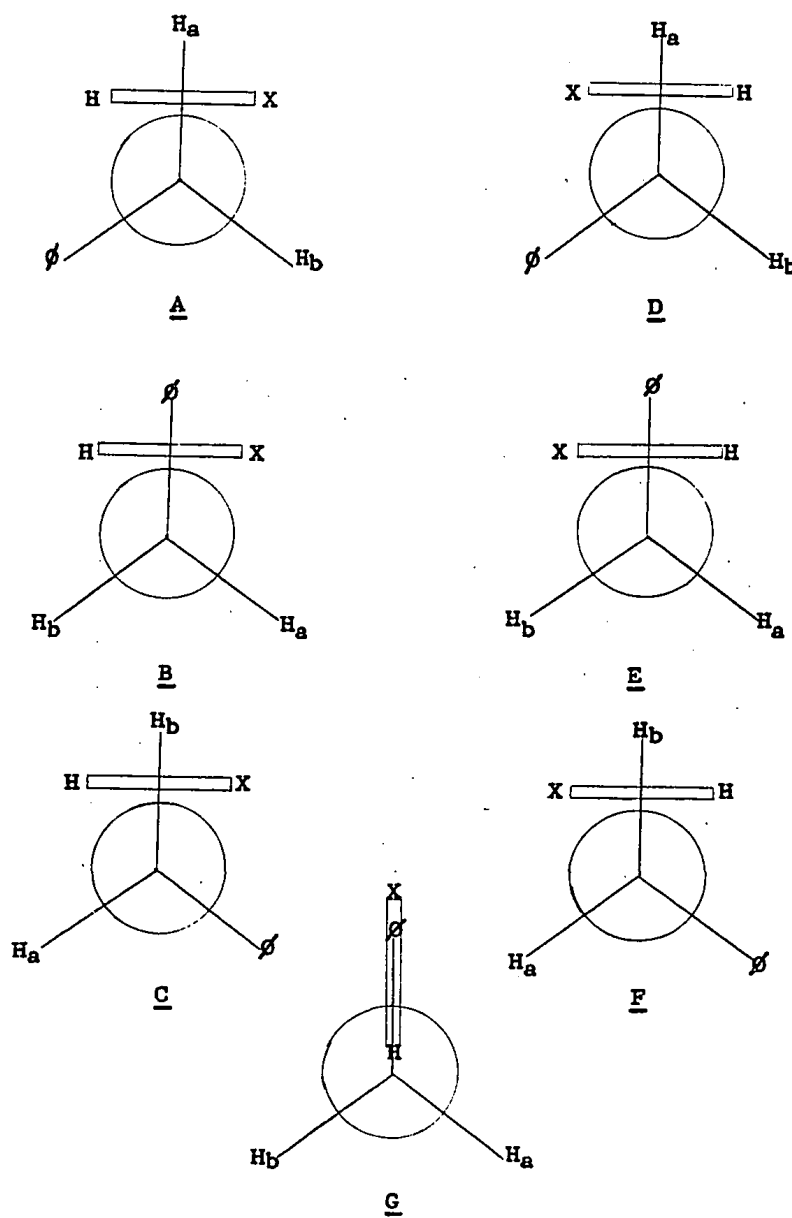
A represents a simplified partial view of the molecule in the direction indicated.



B is obtained from A by a 120° clockwise rotation about the benzyl-carbon bond. Similarly, C is obtained from B by a 120° clockwise rotation about the benzyl-carbon bond. In none of the structures A, B and C are the benzyl protons equivalent, *i.e.* rotation about the benzyl-carbon bond does not make H_a and H_b equivalent.

Structure D is obtained from A by rotation about the aryl C-N bond. In a similar manner, E is obtained from B and F from C. Inspection shows that in D, E and F, H_a is not equivalent to H_b .

Fig. 4

Various Projections of a 2-Benzyl-3-aryl-4(3H)-quinazolinone

Remembering that H_a and H_b are hydrogen atoms, it will be observed that A is enantiomeric with F, B is enantiomeric with E and that C is enantiomeric with D. Now, since enantiomers have identical physical properties, the n.m.r. spectrum of the product (of rotation about the aryl C-N bond) will be identical with that of the starting material. In this sense we are observing a virtual reaction.

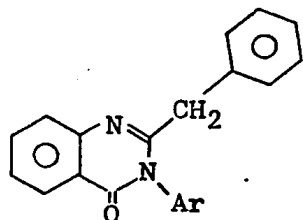
Under conditions of fast rotation about the aryl C-N bond, however, the n.m.r. spectrum will change. When the aryl ring is drawn in the time averaged position, structure G, H_a and H_b are seen to be equivalent.

The chemical shift difference between the benzylic protons is small and they are coupled to each other. As a consequence of the mixing of energy levels an AB quartet results under conditions of slow rotation. When rotation about the C-N bond is fast, the spectrum collapses to a time averaged singlet. Fast rotation of the benzyl group cannot average the environments of the methylene protons and so cause collapse of the AB quartet.

RESULTS AND DISCUSSION

The quinazolinones were prepared by an adaptation of the method of Klosa ³⁵. The structures were assigned by means of their infrared and n.m.r. spectra, elemental analyses (see Experimental section), and from the fact that the compounds are the expected products of the reactions.

Following is a list of the compounds that were synthesised successfully*



Ar

I	2-Chloro-6-methylphenyl
II	<u>o</u> -Bromophenyl
III	<u>o</u> -Tolyl
IV	<u>o</u> -Chlorophenyl
V	<u>o</u> -Fluorophenyl
VI	<u>m</u> -Bromophenyl
VII	β -Naphthyl
VIII	<u>m</u> -Acetylphenyl

It cannot be said with any certainty what the actual motion of the atoms will be during the rotational process about the aryl C-N bond. In principle, the substituent on the aryl ring may rock back and forth over the benzylic methylene hydrogens, or the carbonyl group, or both. It should be noted, however, that for the present purposes

* The syntheses of the o-hydroxyphenyl and o-biphenyl analogues were not successful (Experimental section).

of discussion, this is unimportant provided that it is constant within the series.

ortho-substituted compounds

In an initial investigation aimed at determining the suitability of this type of compound for a study of restricted internal rotation, the room temperature n.m.r. spectrum of the first compound in the series, 2-benzyl-3-(2-chloro-6-methylphenyl)-4(3H)-quinazolinone, was most encouraging. The diastereotopic benzylic methylene protons ³⁶ gave rise to an AB quartet (see spectrum in the Experimental section) indicating slow rotation of the aryl group on the n.m.r. time scale. Furthermore, the chemical shift difference between the protons under consideration was found to be quite large (see Table 2) contrasting sharply with Fehlner's failure to observe a chemical shift difference in a similar compound (see Introduction). In all, the compound seemed to be most suitable for a study of this type.

In spite of the fact that the compound appeared to be "well behaved", the useful data obtained on rotation about the aryl C-N bond were limited. The limiting factor was the degree of steric hindrance. The compound was heated in nitrobenzene solution but the AB pattern did not collapse at the highest temperature attainable. Thus, even at 187°, rotation was slow on the n.m.r. time scale. In consequence, only a minimum value for the free energy of

Table 2

N.m.r. Data and Minimum Free Energies of Activation for Quinazolinones
Having Bulky ortho Substituents

Aryl Moiety	Solvent	Chemical shift difference, p.p.m. ^a	J _{AB} ^b	T ^c	τ^d	$\Delta G^{\ddagger e}$
2-Chloro- 6-methylphenyl	ϕ NO ₂	0.295	14.7	187	0.0194	> 23.7
<u>o</u> -Bromophenyl	ϕ NO ₂	0.210	14.8	177	0.0216	> 23.3
<u>o</u> -Tolyl ^f	CHBr ₃	0.057	14.5		g	g
<u>o</u> -Chlorophenyl	ϕ NO ₂	0.169	15.0	177	0.0222	> 23.3
<u>o</u> -Fluorophenyl ^f	CHBr ₃	0.143	15.1	150	0.0227	> 21.9

(a) 100 MHz spectra measured at room temperature. (b) Coupling constant, Hz. (c) Highest temperature at which the spectrum was studied, °C. (d) Minimum value of the lifetime (sec) at the highest temperature. (e) Minimum free energy of activation (k.cal mole⁻¹) at the specified temperature. (f) In ϕ NO₂ the benzylic protons appear as a singlet. (g) Not determined.

activation is reported. This value was calculated by assuming that the quartet had collapsed at 187°.

With bulky substituents in both ortho positions I is obviously very restricted in the internal rotation process. For this reason it was decided to synthesise compounds in which this process would be less hindered, thereby making the compounds suitable for complete lineshape analysis over a range of temperatures.

In compounds II, III, IV and V, rotation about the aryl C-N bond should be less hindered. All the compounds showed the AB pattern at room temperature that indicates slow rotation on the n.m.r. time scale. With the exception of the o-tolyl compound, the compounds were heated in solution but in no case was collapse of the quartet observed.

The o-tolyl compound was not heated because of the small chemical shift difference of the benzylic methylene protons in that compound (see Table 2). A loss of instrument homogeneity at high temperatures would result in the appearance of a "singlet" even though collapse of the AB pattern is most unlikely since the o-fluorophenyl compound, which is expected to be less hindered, did not show this phenomenon.

It may be a general rule that an o-tolyl group produces little chemical shift difference between diastereotopic protons. This has been shown to be the case in the quinazolinone series (compound III) and will be shown to be true in the thiohydantoin series. It is not surprising,

therefore, that the chemical shift difference between the protons under consideration in Fehlner's compound was too small to be detected.

With the exception of the o-tolyl compound, minimum free energies of activation for rotation about the aryl C-N bond have been reported (Table 2). The values were calculated by assuming that the spectra collapsed at the highest temperature at which the spectra were studied. Since no signs of incipient collapse were observed, it is probable that the true free energies of activation are significantly higher than the values reported. It is possible to assign a minimum free energy of activation to the o-tolyl compound by assuming that the AB quartet collapsed to a singlet at room temperature. This value, however, would be confusing to the casual reader and has been omitted in consequence.

meta-Substituted compounds

At this point, internal rotation in five progressively less hindered quinazolinones had been examined. The result was useful but limited information. Furthermore, it appeared as if the lower limit to hindered rotation in this series had been reached since fluorine is a very small substituent atom. It was decided, therefore, that a meta substituted compound should be examined. In so far as we are aware, this is a novel experiment.

There are two major requirements for this type of study of hindered rotation. First, the rate of rotation must be such that is on the n.m.r. time scale at low temperature but off the n.m.r. time scale at high temperature. Since it is the substituent in the ortho position that is mainly responsible for the steric hindrance to rotation, removal of this bulky substituent in this series of compounds should help by allowing an increase in the rate of rotation. The second requirement concerns the degree of dissymmetry in the molecule. (Without dissymmetry, the methylene protons are equivalent, and as such, will always appear as a singlet in the n.m.r. spectrum). It has been usual to employ ortho substituents to give the molecule the required degree of dissymmetry for a study of this type. The apparent reason being that an ortho substituent maximises the asymmetric shielding of the ring at the rotation axis.

Fortunately, the meta-bromophenyl compound showed an AB quartet at room temperature. The chemical shift difference between the diastereotopic benzylic methylene protons is small but measurable (see Table 3 and the n.m.r. spectrum in the Experimental section), i.e. the heterocyclic moiety is sufficiently bulky in this compound that rotation is slow on the n.m.r. time scale at room temperature even though the blocking substituents on the aryl ring are hydrogen atoms. However, the effective size of the ortho hydrogen atoms is probably increased by buttressing with the adjacent bromine atom. Also implicit is that the meta-

Table 3

N.m.r. Data, Coalescence Temperatures and Free Energies of Activation

for Quinazolinones Lacking Bulky ortho Substituents (Nitrobenzene Solution)

Aryl Moiety	Chemical shift difference, p.p.m. ^a	JAB ^b	Coalescence Temperature ^c	τ^d	ΔG^\ddagger ^e
<u>m</u> -Bromophenyl	0.088	15.1	94	0.022	18.9
β -Naphthyl	0.132	15.1	116	0.016	19.8
<u>m</u> -Acetylphenyl	0.105	15.0	102	0.0195	19.2

(a) 100 MHz spectra measured at room temperature. (b) Coupling constant, Hz.
 (c) Degrees C. (d) Lifetime at coalescence, sec. (e) Free energy of activation (kcal/mole) at the coalescence temperature.

substituted aryl group renders the molecule sufficiently dissymmetric for a study of this type to be feasible.

When the sample was heated, the AB portion of the n.m.r. spectrum collapsed to a singlet. However, since the chemical shift between the diastereotopic benzylic methylene protons is small, it is not practical to obtain activation parameters by complete line shape analysis over a range of temperatures with adequate accuracy. In consequence, only a free energy of activation obtained from the spectra in the region of coalescence is reported in Table 3. The rate constant at coalescence was obtained by computer simulation of the temperature dependent line shape using the programme PLOTAB.

The β -naphthyl and 3-acetylphenyl analogues were synthesised with the expectation that these compounds would show a larger chemical shift difference between the diastereotopic benzylic methylene protons, thus rendering the compounds suitable for complete line shape analysis over a range of temperatures. The chemical shift differences are larger than that of the *m*-bromophenyl compound, but not markedly so. The chemical shift differences of the three quinazolinones that lack bulky ortho substituents do not exceed the magnitude of the coupling constant (Table 3). Only free energies of activation calculated at the coalescence temperature via programme PLOTAB are reported.

As explained in an earlier section, the accuracy of the ΔG^\ddagger values is hard to evaluate. Furthermore, the

three values were obtained at different temperatures, making comparison difficult. It can probably be assumed, however, that differences in the free energy of activation of more than 0.5 kcal mole⁻¹ reflect significantly different values.

The ΔG^\ddagger represents the difference in energy between the ground state and the transition state. Since both of these energy levels may change when the aryl substituent is varied, it is difficult to make conclusions when only slight variations in the ΔG^\ddagger values are observed. For example on the basis of molecular models, it would be predicted that the m-bromophenyl compound would be more highly hindered than the β -naphthyl compound. The basis for this postulate is that the ortho hydrogen atom in the m-bromophenyl compound appears to be more sterically crowded than the corresponding atom in the β -naphthyl compound. Since it is difficult to see the origin of differences in the ground state energies of the two molecules, the apparently anomalous result has tentatively been assigned to differences in solvation.

Coupling constants

The coupling constants of the methylene protons in the quinazolinone series are in the expected region and vary only from 14.5 - 15.1 Hz (Table 2 and Table 3). This implies that the geometry of the moieties attached to the benzylic carbon atom varies only slightly as the aryl part of the molecule is varied.

Chemical shifts

The chemical shifts of the diastereotopic benzylic methylene protons are of some interest. As the aryl moiety is varied, one proton (A) absorbs at a fairly constant value of ca. δ 3.9, while the other proton (B) absorbs between δ 3.6 and δ 3.9 (Table 4). It must be assumed that the assignments made to protons A and B do not invert through the series. The data do not give the configuration at the benzylic carbon atom. It seems probable, however, that proton B is close to the path of either the rotating aryl substituent or the opposite ortho hydrogen atom, and that proton A is relatively far removed from the axis of internal rotation.

Infrared spectra

The infrared carbonyl stretching frequencies of the quinazolinones (Table 5) appear to give no useful information on the stereochemistry of the compounds. The stretching frequencies vary between 1665 and 1690 cm^{-1} but do not follow any discernable pattern. This probably reflects a complex mixture of electronic and steric factors.

Some of the studies on the quinazolinones that do not have bulky ortho substituents have been published ².

Table 4

Chemical Shifts^a of the Diastereotopic Benzylic
Methylene Protons of the Quinazolinones in
Nitrobenzene Solution

Aryl Moiety	δ_A	δ_B
2-Chloro- 6-methylphenyl	3.916	3.621
<u>o</u> -Bromophenyl	3.919	3.709
<u>o</u> -Tolyl ^b		
<u>o</u> -Chlorophenyl	3.923	3.754
<u>o</u> -Fluorophenyl ^b		
<u>m</u> -Bromophenyl	3.854	3.766
β -Naphthyl	3.958	3.826
<u>m</u> -Acetylphenyl	3.966	3.861

(a) 100 MHz spectra measured at room temperature.
(b) The chemical shift difference between the
methylene protons was too small to be detected
in this solvent.

Table 5
Infrared Carbonyl Stretching Frequencies
of the Quinazolinones^a

Aryl Moiety	Stretching Frequency ^b (cm ⁻¹)
2-Chloro- 6-methylphenyl	1670
<u>o</u> -Bromophenyl	1685
<u>o</u> -Tolyl	1665
<u>o</u> -Chlorophenyl	1690
<u>o</u> -Fluorophenyl	1675
<u>m</u> -Bromophenyl	1675
β -Naphthyl	1675
<u>m</u> -Acetylphenyl	c

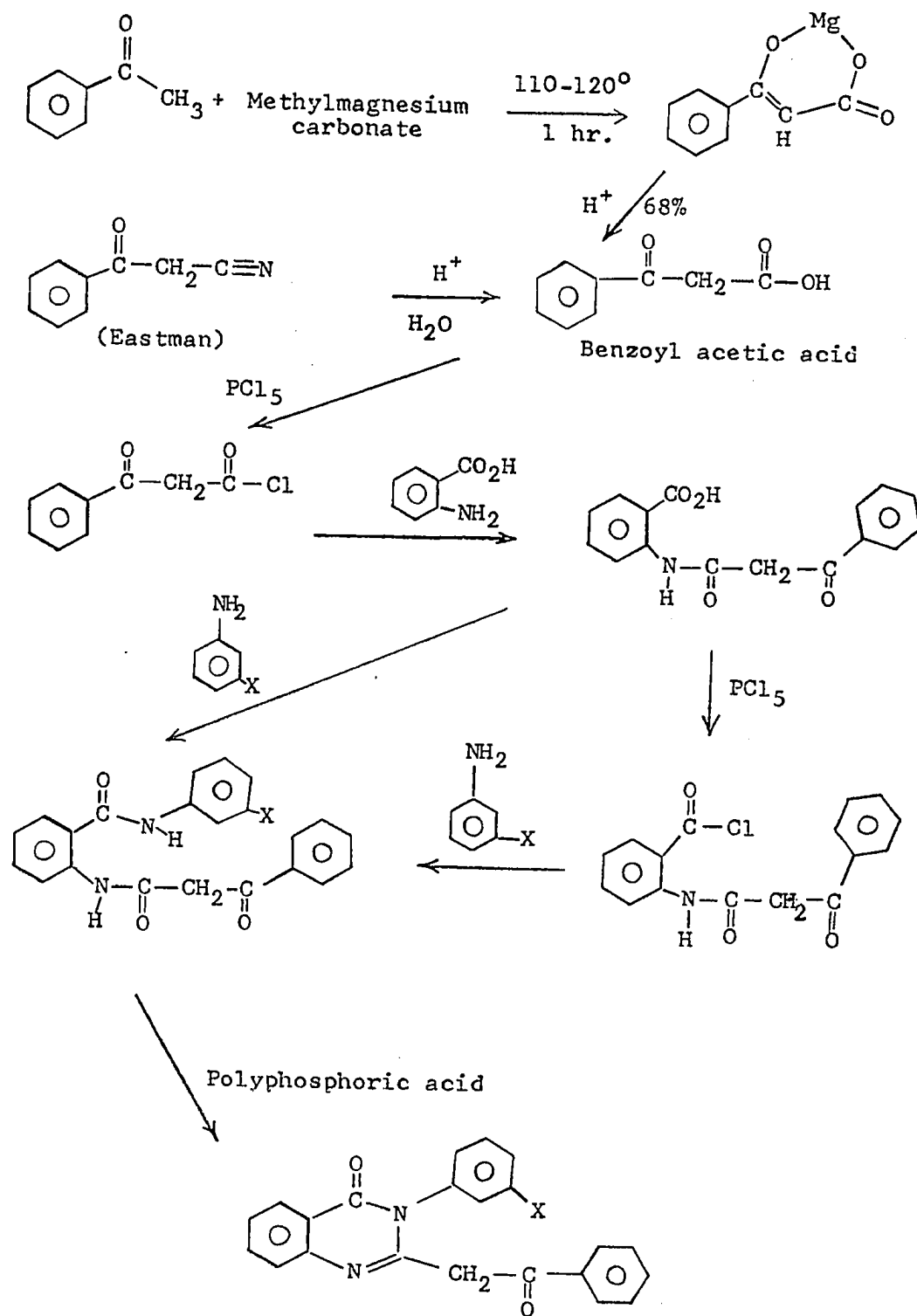
- (a) Taken through fused KBr discs.
(b) Estimated to be accurate to ± 5 cm⁻¹.
(c) Difficult to determine because of interference from the aryl moiety.

SUMMARY

1. Hindered internal rotation has been demonstrated in a new series of compounds, viz 2-benzyl-3-aryl-4(3H)-quinazolinones.
2. Very large rotational barriers were found when a bulky ortho substituent is on the aryl ring. The rate of rotation is so slow on the n.m.r. time scale that line shape analysis is not a suitable tool for the determination of activation parameters.
3. Substantial rotational barriers have been found in compounds lacking a bulky ortho substituent on the aryl ring.

SUGGESTIONS FOR FUTURE WORK

1. The introduction of an asymmetric centre in the molecule would result in the formation of diastereomeric rotational isomers. Hindered internal rotation could then be studied by equilibration rather than line shape methods.
2. It has been observed by Hund⁶, that the introduction of a carbonyl group adjacent to diastereotopic methylene protons causes a large chemical shift difference between the protons. With a large chemical shift difference between the diastereotopic benzylic methylene protons of the compounds lacking bulky ortho substituents, it may be possible to perform complete line shape analysis over a range of temperatures. The following type of synthesis, or adaptations thereof, is suggested. High yields would be expected in all but the last one, or possibly two, steps.³⁸

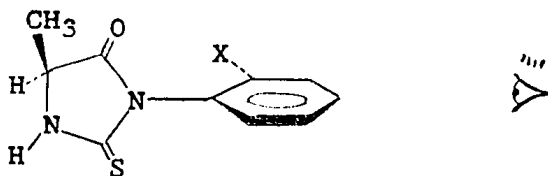


PART II

STUDIES ON THE STEREOCHEMISTRY AND KINETICS
OF ROTATION ABOUT THE ARYL C-N BOND OF
3-ARYL-5-METHYL-2-THIOHYDANTOINS

Causes of Non-Equivalence and Spectra Observed
in Thiohydantoin Asymmetrically Substituted at C-5

If the thiohydantoin molecule is viewed in the direction indicated, i.e., along the aryl C-N bond from the



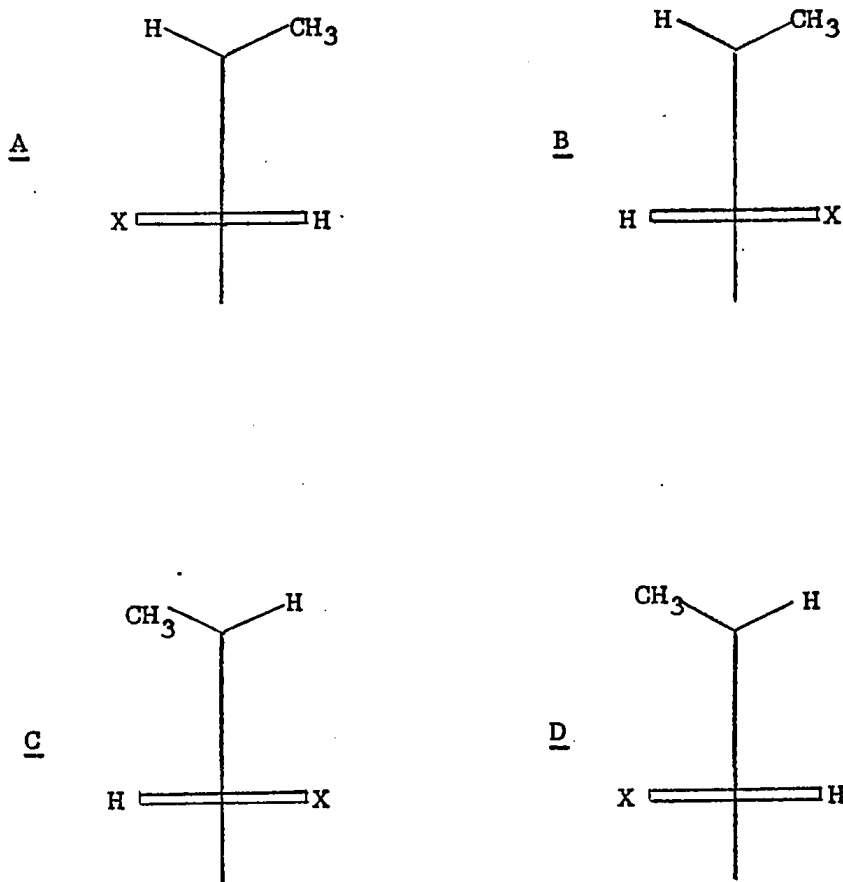
para position of the aryl ring, four isomers are seen to exist (Fig. 5). B is obtained from A by a 180° rotation about the aryl C-N bond. However, the diastereomers A and B have asymmetric centres (*) and have mirror images C and D, respectively. D may be obtained from C by a 180° rotation about the C-N bond.

As enantiomers, A and C will have identical spectra, as will B and D. Thus, only A and B (or C and D) need be considered in interpreting n.m.r. spectra. The key point here is that the rotamers, A and B, are diastereomers. Two methods are available to study the rotation, depending on the rotational stability of the compound.

Low rotational barriers

The methine proton and the methyl group will couple with each other in each diastereomer. Thus, the methyl protons will appear as a pair of doublets, while the methine

Fig. 5

Various Projections of a 3-Aryl-5-methyl-2-thiohydantoin

protons will appear as a pair of quartets if rotation about the aryl C-N bond is slow.* At high temperatures, i.e., under conditions of fast rotation about the aryl C-N bond, these spectra will collapse to a single doublet and a single quartet.

High rotational barriers

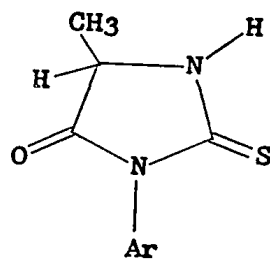
When the rotational barrier is large, the differences in the properties of the diastereomers allows a separation of the two diastereomers. The rotation may then be followed by equilibration (see section on Time Dependent Spectra under Calculation of Thermodynamic Parameters).

* Coupling in the system H-C-N-H was observed only in the o-fluorophenyl compound (see Experimental section).

RESULTS

The thiohydantoins were prepared by an adaptation of the method of Pujari and Rout 39. The structures were assigned by means of infrared and n.m.r. spectra, elemental analyses (see Experimental section), and from the fact that they are the expected products of the reactions.

Following is a list of the compounds that were synthesised successfully



	Ar	
IX		α -naphthyl
X		<u>o</u> -bromophenyl
XI		<u>o</u> -tolyl
XII		<u>o</u> -chlorophenyl
XIII		<u>o</u> -methoxyphenyl
XIV		<u>o</u> -fluorophenyl
XV		β -naphthyl

Equilibrium constants

As mentioned in the introduction (p 6), Fehlner⁴ has reported an equilibrium constant of 1.18 between the diastereomeric rotational isomers of 3- α -naphthyl-5-methyl-2-thiohydantoin in pyridine solution. As will be explained later, the observation of a non-unity equilibrium constant requires an explanation. For this reason it was decided to reappraise the value reported by Fehlner.

The origin of Fehlner's value is not clear. It is most unlikely that the equilibrium constant comes from a single determination but this must be assumed in the absence of an error analysis. Furthermore, no corrections were made for second order characteristics in the n.m.r. spectrum although this is probably not a serious omission.

The integration method that Fehlner used to determine the areas under the diastereomeric methyl peaks is not entirely satisfactory in this case. This integration method works well when there is no overlap of the peaks under consideration but it works badly when there is considerable overlap. It could be argued that the spectrum of the diastereomeric methyl groups of 3- α -naphthyl-5-methyl-2-thiohydantoin forms an intermediate case, since some overlap is present. In any case, the integration method, when applied to this compound, involves arbitrary decisions concerning where one integral ends and another begins.

It may be concluded from this reappraisal that

Fehlner's value of the equilibrium constant is not as reliable as it could be. In fact, the author was convinced that it was erroneous and decided to check the value.

A solution of 3- α -naphthyl-5-methyl-2-thiohydantoin in pyridine, contained in an n.m.r. tube, was heated in boiling water for several hours to allow equilibrium to be reached. After the sample had cooled, six n.m.r. spectra were recorded and the peaks integrated. Small corrections were then made for second order characteristics in the spectra, using the computer programme LAOCOON II, and the equilibrium constant was determined from the ratio of the concentration of diastereomers (Table 6⁴⁰). In addition, the equilibrium constant was determined by resolving the peaks in the spectrum using a curve resolver (see Experimental section for details of this method) and correcting for second order characteristics. The data from the latter method are shown in the same table.

It may be concluded that there is little difference between the results of the two methods but slightly better reproducibility was obtained by curve resolving. It should be noted, however, that this is a special case. When the chemical shift difference between the diastereomeric methyl groups is smaller, as in the rest of the compounds in this series, the integration method would be totally unsatisfactory.

The main conclusion is, therefore, that Fehlner's value is correct, i.e. the equilibrium constant for rotation

Table 6

Comparison of Integration with Curve Resolving in the Determination of the Equilibrium Constant between the Diastereomers of 3- α -Naphthyl-5-methyl-2-thiohydantoin^a

	K by integration	K by curve resolving
	1.254	1.183
	1.268	1.127
	1.169	1.179
	1.334	1.132
	1.244	1.114
	1.154	1.159
Average	1.237	1.149
Standard deviation	0.067	0.029
Equilibrium constant ^b	1.2 \pm 0.1	1.15 \pm 0.06

(a) Corrections were made for second order characteristics in the n.m.r. spectra. (b) 90% confidence limits.

about the aryl C-N bond in 3- α -naphthyl-5-methyl-2-thiohydantoin differs significantly from unity.

With this fact established, it was decided that a series of thiohydantoins should be examined.

Equilibrium constants and kinetics

The diastereomeric methyl signals of 3-o-bromophenyl-5-methyl-2-thiohydantoin, X, show a chemical shift difference in pyridine (Table 7). When the sample was heated to the boiling point of the solvent, however, the signals did not collapse to a doublet. Thus, rotation about the aryl C-N bond is too highly hindered to be studied by complete line shape analysis. Fortunately, in this series of compounds, there is another method that can be used to obtain data. The rotamers are diastereomers (see Introduction) and rotation may be studied by following the equilibration of a sample enriched with one diastereomer as the equilibrium state is approached.

The following methods were not particularly successful in obtaining an enriched sample: slow recrystallisation from ethanol, room temperature recrystallisation from acetone, and chromatography on silica-gel using acetone as the solvent. Slow recrystallisation from methanol, however, gave only the pure, thermodynamically less stable isomer (experimental details are given following an account of the synthesis of this compound).

Table 7

Chemical Shifts and Coupling Constants of the Methyl Groups
of Some 3-Aryl-5-methyl-2-thiohydantoins^a

Aryl Moiety	Solvent	High field methyl ^b	J _c	Low field methyl ^b	J _c	Chemical Shift Difference ^b
α-naphthyl	Pyridine	1.475	7.1	1.546	7.1	0.071
o-bromophenyl	Pyridine	1.491	7.1	1.502	7.1	0.071
o-tolyl	Pyridine	1.413	7.0	1.429	7.1	0.016
o-chlorophenyl	Pyridine	1.423	7.0	1.469	7.0	0.046
o-methoxyphenyl	Pyridine	1.394	7.0	1.433	7.0	0.039
o-fluorophenyl	DMSO-d ₆	1.353	7.1	1.386	7.0	0.033

β-naphthyl ^d	DMSO-d ₆	4.532	7.2	4.543	7.2	0.011

(a) 100 MHz spectra. (b) P.p.m. (c) Coupling constant, Hz. (d) There is no chemical shift difference between the diastereomeric methyl groups in pyridine or DMSO-d₆. The chemical shifts and coupling constants reported are those of the diastereomeric methine protons.

The equilibrium constant between the diastereomeric rotational isomers of 3-o-bromophenyl-5-methyl-2-thiohydantoin (Table 8) was obtained by curve resolving in a manner similar to that used for the α -naphthyl analogue. The equilibration of the thermodynamically less stable diastereomer was studied at various temperatures and the data are shown in Tables 9, 10, 11, 12, 13, and 14. The calculated best fit curves are also reported. Fig. 6 shows the equilibration curves graphically. Fig. 7 shows the n.m.r. spectrum of the methyl region of the diastereomeric rotational isomers of the compound soon after the start of equilibration, while Fig. 8 shows the situation at equilibrium. Table 15 contains the lifetimes calculated at each temperature at which the equilibration was studied together with the calculated errors and the weighting factors used in the Arrhenius calculation. Fig. 9 shows the Arrhenius plot. Table 16 contains the Arrhenius and Eyring activation parameters.

It should be mentioned that some difficulty was encountered in resolving the peaks of the o-bromophenyl compound. In pyridine, the methyl region shows a triplet as a consequence of two almost coincident peaks. It was the central, "double" peak that caused the difficulty since it was not found possible to generate an exact replica in the curve resolver. It is recommended that if the experiment is repeated (or if a similar situation is encountered by any other workers) that the equilibrations be followed on a

Table 8

Equilibrium Constants of the Diastereomeric Rotational
Isomers of some 3-Aryl-5-methyl-2-thiohydantoin

	<u>o</u> -bromophenyl	<u>o</u> -tolyl	<u>o</u> -chlorophenyl	<u>o</u> -methoxyphenyl
	1.931	1.402	1.755	1.432
	1.887	1.396	1.809	1.377
	1.819	1.469	1.709	1.339
	1.809	1.493	1.700	1.359
	1.955	1.472	1.658	1.357
	1.926	1.379	1.639	1.279
	1.949	1.361	1.553	1.355
	1.936	1.339	1.658	1.307
	2.046	1.388	1.586	1.357
	1.937	1.322	1.625	
	1.935	1.365	1.593	
	1.959			
	1.990			
Average	1.927	1.398	1.662	1.351
Standard deviation	0.064	0.056	0.076	0.043
Equilibrium constant ^a	1.9 ± 0.1	1.4 ± 0.1	1.7 ± 0.1	1.35 ± 0.08

(a) 90% confidence limits

Table 9

The Equilibration of the Thermodynamically Less Stable Diastereomer of 3-o-Bromophenyl-5-methyl-2-thiohydantoin in Pyridine at 88.5°C.

Time (minutes)	Experimentally determined ratio of diastereomers ^a	Calculated ratio of diastereomers ^{a,b}
0.0	0.414	0.458
3.0	0.497	0.536
6.0	0.680	0.614
10.0	0.738	0.716
12.0	0.724	0.766
15.0	0.705	0.839
18.0	0.830	0.911
22.0	1.019	1.002
25.0	1.165	1.068
28.0	1.063	1.130
30.0	1.182	1.170
33.0	1.154	1.227
36.0	1.346	1.282
39.0	1.705	1.332
45.0	1.609	1.424
48.0	1.346	1.466
51.0	1.620	1.504
54.0	1.601	1.539
59.0	1.466	1.593
66.0	1.601	1.655
70.0	1.592	1.686
76.0	1.688	1.725
82.0	1.653	1.757
89.0	1.705	1.788
98.0	1.777	1.818
105.0	1.733	1.836
109.0	1.687	1.844
113.0	1.708	1.852

(a) Ratio of less stable to more stable diastereomer.

(b) Assuming an equilibrium constant of 1.9.

Table 10

The Equilibration of the Thermodynamically Less Stable Diastereomer of 3-o-Bromophenyl-5-methyl-2-thiohydantoin in Pyridine at 78.5°C.

Time (minutes)	Experimentally determined ratio of diastereomers ^a	Calculated ratio of diastereomers ^{a, b}
0.0	0.569	0.557
3.0	0.553	0.589
6.0	0.566	0.621
9.0	0.642	0.652
12.0	0.672	0.684
15.0	0.709	0.715
18.0	0.740	0.746
21.0	0.762	0.777
24.0	0.807	0.807
27.0	0.846	0.837
31.0	0.873	0.877
33.0	0.875	0.897
37.0	0.956	0.935
40.0	0.971	0.963
44.0	1.027	1.001
47.0	1.067	1.028
50.0	1.093	1.055
53.0	1.126	1.081
56.0	1.186	1.107
61.0	1.109	1.149
64.0	1.099	1.174
67.0	1.164	1.197
70.0	1.140	1.221
73.0	1.204	1.244
76.0	1.340	1.266
81.0	1.298	1.302
86.0	1.412	1.336
90.0	1.407	1.363
96.0	1.523	1.401
100.0	1.529	1.425
109.0	1.508	1.475
121.0	1.442	1.536
141.0	1.471	1.620
162.0	1.516	1.689

(a) Ratio of less stable to more stable diastereomer.
 (b) Assuming an equilibrium constant of 1.9.

Table 11

The Equilibration of the Thermodynamically Less Stable
Diastereomer of 3-o-Bromophenyl-5-methyl-2-thiohydantoin
in Pyridine at 67.5°C.

Time (minutes)	Experimentally determined ratio of diastereomers ^a	Calculated ratio of diastereomers ^{a,b}
0.0	0.225	0.252
3.0	0.254	0.270
6.0	0.257	0.288
9.0	0.299	0.307
13.0	0.302	0.331
17.0	0.331	0.355
21.0	0.397	0.379
31.0	0.465	0.441
37.0	0.468	0.477
39.0	0.523	0.489
48.0	0.543	0.545
64.0	0.664	0.641
68.0	0.683	0.665
74.0	0.722	0.701
81.0	0.794	0.742
87.0	0.851	0.777
92.0	0.838	0.806
98.0	0.872	0.841
106.0	0.937	0.886
110.0	0.926	0.908
117.0	1.011	0.946
132.0	0.948	1.025
141.0	0.991	1.071
149.0	1.007	1.110
166.0	1.091	1.189
176.0	1.192	1.234
191.0	1.198	1.297
209.0	1.404	1.366
227.0	1.434	1.429
247.0	1.516	1.492
273.0	1.583	1.563
305.0	1.707	1.636
345.0	1.730	1.706
351.0	1.785	1.715

(a) Ratio of less stable to more stable diastereomer.
(b) Assuming an equilibrium constant of 1.9.

Table 12

The Equilibration of the Thermodynamically Less Stable Diastereomer of 3-*o*-Bromophenyl-5-methyl-2-thiohydantoin in Pyridine at 58°C.

Time (minutes)	Experimentally determined ratio of diastereomers ^a	Calculated ratio of diastereomers ^{a,b}
0.0	0.114	0.142
3.0	0.115	0.149
7.0	0.126	0.159
13.0	0.169	0.174
18.0	0.184	0.186
25.0	0.188	0.204
39.0	0.225	0.239
47.0	0.248	0.259
60.0	0.293	0.292
77.0	0.342	0.335
87.0	0.380	0.361
103.0	0.412	0.402
117.0	0.447	0.438
128.0	0.493	0.466
148.0	0.532	0.518
161.0	0.530	0.551
174.0	0.709	0.584
177.0	0.622	0.592
193.0	0.659	0.632
204.0	0.677	0.660
223.0	0.731	0.708
233.0	0.768	0.732
245.0	0.684	0.762
253.0	0.793	0.782
275.0	0.803	0.835
295.0	0.844	0.882
310.0	0.924	0.917
313.0	0.931	0.924
319.0	0.887	0.938
336.0	0.984	0.976
357.0	1.079	1.022
361.0	1.018	1.031
375.0	0.976	1.061
381.0	1.079	1.073
391.0	1.081	1.094
405.0	1.094	1.123
419.0	1.148	1.151
442.0	1.195	1.195
453.0	1.231	1.216
459.0	1.236	1.227

(a) Ratio of less stable to more stable diastereomer.

(b) Assuming an equilibrium constant of 1.9.

Table 13

The Equilibration of the Thermodynamically Less Stable Diastereomer of 3-o-Bromophenyl-5-methyl-2-thiohydantoin in Pyridine at 49°C.

Time (minutes)	Experimentally determined ratio of diastereomers ^a	Calculated ratio of diastereomers ^{a,b}
0.0	0.160	0.116
3.0	0.162	0.120
6.0	0.171	0.125
10.0	0.132	0.130
13.0	0.185	0.135
18.0	0.209	0.142
21.0	0.169	0.146
24.0	0.159	0.150
27.0	0.163	0.155
31.0	0.179	0.161
36.0	0.234	0.168
39.0	0.170	0.172
42.0	0.174	0.177
45.0	0.188	0.181
48.0	0.173	0.185
52.0	0.172	0.191
57.0	0.182	0.199
61.0	0.179	0.204
66.0	0.211	0.212
72.0	0.203	0.221
82.0	0.212	0.235
89.0	0.255	0.246
93.0	0.255	0.252
97.0	0.245	0.258
101.0	0.232	0.264
105.0	0.245	0.269
109.0	0.240	0.275
113.0	0.250	0.281
119.0	0.277	0.290
132.0	0.274	0.309
158.0	0.288	0.349
161.0	0.326	0.353
166.0	0.331	0.361
176.0	0.352	0.376
192.0	0.419	0.400
196.0	0.346	0.406

Table continued overleaf

Table 13 continued

204.0	0.455	0.418
219.0	0.409	0.441
224.0	0.409	0.449
263.0	0.516	0.507
267.0	0.507	0.514
270.0	0.493	0.518
273.0	0.435	0.523
277.0	0.490	0.529
296.0	0.547	0.557
303.0	0.566	0.568
325.0	0.691	0.601
328.0	0.679	0.605
365.0	0.692	0.660
370.0	0.717	0.668
385.0	0.715	0.689
388.0	0.728	0.694

-
- (a) Ratio of less stable to more stable diastereomer.
(b) Assuming an equilibrium constant of 1.9.

Table 14

The Equilibration of the Thermodynamically Less Stable Diastereomer of 3-o-Bromophenyl-5-methyl-2-thiohydantoin in Pyridine at 23.5°C.

Time (hours) ^a	Experimentally determined ratio of diastereomers ^{a,b}	Calculated ratio of diastereomers ^{b,c}
0.07	0.081	0.041
21.50	0.173	0.160
45.69	0.289	0.300
70.07	0.424	0.444
93.62	0.559	0.583
117.86	0.645	0.724
143.30	0.901	0.866
165.82	1.042	0.985

- (a) Average of 3 closely spaced determinations.
(b) Ratio of less stable to more stable diastereomer.
(c) Assuming an equilibrium constant of 1.9.

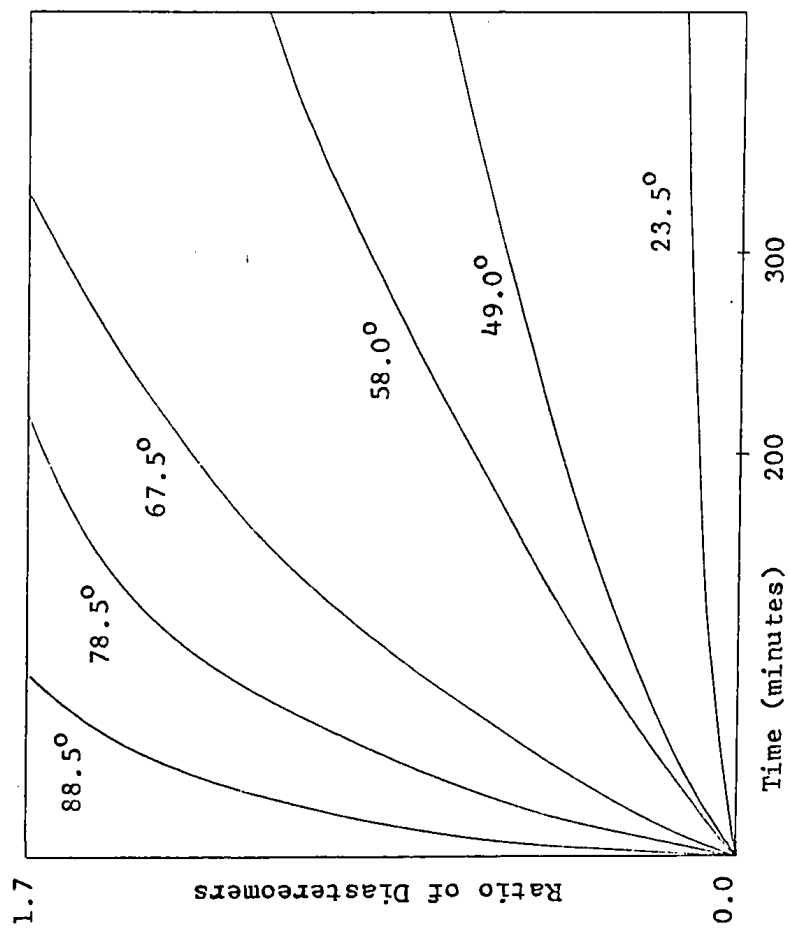


Fig. 6

The Equilibration of the Thermodynamically Less Stable Diastereomer of 3-o-Bromophenyl-5-methyl-2-thiohydantoin in Pyridine at Various Temperatures

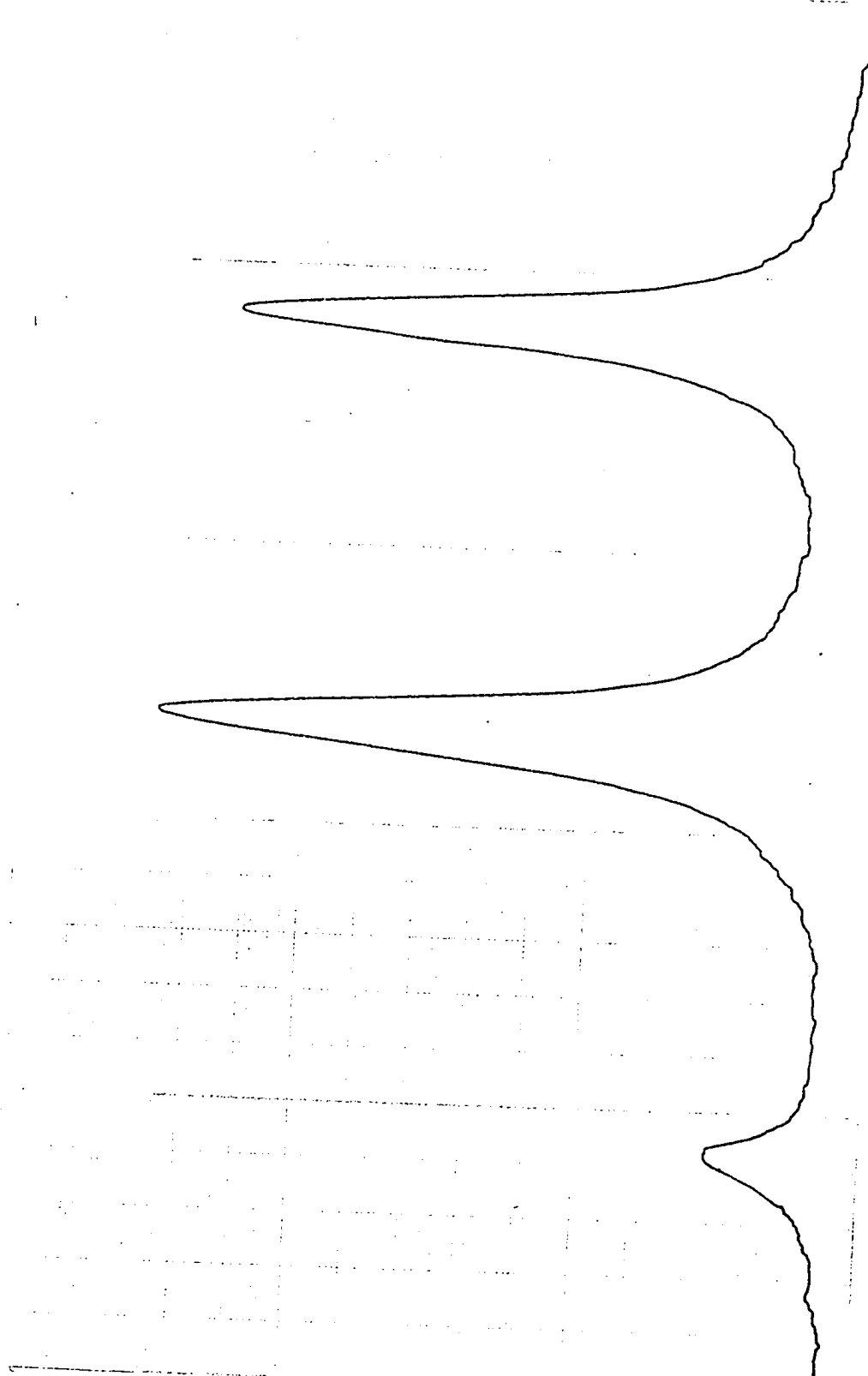


Fig. 7. 100 MHz NMR Spectrum of the Methyl Region of the Diastereomeric Rotational Isomers of 3-o-Bromophenyl-5-methyl-2-thiohydantoin in Pyridine soon after the start of Equilibration (50 Hz scan).

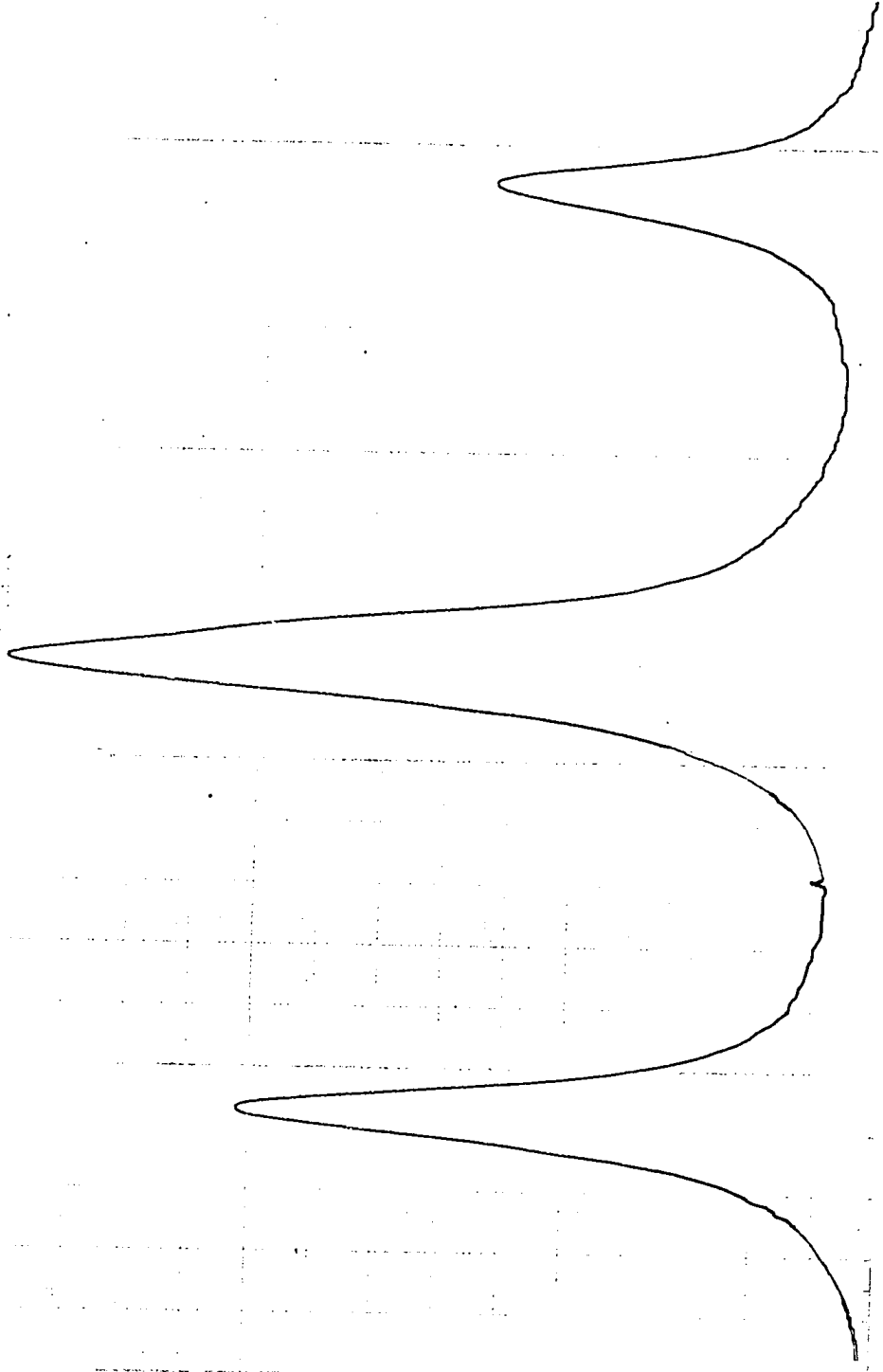


Fig. 8. 100 MHz NMR Spectrum of the Methyl Region of the Equilibrium Mixture of the Diastereomeric Rotational Isomers of 3-o-Bromophenyl-5-methyl-2-thiohydantoin in Pyridine (50 Hz scan)

Table 15

Rotational Lifetimes from the Equilibration of 3-o-Bromophenyl-5-methyl-2-thiohydantoin
in Pyridine at Various Temperatures

Temperature (°C)	Lifetime (sec.)	Error in Lifetime	Weighting Factor
88.5	0.2544×10^4	0.3369×10^3	0.27
78.5	0.6173×10^4	0.4585×10^3	0.46
67.5	0.1085×10^5	0.6626×10^3	0.55
58.0	0.2584×10^5	0.7645×10^3	1.10
49.0	0.4386×10^5	0.6631×10^3	2.13
23.5	0.6711×10^6	0.1467×10^5	1.48

Fig. 9

Arrhenius Plot and Weighted Least Squares Line for the
Thermodynamically Less Stable Diastereomer of
3-o-Bromophenyl-5-methyl-2-thiohydantoin in Pyridine

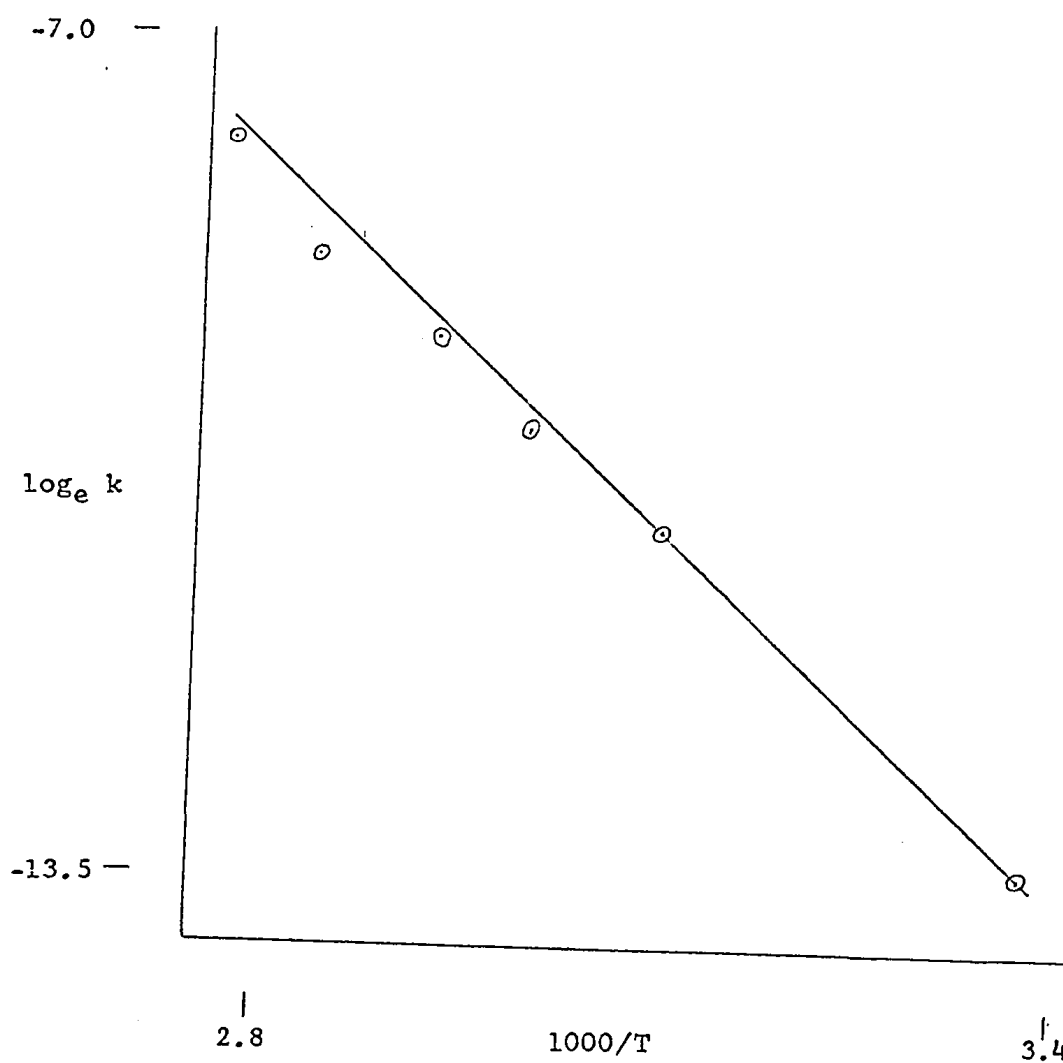


Table 16

Arrhenius and Eyring Activation Parameters for the Restricted
Internal Rotation Process of the Thermodynamically Less
Stable Diastereomer of 3-o-Bromophenyl-5-methyl-2-thiohydantoin

Arrhenius Parameters^a

Activation Energy	18.2 ± 1.7 ^b
log _e (A)	17.6 ± 2.6
log ₁₀ (A)	7.6 ± 1.1

Eyring Parameters^{a, c}

Enthalpy	17.6 ± 1.7 ^b
Entropy	-25.5 ± 5.2 ^d
Free Energy	25.23 ± 0.06 ^b

(a) 90% confidence limits. (b) kcal.mole⁻¹. (c) At 25°C.
(d) e.u.

60 MHz instrument. In this case the chemical shift difference between the methyl signals of the diastereomers will be reduced (in Hertz) and there will be four single peaks in the methyl region of the n.m.r. spectrum.

The principal disadvantage with the equilibration method is that it is time consuming. Usually in complete lineshape analysis six or more carefully chosen spectra will suffice. Considerably more spectra were analysed in the determination of the activation parameters of 3-o-bromophenyl-5-methyl-2-thiohydantoin. In addition, the question arises as to whether it is really desirable to obtain all the activation parameters for all the compounds. For the present purposes of discussion it is not. In consequence, only free energies of activation have been determined from a single equilibration experiment, or from a coalescence point measurement, for the remainder of the compounds in the series.

The spectra of the o-tolyl, o-chlorophenyl, and o-methoxyphenyl compounds (Table 7 gives the chemical shifts of the diastereomeric methyl groups) did not collapse to doublets when heated to the boiling point of pyridine, thus forcing the use of the equilibration method. Table 8 gives the equilibrium constants. Figs. 10, 11, 12 show the n.m.r. spectra at equilibrium. Tables 17, 18, 19 contain the equilibration data obtained at a single temperature. Table 20 gives the rate constants and free energies of activation.

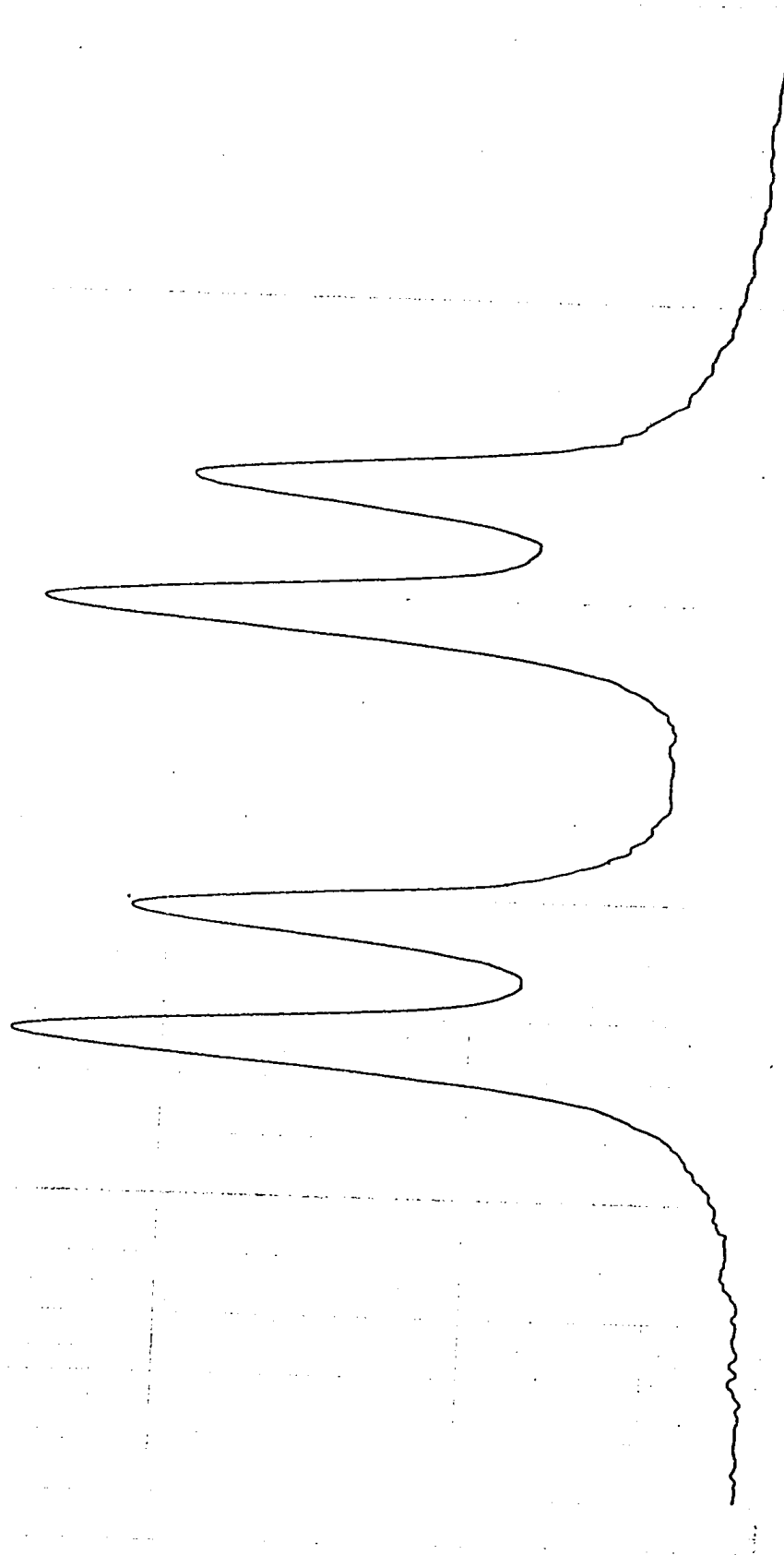


Fig. 10. 100 MHz NMR Spectrum of the Methyl Region of the Equilibrium Mixture of the Diastereomeric Rotational Isomers of 3-o-Tolyl-5-methyl-2-thiohydantoin in Pyridine (50 Hz scan)

Table 17

The Equilibration of the Thermodynamically Less Stable
Diastereomer of 3-o-Tolyl-5-methyl-2-thiohydantoin
in Pyridine at 57.5°C.

Time (minutes)	Experimentally determined ratio of diastereomers ^a	Calculated ratio of diastereomers ^{a,b}
0.0	0.537	0.601
10.0	0.758	0.736
14.0	0.826	0.786
17.0	0.945	0.823
20.0	0.919	0.857
26.0	0.886	0.923
31.0	0.990	0.972
35.0	0.992	1.009
39.0	1.100	1.043
43.0	0.968	1.075
46.0	0.872	1.097
53.0	1.024	1.143
60.0	1.145	1.184
63.0	1.311	1.199
74.0	1.331	1.248
84.0	1.248	1.282
99.0	1.385	1.319
109.0	1.433	1.338
119.0	1.385	1.353
130.0	1.515	1.365

(a) Ratio of less stable to more stable diastereomer.
(b) Assuming an equilibrium constant of 1.4.

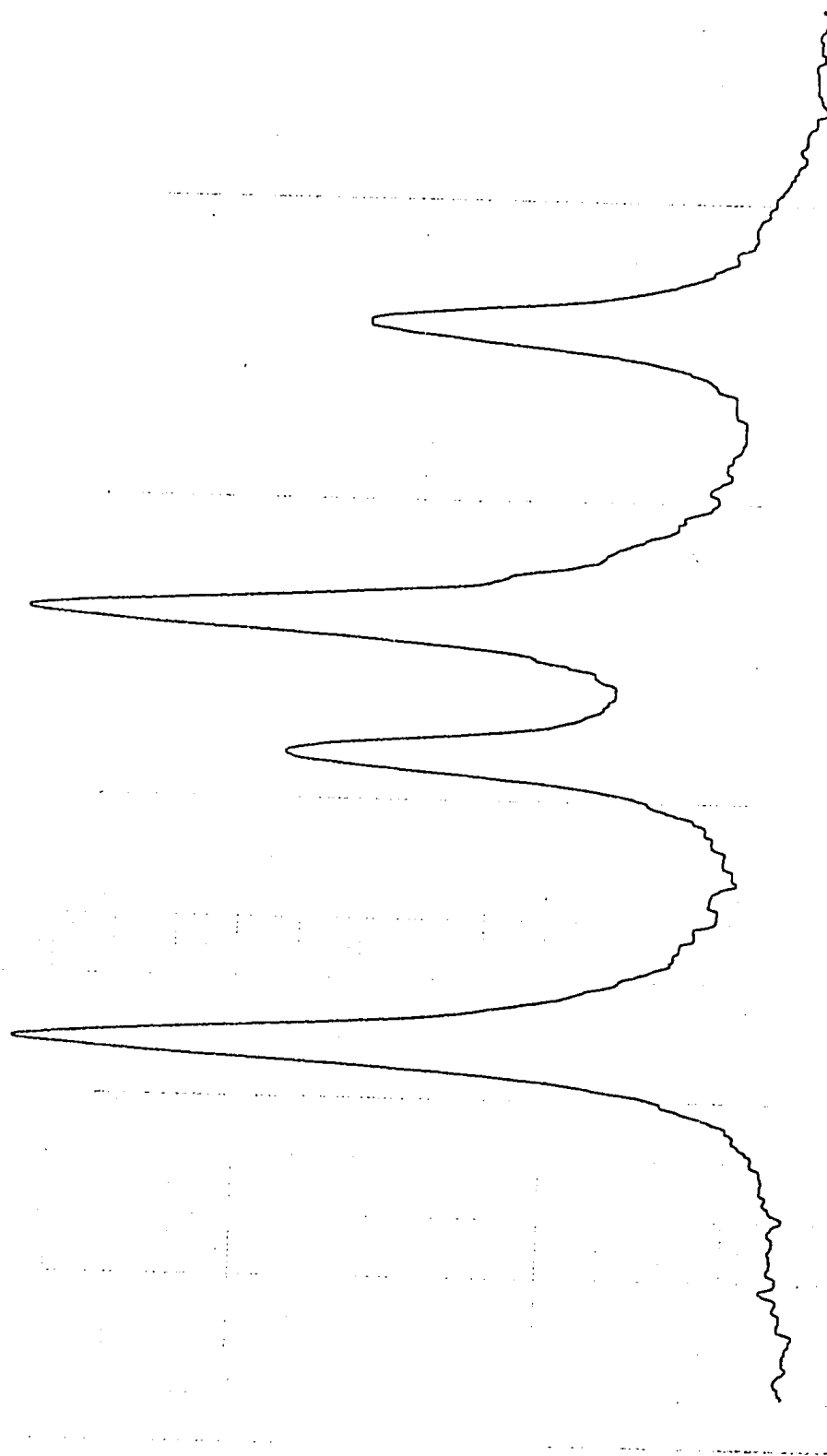


Fig. 11. 100 MHz NMR Spectrum of the Methyl Region of the Equilibrium Mixture of the Diastereomeric Rotational Isomers of 3-o-Chlorophenyl-5-methyl-2-thiohydantoin in Pyridine (50 Hz scan).

Table 18

The Equilibration of the Thermodynamically Less Stable
Diastereomer of 3-o-Chlorophenyl-5-methyl-2-thiohydantoin
In Pyridine at 58.5°C.

Time (minutes)	Experimentally determined ratio of diastereomers ^a	Calculated ratio of diastereomers ^{a,b}
0.0	0.197	0.065
3.0	0.202	0.079
6.0	0.183	0.094
9.0	0.164	0.109
12.0	0.212	0.124
17.0	0.274	0.149
21.0	0.229	0.169
27.0	0.264	0.199
32.0	0.286	0.225
37.0	0.278	0.250
40.0	0.260	0.266
44.0	0.310	0.286
48.0	0.344	0.307
56.0	0.356	0.348
61.0	0.396	0.373
65.0	0.345	0.394
70.0	0.334	0.419
74.0	0.362	0.439
78.0	0.379	0.460
82.0	0.401	0.481
93.0	0.432	0.536
95.0	0.456	0.546
101.0	0.496	0.576
108.0	0.496	0.611
114.0	0.523	0.640
120.0	0.566	0.669
127.0	0.664	0.703
134.0	0.665	0.737
140.0	0.572	0.765
145.0	0.657	0.788
157.0	0.800	0.842

Table continued overleaf

Table 18 continued

161.0	0.900	0.859
169.0	0.958	0.894
176.0	0.935	0.924
181.0	0.970	0.945
185.0	0.960	0.961
188.0	1.000	0.974
191.0	1.000	0.986
211.0	1.188	1.063
215.0	1.146	1.077
220.0	1.000	1.095
228.0	1.155	1.123
237.0	1.121	1.154
247.0	1.127	1.186
259.0	1.193	1.223
294.0	1.382	1.319
310.0	1.607	1.357
322.0	1.545	1.383
344.0	1.612	1.427
354.0	1.551	1.445
358.0	1.515	1.452

(a) Ratio of less stable to more stable diastereomer.
(b) Assuming an equilibrium constant of 1.7.

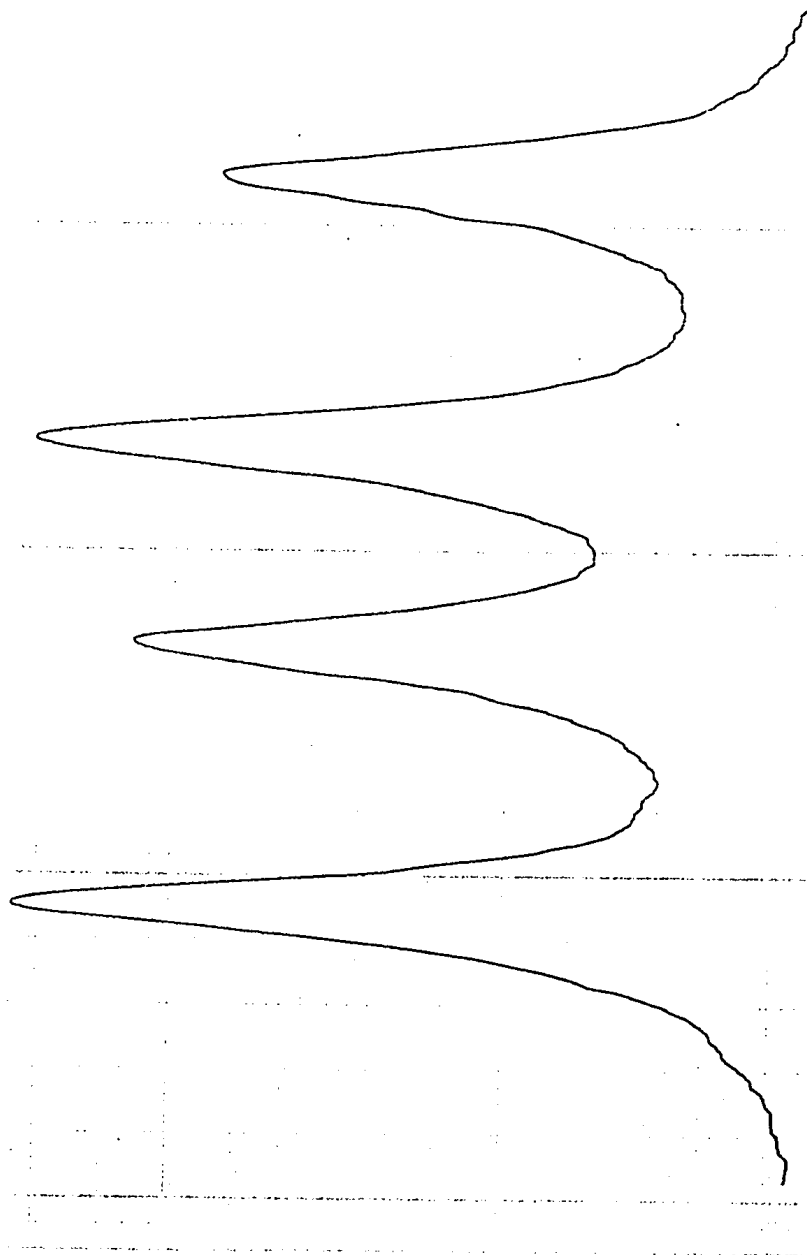


Fig. 12. 100 MHz NMR Spectrum of the Methyl Region of the Equilibrium Mixture of the Diastereomeric Rotational Isomers of 3-O-Methoxyphenyl-5-methyl-2-thiohydantoin in Pyridine (50 Hz scan).

Table 19

The Equilibration of the Thermodynamically Less Stable
Diastereomer of 3-o-Methoxyphenyl-5-methyl-2-thiohydantoin
In Pyridine at 28.5°C.

Time (minutes)	Experimentally determined ratio of diastereomers ^a	Calculated ratio of diastereomers ^{a,b}
0.0	0.030	0.036
4.0	0.038	0.044
9.0	0.064	0.053
18.0	0.058	0.071
25.0	0.088	0.084
36.0	0.095	0.105
46.0	0.119	0.125
56.0	0.143	0.144
63.0	0.166	0.158
74.0	0.171	0.179
92.0	0.208	0.214
103.0	0.239	0.236
112.0	0.241	0.253
125.0	0.271	0.278
136.0	0.303	0.299
151.0	0.324	0.328
161.0	0.363	0.347
179.0	0.394	0.381
192.0	0.417	0.406
205.0	0.434	0.429
219.0	0.491	0.456
293.0	0.597	0.587
297.0	0.599	0.594
304.0	0.611	0.606
313.0	0.633	0.621
327.0	0.648	0.644
350.0	0.639	0.681
353.0	0.652	0.686

(a) Ratio of less stable to more stable diastereomer.
(b) Assuming an equilibrium constant of 1.35.

Table 20

Free Energies of Activation for Rotation about the Aryl C-N Bond in Some 3-Aryl-5-methyl-2-thiohydantoin

Aryl moiety	Solvent	Temperature ^a	Lifetime ^b	ΔG ^{#c}
α -naphthyl	Pyridine	25		25.55 ^{d,e,j}
<u>o</u> -bromophenyl	Pyridine	25		25.23 \pm 0.06 ^{e,f,g,j}
<u>o</u> -bromophenyl	Pyridine	58		26.08 \pm 0.03 ^{e,f,g,j}
<u>o</u> -tolyl	Pyridine	57.5	(3.805 \pm 0.821) 10^3	24.8 \pm 0.1 ^{e,j}
<u>o</u> -chlorophenyl	Pyridine	58.5	(12.539 \pm 0.602) 10^3	25.69 \pm 0.03 ^{e,j}
<u>o</u> -methoxyphenyl	Pyridine	28.5	(31.546 \pm 1.516) 10^3	23.86 \pm 0.03 ^{e,j}
<u>o</u> -fluorophenyl	DMSO-d ₆	86	0.136	19.7 ^{h,i,k}
β -naphthyl	DMSO-d ₆	97.5	0.85	21.7 ^{h,i,k}

(a) °C. (b) sec. (c) Free energy of activation at the specified temperature, kcal/mole. (d) Data from Ref. 4. (e) For thermodynamically less stable diastereomer. (f) Calculated from previous data. (g) 90% confidence limits. (h) Average value for thermodynamically less stable and more stable diastereomers. (i) Estimated error \pm 0.5 kcal/mole. (j) Data obtained by equilibration method. (k) Data obtained by line shape analysis.

The four peak methyl region of the o-fluorophenyl compound did collapse to a single, time averaged doublet when the solution was heated. The chemical shift difference between the diastereomeric methyl groups, however, is rather small (Table 7) and it is not practical to perform complete lineshape analysis. The free energy of activation at the coalescence temperature (see equation, p 16) is reported in Table 20.

The diastereomeric methyl peaks of the β -naphthyl compound do not show a chemical shift difference (see section following an account of the synthesis of this compound). Fortunately, however, the diastereomeric methine protons show a small chemical shift difference in DMSO- d_6 and the room temperature n.m.r. spectrum shows two overlapping quartets. When heated, the spectrum collapsed to a single, time averaged quartet. The rate constant at coalescence was determined by matching the experimental spectra with computer simulated spectra. The computer simulated spectra are shown in Figs. 13, 14, 15. It was assumed that the lifetimes on both sites were equal. In principle this cannot be true but no difference could be discerned in the experimental spectra. The free energy of activation at the coalescence temperature is reported in Table 20.

Infrared spectra

The infrared carbonyl stretching frequencies of

thiohydantoins are shown in Table 21.

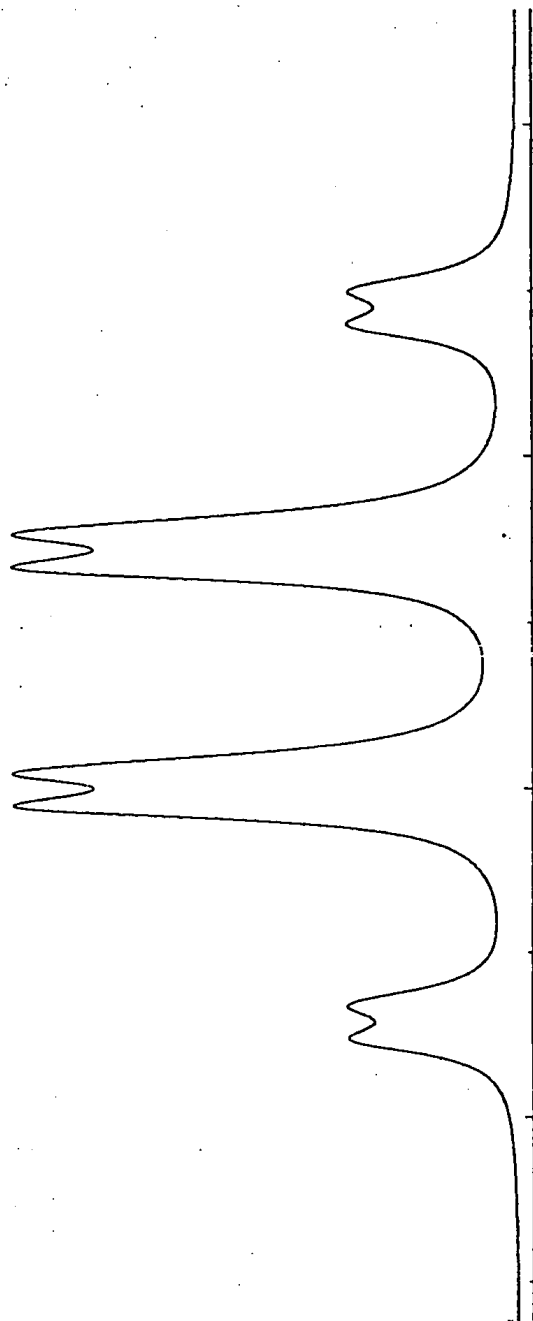


Fig. 13
Simulated Spectrum of the Methine Region
of the Diastereomeric Rotational Isomers
of 3- β -Naphthyl-5-methyl-2-thiohydantoin
with both Rotamers having Lifetimes of
5.00 sec.

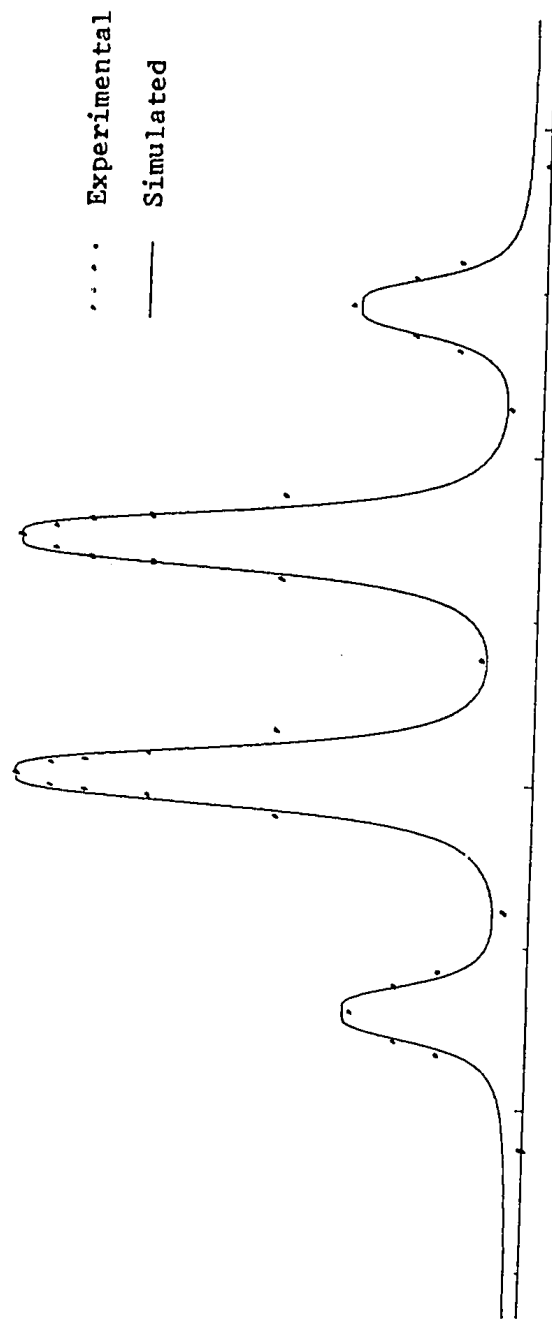


Fig. 14
Simulated Spectrum of the Methine Region
of the Diastereomeric Rotational Isomers
of 3- β -Naphthyl-5-methyl-2-thiohydantoin
with both Rotamers having Lifetimes of
0.85 sec.

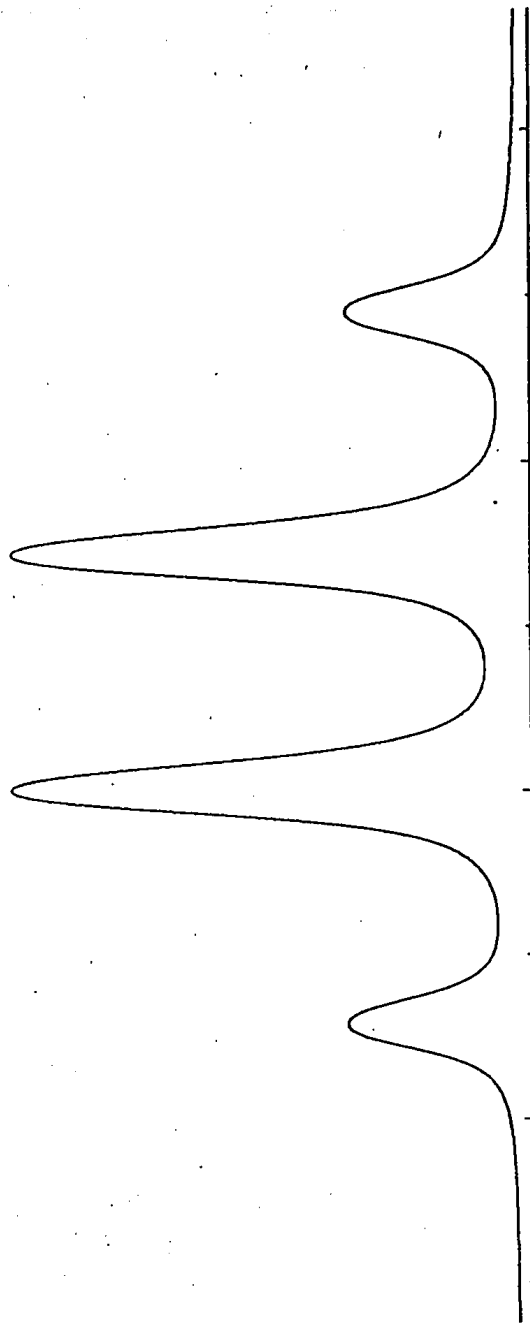


Fig. 15
Simulated Spectrum of the Methine Region
of the Diastereomeric Rotational Isomers
of 3- β -Naphthyl-5-methyl-2-thiohydantoin
with both Rotamers having Lifetimes of
0.55 sec.

Table 21

Infrared Carbonyl Stretching Frequencies
of some 3-Aryl-5-methyl-2-thiohydantoins^a

Aryl Moiety	Stretching Frequency ^b (cm ⁻¹)
α -naphthyl	1720
<u>o</u> -bromophenyl	1720
<u>o</u> -tolyl	1725
<u>o</u> -chlorophenyl	1720
<u>o</u> -methoxyphenyl	1730
<u>o</u> -fluorophenyl	1735
β -naphthyl	1750

(a) Taken through fused KBr discs. (b) Estimated to be accurate to ± 5 cm⁻¹.

X-Ray Structure Determination

Since this is not primarily a crystallographic thesis, only a brief outline of the experimental procedure will be given. The technique has been described by many authors, including Stout and Jensen ⁴¹. Some of the particular experimental techniques that are employed in this department have been published ⁴², while a more complete description will be presented in the forthcoming Ph.D. thesis of Mr. A. R. Fraser.

Recrystallisation of 3-o-bromophenyl-5-methyl-2-thiohydantoin from methanol gave only the thermodynamically less stable diastereomer, as evidenced by the n.m.r. spectrum. The crystals, however, were an approximately equal mixture of orthorhombic and monoclinic forms. Weissenberg photographs of several of the orthorhombic crystals indicated that all the orthorhombic crystals contained the same diastereomer. And it was on a crystal of the orthorhombic form that the structure determination was performed.

Unit cell determination

Monochromatic Mo K α radiation (λ 0.71069 Å) was obtained by Bragg reflection of the direct beam (takeoff angle 2.0°) from the (002) planes of a highly orientated graphite "crystal". The planes in which the diffraction occurs at the monochromator and sample crystal were perpendicular. An incident beam collimator with a 1 mm diameter pinhole

situated 140 mm from the monochromator crystal was used, together with a diffracted beam-receiving aperture 4 mm square, 230 mm from the crystal, and 20 mm in front of a scintillation counter. Accurate values of the four angles 2θ , ω , χ , and ϕ were obtained for 12 Bragg reflections from the specimen crystal, widely separated in the reciprocal lattice and at as high a value of 2θ as compatible with obtaining reasonable intensity (ca. 500 cps). The method used involved systematic missetting of 2θ , ω , and χ until the intensity of diffraction was diminished by half, under automatic control by a PDP 8/S computer using the alignment programme supplied by the Picker-Nuclear Co. This centring process was repeated in the negative range of 2θ for all 12 reflections and the values of 2θ , ω , and χ were appropriately averaged. The unit cell constants given below result from least-squares refinement of approximate values obtained from photographs, together with approximate angles for two reference reflections, against the 12 observed sets of diffraction angles.

Data collection and reduction

For data collection, the takeoff angle was increased to 3.0° , all other parameters were unchanged. A pulse height analyser, used in combination with the scintillation counter, was set to receive 100% of the Mo $K\alpha$ peak. The θ - 2θ scanning technique was used with a base width at low 2θ dependent on the mosaicity of the crystal under study and increasing with 2θ to allow for α_1 - α_2 dispersion. A 2θ scan speed of 1° min^{-1}

was used. Attenuators made of multiple nickel foils were inserted automatically in order to limit the counting rate to less than 10^4 cps. Instrumental and crystal stabilities were checked by monitoring a single reference reflection every 50 measurement cycles and also measuring the intensities of all diffractions on the three reciprocal axes for positive and negative indices before and after data collection. Signals of low intensity were observed on the axes where they should have been absent.

Data reduction was performed using a locally written programme for the CDC 6400 computer. This programme also determined an approximate scale factor and overall thermal parameter from reflection statistics. The reflection intensity, I , was computed as $(N - (B_1 + B_2)t_s/2t_b)$ and the standard deviation $\sigma(I) = (N + (B_1 + B_2)(t_s/2t_b)^2 + (0.02N)^2)^{1/2}$, where N and B are the counts accumulated during the scan time t_s and background time t_b , respectively. All data for which $I < 3\sigma(I)$ were rejected (used in neither structure solution nor refinement) and the data remaining were corrected for Lorentz and polarisation effects, $(Lp)^{-1} = \sin 2\theta_s(\cos^2 2\theta_m + 1)/\cos^2 2\theta_m + \cos^2 2\theta_s$, where $2\theta_s$ and $2\theta_m$ are the diffraction angles at the sample crystal and monochromator, respectively.

Structure solution and refinement

In least squares procedures, the function minimised was $\sum w(F_o - F_c)^2$ where $w = (\sigma(F_o))^{-2}$ and the discrepancy indices referred to are $R = (\sum(F_o - F_c)/\sum F_o)$ and

$R_w = (\sum w(F_o - F_c)^2 \div \sum w/F_o)^{1/2}$. The "goodness of fit" parameter is $(\sum w(F_o - F_c)^2 \div (n - m))^{1/2}$ where n and m are the numbers of observations and variables, respectively.

Scattering factors for neutral bromine were taken from the compilation of Ibers and in the latter (anisotropic) stages of refinement the scattering factors were corrected for anomalous dispersion. The anisotropic thermal parameters used took the form $\exp(-(h^2 b_{11} + k^2 b_{22} + l^2 b_{33} + 2hkb_{12} + 2hlb_{13} + 2klb_{23}))$

Interpretation of Weissenberg $hk0$, hkl , $hk2$, $h0l$ and $h01$, $0kl$, lkl , hll precession photographs uniquely established the space group as P_{bca} (no. 61). The unit cell parameters are: $a = 10.347(6)$, $b = 19.713(11)$, $c = 11.175(4)$ Å. The observed density was 1.63 g cm^{-3} , implying 8 molecules per unit cell. The theoretical density was calculated to be 1.66 g cm^{-3} .

An asymmetric set of 1153 diffraction intensities was collected in the range $4^\circ < 2\theta < 45^\circ$, there being no significantly intense reflections above $2\theta = 45^\circ$, while the backstop intervened below 4° . After data reduction 783 reflections remained.

Inspection of a sharpened three-dimensional Patterson synthesis gave the position of the bromine atom. A three-dimensional Fourier synthesis provided the unambiguous location of all the non-hydrogen atoms. Six cycles of isotropic followed by 4 cycles of anisotropic least squares refinement led to convergence at $R = 6.9\%$. A listing of structure factors is given in Table 22. The final atomic parameters are shown in Table 23. Selected interatomic distances are shown in Table 24. The molecular structure is shown in Fig. 16 and Fig 17. Bond angles are shown in Table 25.

K	L	FOBS	FCAL	K	L	FOBS	FCAL	K	L	FOBS	FCAL	K	L	FOBS	FCAL
0	2	2229	2359	14	7	370	328	7	1	632	658	1	0	422	562
0	4	408	426	16	1	271	242	7	2	207	193	8	3	376	348
0	6	716	706	16	2	272	255	7	4	360	323	8	3	670	634
0	8	280	303	18	0	207	208	7	6	475	463	8	5	213	211
0	10	366	340	18	1	263	201	8	9	362	406	2	7	147	146
2	1	124	130	18	3	153	106	8	1	916	1017	9	0	301	316
2	3	274	337	18	5	106	106	9	3	334	310	9	3	691	666
2	5	159	186	18	7	77	77	9	3	1005	1010	9	3	1236	1118
2	7	459	486	18	9	136	14	9	4	128	65	9	4	1591	1567
2	9	184	179	18	11	564	1023	9	5	331	616	9	5	937	821
2	11	333	283	18	13	1042	1042	9	7	272	231	9	6	428	429
2	13	800	842	18	15	743	781	9	9	317	303	9	7	130	140
2	15	326	300	18	17	254	335	9	11	445	423	9	8	541	533
2	17	1135	1460	18	19	519	546	9	13	204	182	10	2	445	423
4	1	665	681	1	1	315	325	9	15	119	138	10	3	204	182
4	3	1133	1214	1	3	1525	1446	10	17	270	293	10	4	216	236
4	5	359	385	1	5	828	799	10	19	347	391	10	6	470	485
4	7	1137	1198	1	7	454	451	10	21	233	271	10	8	521	513
4	9	442	456	1	9	506	271	10	23	225	242	10	10	128	140
4	11	209	251	1	11	595	307	10	25	1766	1808	10	12	1187	1247
4	13	410	441	1	13	203	227	10	27	1056	1005	11	2	711	707
4	15	1775	1769	1	15	1557	2057	11	29	1067	1005	11	4	127	109
6	1	162	131	2	1	822	558	11	31	316	312	11	6	331	379
6	3	4033	1029	2	3	1235	1238	11	33	468	500	11	8	252	243
6	5	868	857	2	5	126	96	11	35	174	119	11	10	303	273
6	7	1002	978	2	7	437	440	11	37	203	219	11	12	197	186
6	9	520	498	2	9	139	150	11	39	955	921	11	14	767	793
6	11	215	252	2	11	817	800	11	41	282	147	11	16	515	524
6	13	926	886	2	13	105	53	11	43	139	145	11	18	345	342
6	15	945	956	2	15	179	185	11	45	403	403	11	20	575	570
6	17	950	956	2	17	199	190	11	47	663	622	11	22	144	143
6	19	226	279	2	19	157	194	11	49	463	462	11	24	196	180
6	21	877	878	2	21	1009	970	11	51	542	564	11	26	341	255
6	23	172	1257	2	23	731	768	11	53	368	371	11	28	326	290
6	25	446	376	2	25	592	809	11	55	1014	999	11	30	271	288
6	27	208	174	2	27	136	132	11	57	315	304	11	32	307	304
6	29	143	152	2	29	551	558	11	59	1145	1127	11	34	493	504
6	31	711	684	2	31	824	838	11	61	139	110	11	36	180	187
6	33	567	508	2	33	1750	1770	11	63	279	230	11	38	514	500
6	35	603	618	2	35	692	676	11	65	522	514	11	40	614	600
6	37	367	378	2	37	250	202	11	67	147	134	11	42	223	210
6	39	1057	1024	2	39	366	361	11	69	928	928	11	44	142	154
6	41	251	252	2	41	1005	1006	11	71	316	320	11	46	149	117
6	43	347	378	2	43	276	251	11	73	91	65	11	48	201	169
6	45	654	643	2	45	1005	986	11	75	846	838	11	50	174	197
6	47	148	168	2	47	746	744	11	77	382	410	11	52	153	193
6	49	743	715	2	49	344	357	11	79	274	262	11	54	411	451
6	51	147	149	2	51	501	499	11	81	407	433	11	56	316	321
6	53	446	437	2	53	3275	3094	11	83	889	879	11	58	944	909
6	55	190	174	2	55	261	253	11	85	308	300	11	60	653	640
6	57	174	174	2	57	104	104	11	87	148	148	11	62	234	240
6	59	391	474	2	59	276	251	11	89	181	173	11	64	173	173
6	61	654	643	2	61	1005	986	11	91	181	173	11	66	1003	1003
6	63	148	168	2	63	746	744	11	93	121	113	11	68	181	181
6	65	743	715	2	65	344	357	11	95	838	811	11	70	499	497
6	67	147	149	2	67	501	499	11	97	1080	1068	11	72	1000	1068
6	69	446	437	2	69	163	148	11	99	746	742	11	74	208	177
6	71	190	174	2	71	261	253	11	101	175	151	11	76	180	177
6	73	391	474	2	73	104	104	11	103	142	142	11	78	149	149
6	75	654	643	2	75	1005	986	11	105	846	838	11	80	174	197
6	77	148	168	2	77	746	744	11	107	382	410	11	82	153	193
6	79	743	715	2	79	344	357	11	109	407	433	11	84	411	451
6	81	147	149	2	81	501	499	11	111	308	300	11	86	944	909
6	83	446	437	2	83	3275	3094	11	113	148	148	11	88	653	640
6	85	190	174	2	85	104	104	11	115	181	173	11	90	234	240
6	87	391	474	2	87	276	251	11	117	181	173	11	92	173	173
6	89	654	643	2	89	1005	986	11	119	181	173	11	94	1003	1003
6	91	148	168	2	91	746	744	11	121	121	113	11	96	181	181
6	93	743	715	2	93	344	357	11	123	838	811	11	98	499	497
6	95	147	149	2	95	501	499	11	125	1080	1068	11	100	1000	1068
6	97	446	437	2	97	163	148	11	127	746	742	11	102	208	177
6	99	190	174	2	99	261	253	11	129	175	151	11	104	180	177
6	101	391	474	2	101	104	104	11	131	142	142	11	106	149	149
6	103	654	643	2	103	1005	986	11	133	846	838	11	108	174	197
6	105	148	168	2	105	746	744	11	135	382	410	11	110	153	193
6	107	743	715	2	107	344	357	11	137	407	433	11	112	411	451
6	109	147	149	2	109	501	499	11	139	308	300	11	114	944	909
6	111	446	437	2	111	3275	3094	11	141	148	148	11	116	653	640
6	113	190	174	2	113	104	104	11	143	181	173	11	118	234	240
6	115	391	474	2	115	276	251	11	145	181	173	11	120	173	173
6	117	654	643	2	117	1005	986	11	147	181	173	11	122	1003	1003
6	119	148	168	2	119	746	744	11	149	121	113	11	124	181	181
6	121	743	715	2	121	344	357	11	151	838	811	11	126	499	497
6	123	147	149	2	123	501	499	11	153	1080	1068	11	128	1000	1068
6	125	446	437	2	125	163	148	11	155	746	742	11	130	208	177
6	127	190	174	2	127	261	253	11	157	175	151	11	132	180	177</

K	L	FOBS	FCAL	K	L	FOBS	FCAL	K	L	FOBS	FCAL	K	L	FOBS	FCAL	K	L	FOBS	FCAL	K	L	FOBS	FCAL	
13	5	141	96	7	0	191	191	2	2	360	373	11	4	192	155	13	2	145	130					
14	6	527	471	7	1	266	272	3	3	591	568	12	0	199	155									
15	1	172	142	7	2	284	272	3	5	721	702	12	2	532	505									
15	2	306	237	7	5	566	549	2	0	6	245	156	12	3	169	175								
15	3	156	203	7	7	666	643	2	0	2	284	274	12	4	137	165								
15	4	165	142	7	9	255	159	3	0	0	759	758	12	5	270	255								
16	5	215	226	7	0	303	334	3	0	0	624	623	13	0	152	259								
16	3	239	240	7	1	182	161	1	1	1	142	141	13	1	0	475	463							
16	4	149	74	7	2	173	151	3	1	3	182	182	14	1	0	145	98							
17	1	362	455	7	3	706	698	3	0	4	472	478	14	2	639	665								
				8	4	199	195	4	1	1	724	727	14	2	475	462								
				8	2	562	510	4	1	3	670	681	15	0	163	241								
				9	3	603	670	4	2	4	669	621	2	1	232	237								
				9	4	312	350	4	2	5	423	426	2	1	326	326								
				9	5	706	680	4	2	6	593	593	2	2	789	806								
				9	6	155	139	5	1	1	512	511	2	3	155	133								
				9	7	363	326	5	2	2	104	94	2	4	487	474								
				9	8	245	255	5	3	4	294	247	2	7	159	109								
				10	0	342	374	5	4	5	374	406	3	0	405	406								
				10	1	555	652	5	5	6	160	226	3	1	146	172								
				10	2	393	343	6	3	3	390	343	3	1	224	193								
				10	3	593	372	6	4	4	125	119	3	1	405	406								
				10	4	174	133	6	5	5	104	94	3	2	146	172								
				10	5	374	406	6	6	6	160	226	3	3	146	172								
				10	6	537	564	6	7	7	1233	1231	3	4	330	320								
				10	7	1233	1231	6	8	8	168	161	2	5	206	242								
				10	8	125	119	6	9	9	168	161	2	6	330	320								
				10	9	150	133	6	10	10	168	161	2	7	201	205								
				11	0	189	211	7	1	1	110	165	3	8	201	205								
				11	1	393	343	7	2	2	372	766	3	9	314	317								
				11	2	151	203	7	3	3	597	600	3	10	519	519								
				11	3	151	203	7	4	4	160	91	3	11	199	210								
				11	4	281	219	7	5	5	198	174	4	1	419	468								
				11	5	186	176	7	6	6	168	161	4	2	366	355								
				11	6	1670	1644	7	7	7	282	286	4	3	135	248								
				11	7	282	286	7	8	8	1670	1644	4	4	201	205								
				11	8	257	250	8	9	9	132	199	4	5	201	205								
				11	9	245	219	8	10	10	141	19	5	6	129	129								
				11	10	1670	1644	8	11	11	223	256	5	7	173	173								
				11	11	125	130	8	12	12	441	19	5	8	744	817								
				11	12	245	219	8	13	13	125	130	5	9	240	258								
				11	13	348	332	8	14	14	405	460	5	10	214	235								
				11	14	245	219	9	1	1	165	703	6	11	159	157								
				11	15	142	117	9	2	2	465	460	6	12	456	455								
				11	16	372	372	9	3	3	276	287	6	13	473	510								
				11	17	570	576	9	4	4	118	95	6	14	397	254								
				11	18	246	260	9	5	5	246	260	6	15	207	156								
				11	19	179	168	9	6	6	179	168	7	16	474	390								
				11	20	159	131	9	7	7	159	131	7	17	646	642								
				11	21	166	123	9	8	8	166	123	7	18	305	326								
				11	22	152	184	9	9	9	152	184	7	19	201	262								
				11	23	167	206	9	10	10	167	206	8	20	578	566								
				11	24	360	314	9	11	11	360	314	8	21	196	174								
				11	25	597	646	9	12	12	597	646	8	22	153	91								
				11	26	360	314	9	13	13	360	314	9	23	261									
				11	27	440	440	9	14	14	440	440	9	24	148	131								
				11	28	149	157	9	15	15	149	157	9	25	132	210								
				11	29	467	443	10	16	16	467	443	10	26	245	276								
				11	30	140	108	10	17	17	140	108	10	27	194	151								
				11	31	544	546	10	18	18	544	546	10	28	202	225								
				11	32	207	209	11	19	19	207	209	11	29	388	388								
				11	33	131	131	11	20	20	131	131	11	30	144	191								
				11	34	467	448	11	21	21	467	448	11	31	572	565								
				11	35	137	87	11	22	22	137	87	11	32	389	357								
				11	36	112	404	11	23	23	112	404	11	33	144	382								
				11	37	145	150	11	24	24	145	150	11	34	185	241								
				11	38	298	341	11	25	25	298	341	11	35	185	241								

Table 22 . Continued

Table 23

Final Positions and Thermal Parameters with ESD'S a, b

Atom	x	y	z
N(1)	.2934(11)	.0064(6)	.1651(10)
C(2)	.3616(14)	.0574(7)	.1226(13)
N(3)	.3079(12)	.0789(6)	.0138(11)
C(4)	.2027(16)	.0394(8)	-.0132(14)
C(5)	.1844(14)	-.0121(8)	.0900(12)
S(6)	.4954(4)	.0931(2)	.1771(4)
C(7)	.1929(13)	-.0847(7)	.0387(14)
O(8)	.1351(9)	.0429(5)	-.1036(9)
C(9)	.3585(17)	.1285(7)	-.0718(13)
C(10)	.3006(13)	.1921(11)	-.0709(13)
C(11)	.3340(17)	.2444(8)	-.1519(16)
C(12)	.4338(18)	.2282(9)	-.2279(15)
C(13)	.4939(15)	.1588(11)	-.2232(16)
C(14)	.4590(12)	.1056(7)	-.1483(11)
Br(15)	.1625(2)	.21447(9)	.0375(2)

continued

Table 23 continued

Atom	B(1,1)	B(2,2)	B(3,3)	B(1,2)	B(1,3)	B(2,3)
N(1)	724(184)	208(43)	683(134)	-53(71)	291(130)	128(68)
C(2)	785(217)	214(54)	365(161)	322(99)	-223(159)	-112(82)
N(3)	844(175)	171(45)	732(157)	-63(76)	-125(134)	26(68)
C(4)	803(249)	212(52)	567(190)	100(103)	-11(154)	-145(91)
C(5)	660(194)	305(62)	442(147)	-124(92)	-147(159)	140(84)
S(6)	1072(57)	309(16)	884(47)	-97(27)	-414(49)	75(25)
C(7)	1020(215)	145(51)	1216(180)	-91(84)	23(181)	-12(89)
O(8)	667(133)	368(41)	584(103)	39(61)	-80(103)	-11(60)
C(9)	1193(249)	91(50)	783(212)	-127(99)	-902(207)	-40(89)
C(10)	445(195)	518(81)	441(176)	-113(103)	-103(138)	-182(101)
C(11)	1060(230)	377(62)	503(158)	-322(124)	-232(192)	40(94)
C(12)	1110(250)	470(90)	681(207)	-344(118)	-363(190)	76(108)
C(13)	681(214)	527(78)	1028(237)	29(129)	-478(185)	-486(125)
C(14)	74(148)	235(52)	-92(122)	-78(78)	257(112)	30(67)
Br(15)	1414(24)	454(7)	1250(21)	249(13)	117(24)	-214(12)

(a) The anisotropic thermal parameters have been multiplied by 10^5 . (b) Esd's are shown in parentheses. They are right justified to the least significant digit of the preceding number.

Table 24

Selected Interatomic Distances, (Å)^o^a

N1	C2	1.32(2)
N1	C5	1.45(2)
C2	N3	1.40(2)
C2	S6	1.67(1)
N3	C4	1.37(2)
N3	C9	1.46(2)
C4	C5	1.55(2)
C4	O8	1.23(2)
C5	C7	1.54(2)
C8	Br15	3.74(1)
C9	C10	1.39(2)
C9	C14	1.42(2)
C10	C11	1.41(2)
C10	Br15	1.92(1)
C11	C12	1.37(2)
C12	C13	1.50(3)
C13	C14	1.39(2)

(a) The estimated standard deviations are shown in brackets.

Table 25

Bond Angles (Deg.) ^a			
C2	N1	C5	114(1)
N1	C2	N3	109(1)
N1	C2	S6	129(1)
N3	C2	S6	121(1)
C2	N3	C4	109(1)
C4	N3	C9	121(1)
N3	C4	C5	108(1)
N3	C4	O8	127(1)
C5	C4	O8	125(1)
N1	C5	C4	100(1)
N1	C5	C7	114(1)
C4	C5	C7	109(1)
N3	C9	C10	116(1)
N3	C9	C14	116(1)
C10	C9	C14	127(1)
C9	C10	C11	123(1)
C9	C10	Br15	122(1)
C11	C10	Br15	115(1)
C10	C11	C12	114(1)
C11	C12	C13	120(1)
C12	C13	C14	127(1)
C9	C14	C13	108(1)

(a) The estimated standard deviations are shown in brackets.

DISCUSSION

Equilibrium constants and ground state conformations.

X-Ray molecular structure determination.

The origin of the non-unity equilibrium constants.

The dihedral angle and the equilibrium constants.

Comparison of the rotational free energies of activation of thiohydantoins and hydantoins.

Relative solubilities of the diastereomeric isomers.

The "rotational entropy of activation".

The "rotational enthalpy of activation".

The effective sizes of methyl and chlorine.

Other compounds in the thiohydantoin series.

Comparison of the α -fluorophenyl and β -naphthyl compounds.

Infrared spectra.

Notes on the ring closure step in the synthesis.

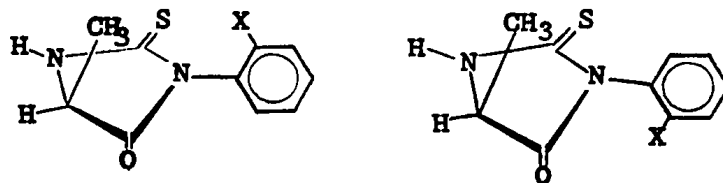
Summary.

Suggestions for future work.

Equilibrium constants and ground state conformations

The equilibrium constant between the rotational diastereomers is not unity for any of the compounds studied (Table 6 and Table 8). This means that the lifetime of one rotamer is greater than that of the other. One or more of three possible circumstances would cause this phenomenon: (1) the thiohydantoin ring being puckered (2) an unsymmetrical solvent shell around the carbonyl group (3) repulsive interaction between the C₅-methyl and the ortho substituent on the aryl ring.

(1) If the thiohydantoin ring is puckered, the methyl group may be pulled in towards the centre of the thiohydantoin ring. In this event, there may be a repulsive interaction between the methyl group and the ortho substituent on the



aryl ring in one of the rotational diastereomers. In the diagrams above, the carbon atom of the carbonyl group has been drawn with its position below the plane joining C₅, N₁, C₂, and N₃. It could be argued that puckering of the heterocyclic ring would lead to the methyl group being pushed away from the heterocyclic ring. In any event, it is easy to see that puckering of the heterocyclic ring may lead to

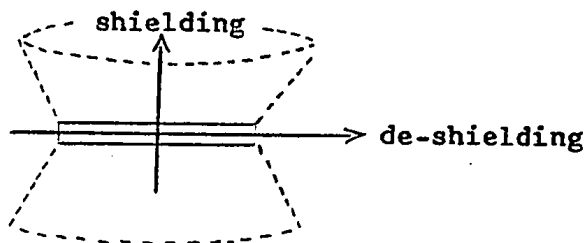
repulsive interactions in the two rotamers that are quite different.

(2) The steric bulk of the C₅-methyl group may be expected to force an unsymmetrical solvent shell around the carbonyl group. In this event, the ground state energies of the two rotamers would be different as a result of different steric interactions. This would lead to a non-unity equilibrium constant. Unfortunately, it is not easy to test this hypothesis. If it were true, the equilibrium constants should show solvent dependence. The thiohydantoins, however, have limited solubility and only a small range of solvents, all highly polar, could be used. Furthermore, the equilibrium constants can only be measured to within about 10%, so small effects would not be noticed. It may be possible to overcome the solubility problem through the use of pulsed Fourier transform spectroscopy, however. This technique⁴³ gives increased sensitivity. The spectrum may be scanned many times while the information is stored in "memory" and the resulting spectrum is a "sum" of all the individual scans. Thus, "noise" is averaged out and low intensity signals may be detected.

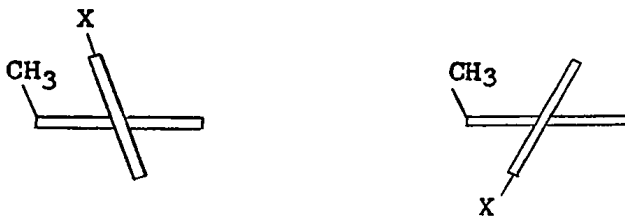
(3) A repulsive interaction between the C₅-methyl group and the bulky ortho substituent on the aryl ring seems to be unlikely simply because the two moieties are so far away from each other, as shown by the inspection of molecular models.

Any meaningful discussion on the origin of the non-unity equilibrium constants must revolve around the stereochemistry of the molecules. Thus, the n.m.r. chemical shifts were examined in an attempt to elucidate the stereochemical configurations of the rotational isomers. The datum is that the chemical shift of the methyl group of the thermodynamically less stable diastereomeric rotational isomer is always upfield from that of the other isomer (see Experimental section).

The zone of maximum shielding of a benzene ring is normal to the plane of the ring, while the zone of maximum de-shielding is in the plane of the ring ⁴⁴.



The diagrams following represent the two rotational diastereomers in which the bulky ortho substituent lies cisoid and transoid to the methyl group, respectively. These two cases were examined since they represent the two diastereomeric rotational isomers, as shown by the inspection of molecular models.



Unfortunately, when the models are viewed in three dimensions,

it is clear that the assignment of chemical shifts rests on the knowledge of the dihedral angle in each isomer. Thus, n.m.r. chemical shifts are not helpful in elucidating the stereochemistry of these molecules.

The variation of the equilibrium constant with the aryl moiety is of interest. The equilibrium constant reflects the differences in ground state energies between the rotational isomers. In the thiohydantoins for which the equilibrium constant was measured, this difference is largest for the o-bromophenyl compound. Thus, steric factors are seen to be of importance. That electronic factors are also important is seen after a comparison of the o-tolyl and o-chlorophenyl compounds. The equilibrium constant for the o-chlorophenyl compound (1.7 ± 0.1) is significantly larger than that of the o-tolyl analogue (1.4 ± 0.1) even though a chlorine atom is smaller than a methyl group. This effect is attributed to an electronic interaction between the chlorine atom and the carbonyl group. The phenomenon (reversal of the effective sizes of methyl and chlorine) will be discussed more fully later in the thesis in terms of the effect on the rotational activation energies. Also included will be a discussion of Granata's ⁸ failure to observe through bond electronic effects. In a similar manner, the equilibrium constant for the o-methoxyphenyl compound is quite large (1.35 ± 0.08) although the size of the moiety is rather small.

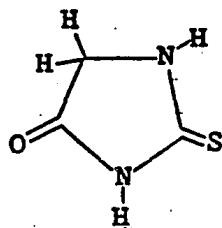
The difference in ground state energies between the diastereomeric rotational isomers may be calculated from the

following equation ⁴⁵.

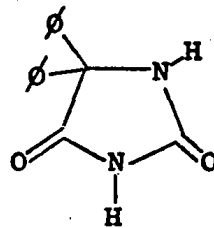
$$\Delta G = -RT \log_e K$$

The calculation has been performed for all the thiohydantoins for which we were able to obtain equilibrium constants. These results are recorded in Table 26.

The key point in this section is that we had observed large values of the equilibrium constants between diastereomeric rotational isomers but their origin was not understood. Clearly, the key to the problem lies in the relationship of the ortho substituent on the aryl ring with the C₅-methyl group. The question arises as to how one moiety "senses" the presence of the other. Of the reasons suggested at the beginning of this section, the most attractive seems to be the one involving a puckered heterocyclic ring. The main objection to this proposal stems from X-ray crystal structure determinations of 2-thiohydantoin ⁴⁶ and 5,5-diphenyl hydantoin ⁴⁷. In both



2-thiohydantoin



5,5-diphenyl hydantoin

structures, the heterocyclic rings were found to be planar.

It is evident from the forgoing discussion that the nature of the interactions leading to the large equilibrium constants was unclear. Furthermore, the stereochemistry of

Table 26

Equilibrium Constants and Corresponding Ground State Free Energy Differences of the Rotational Isomers

Aryl Moiety	K^a	ΔG (cal mole ⁻¹) ^{a,b}
α -naphthyl	1.15 ± 0.06	84 ± 30
o -bromophenyl	1.9 ± 0.1	384 ± 30
o -tolyl	1.4 ± 0.1	201 ± 41
o -chlorophenyl	1.7 ± 0.1	317 ± 34
o -methoxyphenyl	1.35 ± 0.08	179 ± 35

(a) Errors stated at 90% confidence limits.
 (b) Calculated at 302°K.

these molecules was not known. For these reasons, an X-ray crystal structure was determined employing the thermodynamically less stable diastereomer of 3-o-bromophenyl-5-methyl-2-thiohydantoin. It is recognised that there may be major differences between the crystal structure and the structure of the compound in solution. The crystal structure, however, can answer two important questions: Is the thiohydantoin ring puckered and does the ortho substituent lie cisoid or transoid to the C₅-methyl group in the less favoured diastereomer?

X-ray molecular structure determination

The work described in this thesis is not presented in the chronological order in which it was performed. Thus, a discussion of the results of the X-ray crystal structure determination is introduced at this point. This avoids the lengthy presentation of some theories that have been discarded since the structure was determined. The need for a structure determination has been demonstrated in the discussion of the equilibrium constants. The crystal structure will be referred to again in other sections.

The key results from the X-ray structure determination of the thermodynamically less stable diastereomer of 3-o-bromophenyl-5-methyl-2-thiohydantoin are:

1. The heterocyclic ring was found to be planar.
2. The bromine atom lies transoid to the methyl group.

Views of the molecule are given in Fig. 16 and Fig. 17. The bond lengths are recorded in Table 24 and the bond angles are recorded in Table 25.

Reliability of the solution

Although the structure was solved to a relatively low R factor (6.9%), the bond lengths and bond angles of the aryl ring are not those commonly observed (Tables 24 and 25). The geometry of the heterocyclic ring, however, is in good agreement with the results obtained on the crystal structure of 2-thiohydantoin⁴⁶. Thus, it is concluded that while the gross molecular structure is acceptable, some of the finer details are open to question.

The lack of good refinement on the aryl ring is most easily ascribed to a "chemical" rather than a "crystallographic" problem. After data collection, the previously white thiohydantoin crystal was observed to be pink. This was probably caused by the fracture, in some molecules, of the bromine-aryl bond as a consequence of the high energy incident radiation.

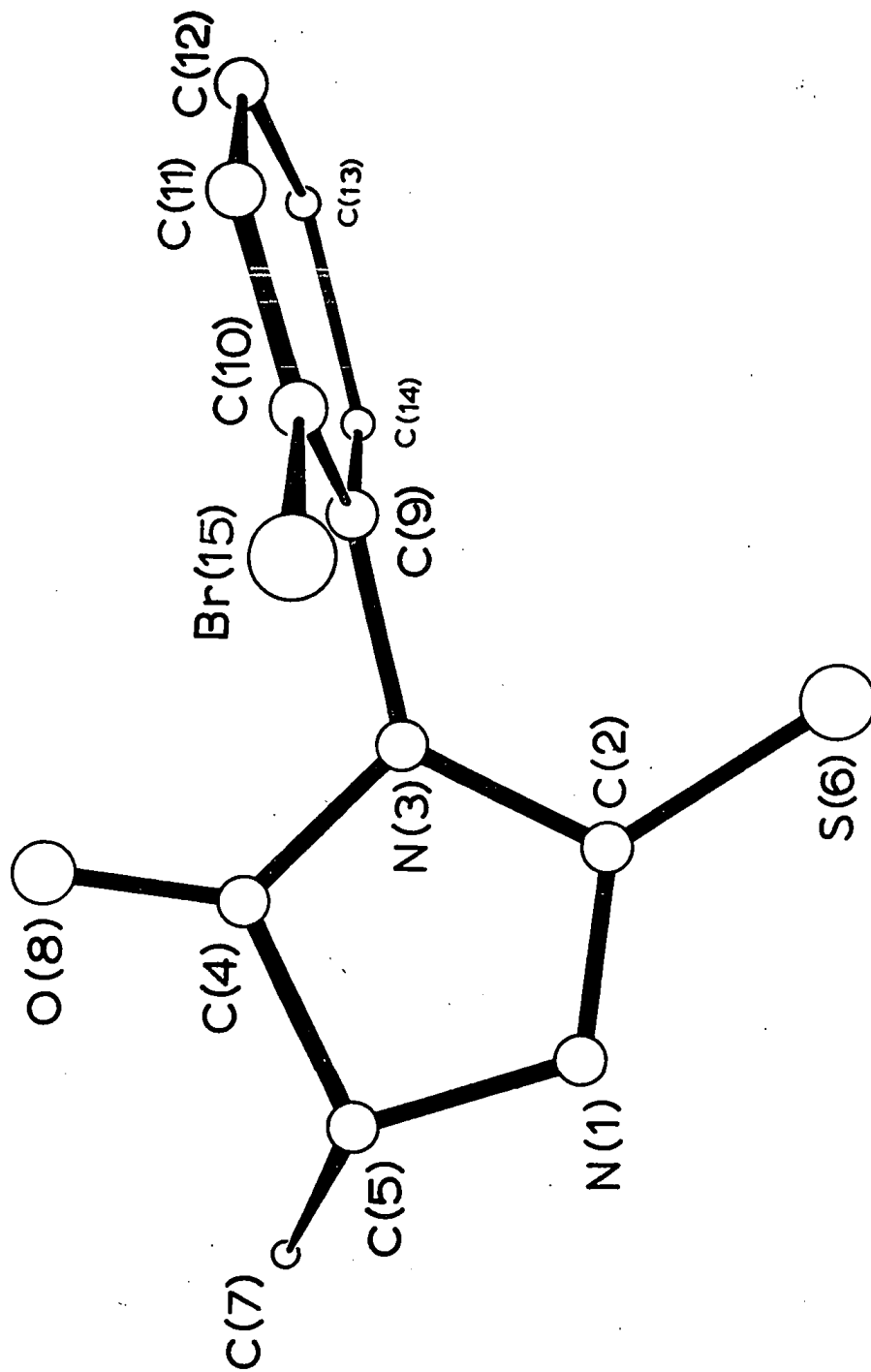


Fig. 16. The Structure of the Thermodynamically Less Stable Diastereomer of 3-O-bromophenyl-5-methyl-2-thiohydantoin

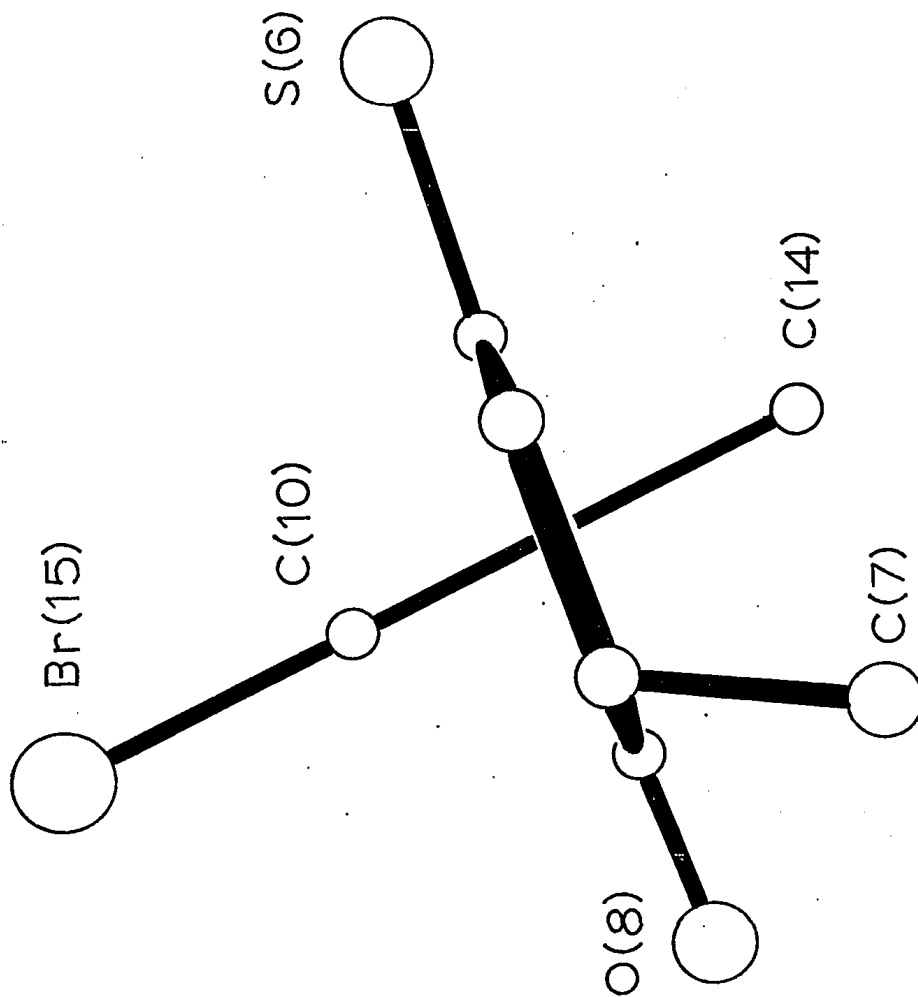
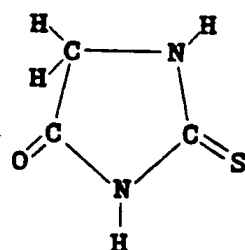


Fig. 17. A Sketch of the Thermodynamically Less Stable Diastereomer of 3-o-Bromophenyl-5-methyl-2-thiohydantoin Viewed Along the Aryl C-N Bond From a Position Midway Between N(1) and C(5).

The question of inversion at N(3)

The data obtained on this crystal structure are not sufficiently good to allow us to state that there are no nitrogen invertamers in the compound. The data obtained on 2-thiohydantoin⁴⁶ may be considered, however. The authors were

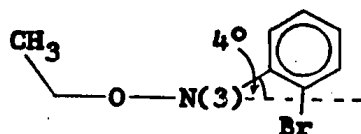


2-thiohydantoin

able to locate all the hydrogen atoms but this would not be the case if inversion were taking place at either or both nitrogen atoms. In addition, the angles around both nitrogen atoms add up to 360° . Thus, the bonds around nitrogen are co-planar and there are no invertamers. This is to be expected in amide and thioamide type nitrogens where there is considerable double bond character in the carbon-nitrogen bonds.

The "angle at N(3)"

The angle referred to is the minimum acute angle between the plane of the thiohydantoin ring and a line from the centroid of the benzene ring through N(3). The angle was found to be 4° , with the aryl ring displaced to the "methyl side" of the heterocyclic ring. The diagram following exaggerates the situation for the sake of clarity.



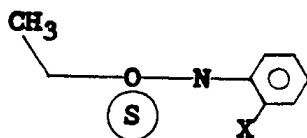
This geometry is probably a result of steric interaction between the bromine atom and the carbonyl group. Thus, as the bromine atom is forced away from the carbonyl group, the aryl ring is forced "up" (as drawn above). If this geometry is not primarily a result of crystal packing forces, it is to be assumed that a similar arrangement exists when the compound is in solution.

Delocalisation

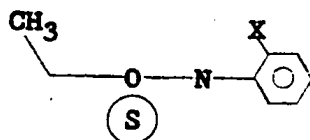
There is no direct crystallographic evidence for, or against, π delocalisation over the system S(6)-C(2)-N(3)-C(4)-O(8). The bond lengths of the carbonyl and thiocarbonyl groups (Table 24) are similar to those observed for simple ketones and thioketones⁴⁸. Bond length data, however, are not very sensitive to limited delocalisation. For example, the average C=C bond length is 1.34 Å, whereas the C=C bond length in the C=C-C=C moiety has also been measured as 1.34 Å⁴⁸.

The origin of the non-unity equilibrium constants

From points 1 and 2 in the previous section, it is deduced that the non-unity equilibrium constants are caused by unsymmetrical solvent shells around the carbonyl groups. Thus, in solution, if the methyl group is "up", the solvent shell around the carbonyl group prefers to be mainly "down". There is a choice in the position of the bromine, however, as it may be "up" or "down". If it is "up", steric interactions



less stable diastereomer



more stable diastereomer

between the ortho substituent on the aryl ring and the solvent are minimised. This is the more stable diastereomer and the ortho substituent on the aryl ring and the methyl group are cisoid. Conversely, in the less stable isomer, the ortho substituent and the methyl group are transoid. Clearly, the hypothesis would not be true if there were an important

repulsive interaction between the bromine and the methyl group. In addition, the heterocyclic ring is planar. Thus, we are left with only one of the three possibilities that have been suggested to explain the non-unity equilibrium constants.

The dihedral angle and the equilibrium constants

As expected, because of severe repulsive interactions, the crystal structure of the *o*-bromophenyl compound shows that there is a large angle, 82° , between the heterocyclic ring and the aryl ring, with the bromine lying on the oxygen side of the heterocyclic ring. The angle of 82° was measured for the solid state and probably reflects, in part, the nature of the molecular packing in the crystal. For this reason, it is most unlikely that the value represents the average position of the less stable diastereomer in solution. It is probable, however, that there will be only a small change in solution.

That the bromine atom lies on the oxygen side of the ring is most reasonably explained by a consideration of the sizes of oxygen and sulphur. Oxygen is smaller than sulphur (the van der Waals radii are 1.40 \AA and 1.85 \AA , respectively)²⁰ and in order to minimise repulsive interactions the bromine prefers to be on the oxygen side of the heterocyclic ring.

There are two opposing forces that govern the values of the dihedral angles in these compounds. The aryl and heterocyclic rings would prefer to be co-planar in order to increase π delocalisation, while steric and repulsive electronic interactions between the ortho substituents on the aryl ring and the carbonyl and thiocarbonyl groups tend to twist the two rings far apart. It is presumed that the dihedral angle decreases as the sum of the steric and electronic repulsions between the ortho aryl substituents and the carbonyl and thiocarbonyl groups decreases. That is, it is presumed that the dihedral angle in any given diastereomer decreases as the equilibrium constant between the diastereomer and its rotamer decreases.

Williams ⁷, who studied the ¹³C spectra of a number of 3-aryl-5,5-dimethyl-hydantoins, found some evidence that the dihedral angle varies with the effective size of the substituent on the aryl ring. If the dihedral angle gets smaller as the effective size of the substituent gets smaller, it is expected that there will be more conjugation between the aryl ring and the C₂ and C₄ carbonyls. The carbonyl groups, however, are already involved in a conjugated π -electron system and further conjugation with the aryl ring results in sharing of the two p-electrons of N(3) with the aryl ring. Thus, it is expected that there will be less electron density around the carbonyl atoms, and in the ¹³C n.m.r. spectrum there should be a downfield shift with a decreasing effective size of the ortho substituent on the aryl ring. This is precisely what Williams observed.

Comparison of the rotational free energies of activation
of thiohydantoins and hydantoins

Any comparison of the relative rotational stabilities of thiohydantoins and hydantoins must revolve around the effective sizes of the thiocarbonyl and carbonyl groups.

The X-ray crystal structure of the o-bromophenyl compound shows that the thiocarbonyl bond length is considerably larger than the carbonyl bond length. In addition, sulphur is larger than oxygen as previously discussed. In consequence, there occurs a stronger repulsive interaction between the sulphur atom and the groups in the ortho positions of the aryl ring when the thiohydantoin molecule is in its rotational transition state than is the case in the hydantoin molecule. It is presumed that the bulky ortho substituent passes over the carbonyl group in the transition state, while the ortho hydrogen atom passes over the thiocarbonyl group. (The figure on the following page depicts the two possible transition states and includes the van der Waals radii of the atoms most important in the torsional transition state). Additional evidence for this hypothesis comes from the dihedral angle found in the crystal structure (discussed previously).

From the above discussion, it appears that the differences in rotational stabilities of the thiohydantoins and hydantoins principally result from differences in repulsive interactions between the ortho hydrogen atom and the sulphur atom, and the ortho hydrogen atom and the oxygen atom. Thus, the thiohydantoins show a larger degree of rotational stability than the hydantoins. This is reflected

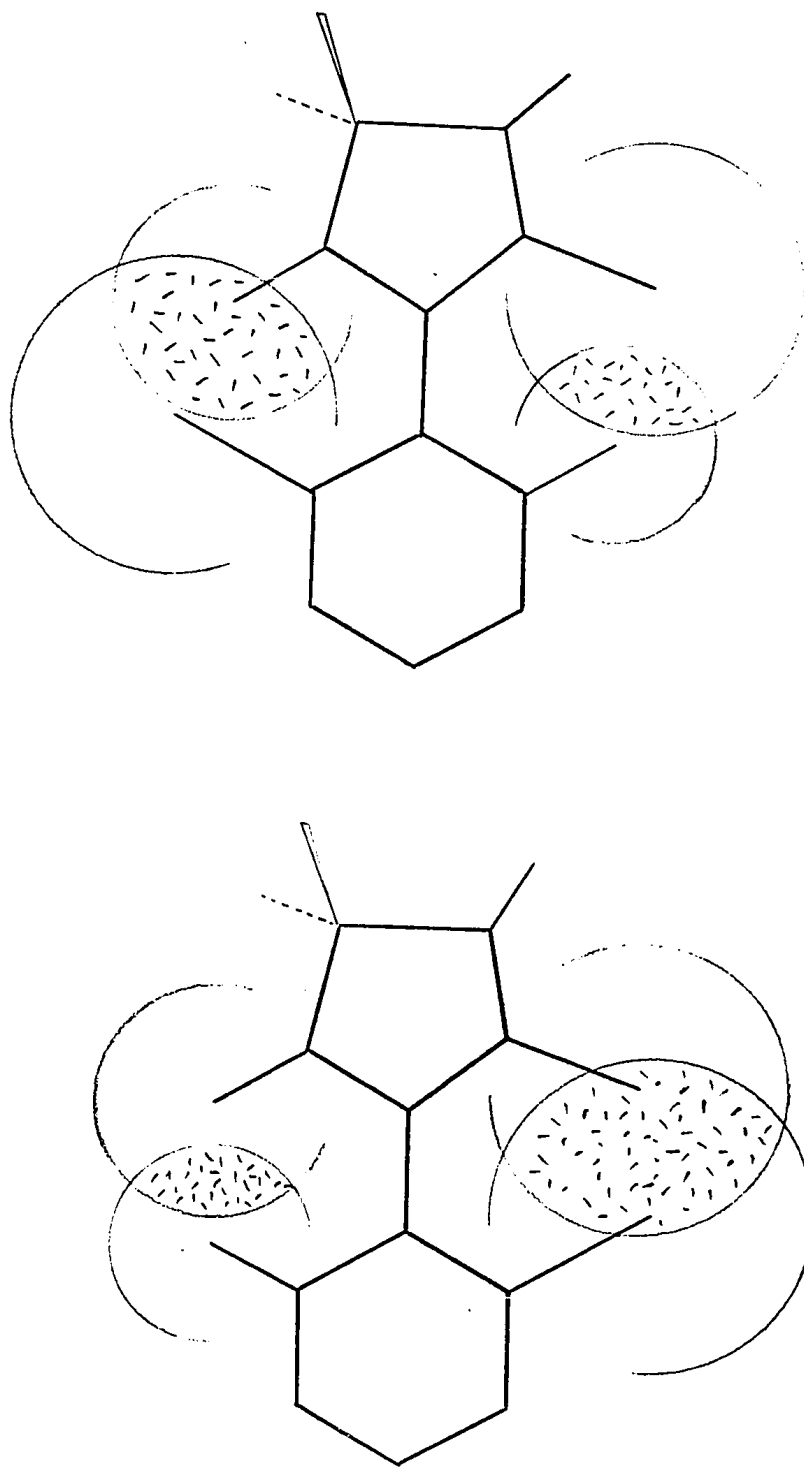


Fig. 18. The Two Possible Rotational Transition States
For 3-o-Bromophenyl-5-methyl-2-thiohydantoin.
(Bond bending has been ignored)

in the ΔG^\ddagger values. For example, the free energy of activation of 3-o-chlorophenyl-5-methyl-2-thiohydantoin (XII) is some 6.5 kcal mole⁻¹ higher than that measured by Fehlner⁴ for the corresponding hydantoin.

Electronic factors may play an important role, however. Thus, the ability of sulphur to accommodate electrons and increase the bond length of the thiocarbonyl group may be accompanied by a relative decrease of the electron density on N(3). This would have the effect of decreasing the aryl C-N bond length in the rotational transition state and increasing the rotational barrier.

Relative solubilities of the diastereomeric isomers

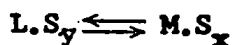
It was observed (Experimental section) that recrystallisation of a mixture of diastereomers invariably yielded only the thermodynamically less stable diastereomer. That is, in the solvents employed (ethanol and methanol) the less stable isomer is the less soluble isomer.

It is presumed that the solubilities are a function of the relative abilities of the carbonyl groups in the two isomers to be solvated. Thus, the less stable isomer, with the methyl group and the ortho substituent on the aryl group transoid to each other, has the carbonyl group sterically protected from both sides of the thiohydantoin ring. This molecular geometry decreases the solvation of the isomer relative to that of the other isomer, where there are no bulky groups on one side of the thiohydantoin ring.

The "rotational entropy of activation"

The "rotational entropy of activation" of the o-bromophenyl compound was found to be very negative (-25.5 + 5.2 e.u.). The value is similar to that found by Fehlner⁴ for the α -naphthyl analogue and is similar to the values obtained in analogous compounds in the hydantoin series. These very negative values are discussed in terms of the role of the solvent.

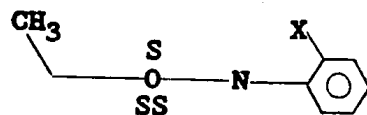
Consider two diastereomeric rotational isomers L and M in solution. L is the less stable isomer and M is the more stable isomer. In solution each species is solvated, presumably by different numbers of solvent molecules. Thus, the equilibration may be represented as



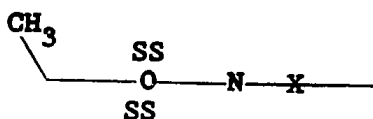
where S is the solvent and y and x are the numbers of solvent molecules. As discussed in the section on the relative solubilities of the diastereomers, it is assumed that y is smaller than x. In the rotational transition state it is assumed that the position of the ortho substituent on the aryl ring allows an increase in solvation around the carbonyl group. Thus, including the transition state, the equilibrium may be represented as



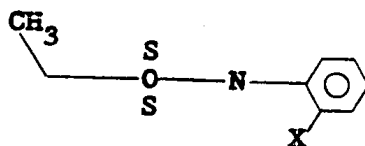
where T represents the transition state and z is greater than y and x. The diagram following depicts the situation.



more stable diastereomer



rotational transition state

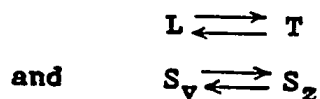


less stable diastereomer

S = solvent

It is not intended that the number of "S's" be taken to quantitatively represent the number of solvent molecules involved.

If the hypothesis is true, the activation parameters reflect two processes, as follows



Thus, the term "rotational entropy of activation" is something of a misnomer.

The data, i.e., the large negative "rotational entropies of activation", are consistent with this hypothesis. In the proposed mechanism, one or more solvent molecules are added to the solute-solvent complex in the transition state, and the thiohydantoin molecule becomes more ordered.

There is, of course, a contribution to the negative "entropy of activation" from the bare molecule because of torsional strain. It is not possible to estimate the value in these systems but it is probably in the region of about -5 e.u. ¹¹.

At the present time, we do not have sufficient data to compare the entropies of activation for pairs of compounds symmetrically and unsymmetrically substituted at the C₅ position in either the hydantoin or thiohydantoin series.

The "rotational enthalpy of activation"

The "rotational enthalpy of activation" is usually taken as the best indication of the steric opposition to rotation. The value obtained for the *o*-bromophenyl compound is 17.6 ± 1.7 kcal mole⁻¹. The quantitative interpretation of this datum is not simple, however.

There are two important contributions to the value determined. First, there is the enthalpy of activation of the bare molecule, and secondly, there is the contribution from the (proposed) change in solvation as the molecule goes from the ground state to the transition state.

The reaction, *i.e.*, rotation to the transition state is clearly endothermic overall. However, the proposed change in solvation should make an exothermic contribution, since the transition state is stabilised by a greater solvation. Thus, there are two opposing contributions to the value of the "rotational enthalpy of activation".

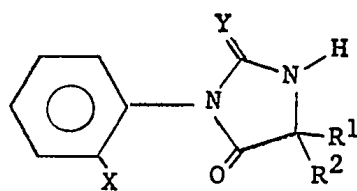
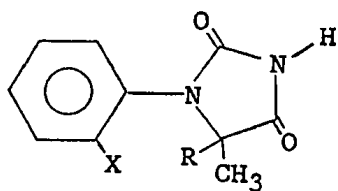
It is seen then, that the role of the solvent is important in determining the rotational stability of the molecule. The effect of the solvent on ΔH^\ddagger is such that it decreases the rotational stability, whereas the effect of the solvent on ΔS^\ddagger increases the rotational stability.

The effective sizes of methyl and chlorine ³

The results presented in this thesis on this study follow the work of Fehlner ⁴ and were coincident with the studies of Icli ⁹ and Granata ⁸. The work is now presented as a whole.

It has commonly been observed ^{49,50} that a methyl group exerts a greater steric effect than that of a chlorine atom, for example in restricting internal rotation in hindered biphenyls ⁴⁹. This order is consistent with the relative sizes of these groups as determined by X-ray crystallographic measurements of van der Waals radii ²⁰.

Icli ⁹, in a study of restricted rotation about the aryl C-N bond of 1-aryl hydantoins has found that the same order of relative sizes applies. The free energies of activation for rotation about the C-N bond joining the aryl and heterocyclic moieties are 0.5-1.5 kcal mole⁻¹ higher for the ortho methyl compounds than for the ortho chloro compounds (Table 27).



	X	R
(Ca)	CH ₃	H
(Cb)	Cl	H
(Cc)	CH ₃	CH ₃
(Cd)	Cl	CH ₃

	X	R ¹	R ²	Y
(Ma)	CH ₃	CH ₃	CH ₃	O
(Mb)	Cl	CH ₃	CH ₃	O
(Mc)	CH ₃	H	C ₆ H ₅	O
(Md)	Cl	H	C ₆ H ₅	O
(Me)	CH ₃	H	CH ₃	O
(Mf)	Cl	H	CH ₃	O
(XI)	CH ₃	H	CH ₃	S
(XII)	Cl	H	CH ₃	S

Table 27

Free Energies of Activation for 1-Aryl Hydantoins 9					
	Solvent	Temperature ^a	ΔG^\ddagger b,c	ΔG^\ddagger b,d	
Ca	Acetone-d ₆ :DMSO-d ₆ (4:1)	-32 ^e	12.6 ± 0.1		
Cb	Acetone-d ₆ :DMSO-d ₆ (4:1)	-63 ^e	11.1 ± 0.1	1.5	
Cc	DMSO-d ₆	60	18.1 ± 0.1		
Cd	DMSO-d ₆	60	17.4 ± 0.1	0.7	
Cc	Pyridine	60	17.6 ± 0.1		
Cd	Pyridine	60	17.1 ± 0.1	0.5	

(a) Degrees C. (b) kcal mole⁻¹. (c) 90% confidence limits.
 (d) $\Delta G_{CH_3}^\ddagger - \Delta G_{Cl}^\ddagger$. (e) Coalescence temperatures.

In contrast, the free energies of activation for rotation of the 3-aryl hydantoins and the 3-aryl 2-thiohydantoins (Table 28) indicate a reversal in the relative steric effects of the ortho methyl and ortho chloro substituents on the aryl ring. The free energy barriers to rotation about the aryl C-N bonds are 0.9 - 2.1 kcal mole⁻¹ higher for the chloro than for the methyl compounds. This reversal in the relative influences of the ortho chloro and the ortho methyl substituents is attributed to the nature of the interactions within the molecules in the transition states for internal rotation.

The rate constants for the internal rotation process in the 1-aryl and the 3-aryl hydantoins were obtained by complete n.m.r. line shape analysis of the temperature dependent 5-methyl or ortho tolyl methyl signals over a range of temperatures, using an iterative fitting procedure. The linear least squares method was used to fit the Arrhenius equation to the data. Except in the cases of Ca and Cb, the free energies of activation are reported (Tables 27 and 28) for a temperature common to, or falling between, the ranges used for the pair of compounds being compared. For compounds Ca and Cb, which could not be studied over an extended temperature range, the rate constants were obtained in the coalescence point region and are reported for the coalescence temperature. Because of the high rotational barriers, the spectra of the thiohydantoins

Table 28

Free Energies of Activation for 3-Aryl hydantoins
and 3-aryl 2-thiohydantoins

	Solvent	Temperature ^a	$\Delta G^\ddagger_{b,c}$	$\Delta G^\ddagger_{b,d}$
Ma	Pyridine	60	18.3 \pm 0.1	
Mb	Pyridine	60	19.8 \pm 0.2	-1.5
Mc	DMSO-d ₆	70	18.7 \pm 0.2	
Md	DMSO-d ₆	70	20.8 \pm 0.2	-2.1
Me	DMSO-d ₆	70	19.0 \pm 0.1	
Mf	Pyridine	70	20.0 \pm 0.1	-1.0
XI	Pyridine	57.5	24.8 \pm 0.1	
XII	Pyridine	58.5	25.7 \pm 0.1	-0.9

(a) Degrees C. (b) kcal mole⁻¹. (c) 90% confidence limits.
(d) $\Delta G^\ddagger_{CH_3} - \Delta G^\ddagger_{Cl}$

do not show collapse at the boiling point of the solvent. Rate constants (at a single temperature) were obtained for XI and XII by following the equilibration of the thermodynamically less stable diastereomer by repetitively recording the n.m.r. spectrum and measuring the areas under the peaks. The values of ΔG^\ddagger quoted for Ca, Cb, Mc, Md, Me, Mf, XI, and XII correspond to conversion of the less to the more thermodynamically stable rotamer.

In their internal rotational ground states, these molecules are expected to adopt conformations with large dihedral angles between the aryl and heterocyclic ring systems because of steric interaction between the ortho substituents on the aryl group and the hetero ring. The existence of significant chemical shifts between diastereotopic groups and between protons, located on the hetero ring, of diastereomeric rotational isomers is consistent with anisotropic shielding by the unsymmetrically substituted aryl groups which are constrained to adopt conformations not co-planar with the hetero ring. Since the molecules should have sufficient flexibility in the ground states to minimise steric repulsions between the two ring systems it is probable that most of the influence on the values of ΔG^\ddagger in these series of compounds of importance in this study arises from interactions in the transition states.

Ground state effects of substituents are most easily recognised when the rotational isomers are diastereomeric, so that the equilibrium constant is not unity.

Comparison of the equilibrium ratios of rotamers of the methyl and chloro compounds reveals differences consistent with the reversal of the effective sizes of these groups in the 1-aryl and 3-aryl series. Difficulties in obtaining satisfactory low temperature spectra of Ca and Cb precluded accurate measurement of the equilibrium constants, but it is clear that the deviation from unity in the equilibrium ratio is greater for the methyl compound, Ca, than for the chloro compound, Cb. This is expected if the methyl group is effectively larger than chlorine in the rotational ground states. In contrast, the equilibrium constants at ambient temperature of the 3-aryl 2-thiohydantoins, XI and XII are 1.4 ± 0.1 and 1.7 ± 0.1 (90% confidence limits), respectively, the chloro substituent exerting a greater influence than the methyl group in the ground state. Ground state free energy differences between rotamers are, in all cases, smaller than the differences in free energies of activation reported in Tables 27 and 28.

In the 1-aryl hydantoins there are two possible transition states for rotation, the ortho aryl substituent passing either the substituents in the 5-position or the 2-carbonyl group. The significant differences between the rotational barriers of 1-aryl hydantoins and 3-aryl hydantoins (in which the ortho aryl substituent must pass a carbonyl group) (Tables 27 and 28), the large increase in ΔG^\ddagger on the introduction of a second methyl group in the 5-position (Table 27), and the failure in this laboratory to observe

restricted rotation at temperatures as low as -78°C in 1-aryl hydantoins lacking a substituent in the 5-position, are taken as evidence that the more bulky ortho substituent must pass the 5-position in the preferred transition state for rotation in the 1-aryl series. This conclusion is supported by an examination of Dreiding models. In this series, the interaction between the substituents in the 5-position of the heterocyclic moiety and the ortho chloro or ortho methyl group should be of a normal steric character.

In the 3-aryl hydantoin or 3-aryl 2-thiohydantoin series, the ortho chloro or ortho methyl substituent must pass a carbonyl group oxygen atom in the transition state for rotation. The preferred pathway in the 2-thiohydantoins must be the one in which the bulky ortho substituent passes the carbonyl rather than the more bulky thiocarbonyl group. The two possible transition states in the 3-aryl hydantoins appear to be very similar in energy, the ortho aryl substituent passing either the 2- or the 4-carbonyl oxygen atom. Available evidence does not indicate which of these is the preferred pathway or if there is a significant energy difference between them. It is likely that the increase in the effective size of chlorine relative to methyl results from electrostatic repulsion between the electronegative chlorine and oxygen atoms which increases the energy of the transition state. This influence is lacking in the preferred transition state for rotation in the 1-aryl hydantoins.

In addition to its steric effects and through-space electronic effects as an ortho substituent on the aryl group, a chlorine substituent may possibly influence the barriers to rotation by through-bond field or mesomeric effects. Mesomeric effects are likely to be significant only in or near the transition state for rotation of the aryl group. In the transition state, the aryl and heterocyclic moieties must be approximately co-planar, allowing maximum or near maximum conjugation between the aryl π -electron system and the lone pair of electrons on the heterocyclic nitrogen atom at the point of attachment. Through-bond field effects may operate in both the transition and ground states. By influencing the electron distribution in the hetero ring, a chloro substituent might cause sufficient changes in bond lengths and bond angles in the ground and transition states to influence the free energies of activation.

In order to determine the electronic influence of a chlorine substituent on the rotational barriers, the free energies of activation of 3-(2-methyl-4-chlorophenyl)-5-methylhydantoin, Mg, and 3-(2-methyl-4-chlorophenyl)-5-phenylhydantoin, Mh, both containing a para chloro substituent, were compared (at the same temperature) with those of Me and Mc, respectively. No significant changes in the values of ΔG^\ddagger were observed on the addition of this substituent. Since the through-bond influence of an ortho chloro substituent should be similar to that of a para chloro

substituent, it is concluded that the observed influence of an ortho chloro substituent is primarily a through-space effect.

Other compounds in the thiohydantoin series

3-o-Methoxyphenyl-5-methyl-2-thiohydantoin

The C₅-methyl groups of the rotational diastereomers of this compound showed a chemical shift difference. This was fortunate, as many workers, e.g. Icli⁹, have found that the chemical shift difference induced by an o-methoxyphenyl group is too small to be detected.

The effective size of an o-methoxy group is usually considered to be quite small since the methyl portion of the moiety can take up a conformation in which its steric effect is minimised. The rotation in this compound is highly hindered, however, and in an equilibration study a $\Delta G_{28.5}^\ddagger$ of 23.86 ± 0.03 kcal mole⁻¹ was determined. As discussed for the case of the o-chlorophenyl analogue, the reason for the high degree of rotational stability appears to be a repulsive electronic interaction, in this case between the oxygen of the methoxy moiety and the oxygen of the carbonyl group.

The effect is also seen in the rotational ground states. Thus, the equilibrium constant between the rotational isomers differs significantly from unity (1.35 ± 0.08) and the value is larger than that of the α -naphthyl analogue (1.15 ± 0.06) although the rotational stability of the α -naphthyl compound is much higher.

3-o-Fluorophenyl-5-methyl-2-thiohydantoin

At present, we have no data from the hydantoin series to compare with the data obtained on this compound. Within the thiohydantoin series, however, the data are consistent. Thus, fluorine was the smallest non-hydrogen ortho substituent employed (van der Waals radius 1.35 \AA) and the compound has the lowest rotational stability in the series of compounds (ΔG^\ddagger at 86° is $19.7 \text{ kcal mole}^{-1}$). It should be noted, however, that the results obtained on this compound and the β -naphthyl analogue may not be compared quantitatively with the results obtained on the other thiohydantoins, as a different solvent was employed in order to obtain a larger chemical shift difference between the methyl groups of the diastereomeric rotational isomers.

3- β -Naphthyl-5-methyl-2-thiohydantoin

This compound is one of the five examples² that we have found in which there are substantial barriers to rotation in the absence of bulky ortho substituents and in which the asymmetric shieldings of the aryl rings are sufficient

to cause chemical shift differences between diastereotopic groups or between diastereomeric rotational isomers. In this case the rotamers are diastereomers. As in the cases of the other four compounds, the high rotational stability is attributed to the bulk and geometry of the heterocyclic moiety.

The reason for a lack of a chemical shift difference shift difference between the diastereomeric methine protons is not clear, but this probably reflects the smaller distance of the methine protons from the centre of asymmetry.

The results obtained on this compound and the o-fluorophenyl analogue may not be compared quantitatively with the results obtained on the other thiohydantoins as a different solvent was employed.

Comparison of the o-fluorophenyl and β -naphthyl compounds

The o-fluorophenyl compound has a larger ortho substituent on the aryl ring (fluorine, van der Waals radius 1.35 Å) than the β -naphthyl compound (hydrogen, van der Waals radius 1.2 Å), yet the former has a lower degree of rotational stability than the latter. The observation is attributed to the inductive effect of the fluorine atom. It is presumed that in the torsional transition state, electrons are withdrawn from the carbonyl group and/or the thiocarbonyl group making the C=O and/or the C=S bonds shorter, thus decreasing the barrier to internal rotation.

Infrared Spectra

The infrared spectra of a number of hydantoins have been reported by Elliot and Natarajan⁵¹, and Kimmel and Saifer⁵² have reported the infrared spectra of a number of thiohydantoins.

The most easily characterised peak is that corresponding to the carbonyl stretching mode. In the thiohydantoins studied, the position of this absorption varies from 1720 cm^{-1} to 1750 cm^{-1} (Table 21). Although infrared spectra were sometimes run on a mixture of diastereomers, the two carbonyl peaks were never resolved. This may be possible, however, through the use of solutions rather than KBr pellets and through the use of an instrument with a better resolving power. The variation in the position of the carbonyl absorption with aryl substituent does not appear to give any useful information on the stereochemistry of the molecule.

Notes on the ring closure step in the synthesis

In the synthesis of the thiohydantoins, the mode of ring closure is of some interest. Fehlner⁴ examined the crude product in the synthesis of 3- α -naphthyl-5-methyl-2-thiohydantoin (see Experimental section for synthetic scheme). Unfortunately, not all of the mixture would dissolve in pyridine but the n.m.r. spectrum did show a marked preponderance of the thermodynamically less stable diastereomer. He concluded that the less stable diastereomer is probably formed preferentially.

Some thought was given to experiments that would answer this question definitively and quantitatively but this is not a trivial problem

Two processes may be important in determining the nature of the product

(1) A preference for the formation of one diastereomer during the formation of the thiohydantoin, i.e., during the ring closure.

(2) A preference for the formation of one diastereomer during the formation of thiohydantoin crystals.

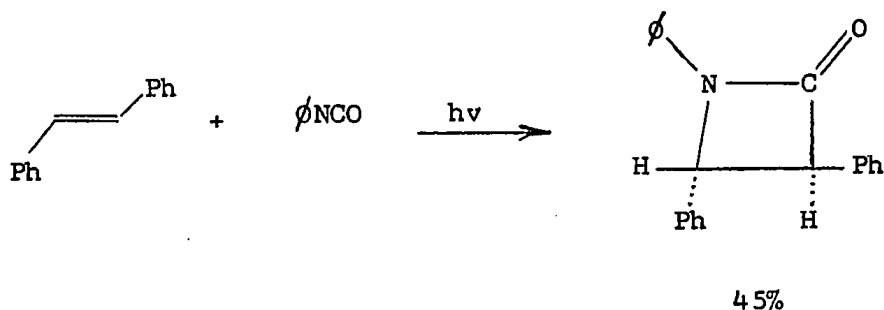
For a quantitative study, the two processes should be clearly identified. Experimentally this is most difficult. Since the possible results of such a study do not justify the required effort, the work has been omitted.

SUMMARY

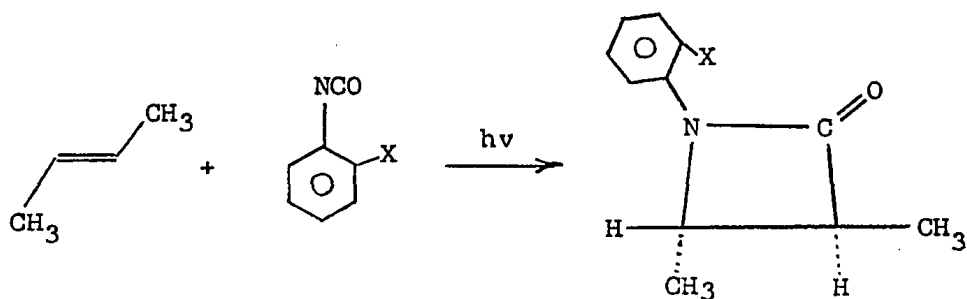
1. Restricted internal rotation about the aryl C-N bond has been examined in a number of 3-aryl-5-methyl-2-thiohydantoins.
2. Substantial rotational barriers were found in all the compounds, even in a compound where there are no bulky ortho substituents on the aryl ring.
3. Strong conformational preferences were observed between some of the diastereomeric rotational isomers. It is proposed that this is a consequence of the effect of the C₅-methyl group being transmitted to the aryl group via an unsymmetrical solvent shell around the carbonyl group.
4. Through space repulsive electronic interactions have been shown to have an important influence on the rotation process and on the relative stabilities of the rotational ground states. Most dramatically, an ortho chloro group is effectively larger than an ortho methyl group in both the rotation process and the rotational ground states.

SUGGESTIONS FOR FUTURE WORK

Recently, Tadatoshi and Sakuri⁵³ have reported the following synthesis



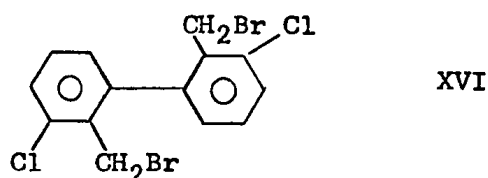
In principal, the synthesis could easily be adapted to give compounds that may exhibit hindered rotation about the aryl C-N bond as follows



It should be noted, however, that a ground state route to this compound may prove to be more feasible. In any event, this would probably be an interesting series of compounds and would be a logical extension of the present work.

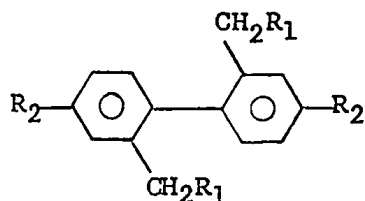
PART III

MISCELLANEOUS COMPOUNDS

Miscellaneous Compounds2,2'-bis-(Bromomethyl)-3,3'-dichlorobiphenyl

A sample of this compound was supplied by Prof. D.E. Pearson of Vanderbilt University. The study was undertaken to supplement the work of W.E. Bentz ⁵.

Bentz studied hindered rotation about the phenyl-phenyl bond of several 2,2'-disubstituted biphenyls



by means of complete n.m.r. line shape analysis. For the compound $R_1 = \text{Br}$, $R_2 = \text{H}$, he reported a free energy of activation of $21.03 \text{ kcal mole}^{-1}$ (S.D. 0.03) at 25°C .

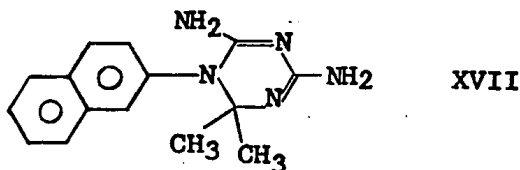
The benzylic protons of XVI are non-equivalent and show an AB pattern in the n.m.r. spectrum at room temperature, indicating slow rotation about the phenyl-phenyl bond. In nitrobenzene solution the following chemical shifts and coupling constant were observed, $\delta_A 4.146$, $\delta_B 4.397$, $J 10.1 \text{ Hz}$.

Under conditions of fast rotation about the phenyl-phenyl bond, it is to be expected that the AB pattern would collapse to a singlet. However, no collapse whatsoever was evident when a sample of the compound was heated to 187°C, indicating that, even at this temperature, rotation is slow on the n.m.r. time scale.

The minimum free energy of activation about the phenyl-phenyl bond at 187° was calculated to be 23.9 k.cal mole⁻¹ (minimum lifetime = 0.0255 sec.).

The clear implication is that the introduction of chlorine groups in the meta positions causes a buttressing effect so that steric interaction between the two moieties in the transition state is severe.

1-(β-naphthyl)-1,2-dihydro-2,2-dimethyl-4,6-diamino-s-triazine



The compound was supplied as the hydrochloride salt by Dr. A. Rosowsky of the Children's Cancer Research Foundation, Inc., Boston. The study was undertaken to supplement the work of Fehlner⁴ and Bentz⁵.

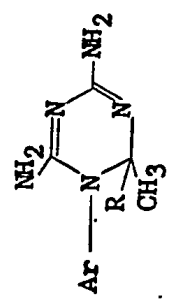
At 109° in perfluorobutyric acid (bp 120.5-121.0⁵⁴) the diastereotopic methyl groups give rise to two lines, at δ 1.418 and δ 1.450, indicating slow rotation of the aryl group. When the sample was heated in a sealed tube, the spectrum arising from these protons collapsed to a singlet. The coalescence temperature was 141°.

Unfortunately, the collapse of the methyl doublet was accompanied by some decomposition. In consequence, only the free energy of activation at the coalescence point was determined. The rate constant in the coalescence point region was obtained by matching computer simulated spectra to the experimental spectra. The free energy of activation for rotation about the aryl C-N bond at 141° is 23.1 kcal mole⁻¹. It is estimated that the error in ΔG^\ddagger is +0.5 kcal mole⁻¹.

The aryl group of this compound does not have a bulky ortho substituent but still has a substantial barrier to rotation about the aryl C-N bond. The work on this compound has been published² together with studies on the quinazolinones that do not have bulky ortho substituents and studies on 3- β -naphthyl-5-methyl-2-thiohydantoin. In addition, studies on XVII enlarge the data, obtained in these laboratories, on hindered rotation about the aryl C-N bond in 1-aryl substituted triazines (Table 29).

Table 29

Free Energies of Activation for Rotation About the Aryl C-N Bond in Some 1-Aryl Substituted Triazines



Ar	R	Acid Solvent	T ^a	[#] b ΔG
α-naphthyl ^c	CH ₃	Perfluorobutyric	128	19.6 ^d
o-chlorophenyl ^c	CH ₃	Perfluorobutyric	132.5	20.4 ^d
o-tolyl ^e	H	Trifluoroacetic	25	24.1 ^{f,g}
o-chlorophenyl ^e	H	Pentafluoropropionic	25	21.5 ^{f,h}
β-naphthyl	CH ₃	Perfluorobutyric	141	23.1 ^{i,j}

(a) Temperature, °C. (b) Free energy of activation at the specified temperature, kcal/mole. (c) Data from Ref. 4. (d) Minimum value, spectrum did not collapse. (e) Data from Ref. 1 and Ref. 5 (f) For thermodynamically least stable diastereomer. (g) Data obtained by the equilibration method. (h) Data obtained by lineshape analysis. (i) Data obtained from coalescence studies. (j) Estimated to be accurate to ±0.5 kcal/mole.

EXPERIMENTAL

General

- (1) Melting points and boiling points.
- (2) Infrared spectra.
- (3) Nuclear magnetic resonance spectra.
- (4) Elemental analyses.
- (5) Curve resolving.
- (6) Mass spectra.
- (7) Computer simulation of n.m.r. spectra.

(1) Melting points and boiling points.

Where the value is given as a range between two temperatures the determination was performed on a Gallenkamp melting point apparatus. Where the value is given as a single temperature, the determination was performed on a Mettler FP 1 melting point apparatus employing a temperature rise of $2^{\circ} \text{ min}^{-1}$. Both melting points and boiling points are uncorrected.

(2) Infrared spectra.

The infrared spectra of the products that are solids were taken through fused potassium bromide discs. The spectra of the liquid products were taken through neat liquid films held between sodium chloride plates. In all cases, the spectra were recorded on both a Perkin-Elmer Infracord for presentation in this thesis and a Perkin-Elmer 457 for more quantitative comparisons. The 1602 cm^{-1} polystyrene absorption was routinely used for calibration purposes. Where peak positions are reported, they are probably accurate to $\pm 5 \text{ cm}^{-1}$.

(3) Nuclear magnetic resonance spectra.

The spectra were recorded on a Varian HA 100 spectrometer employing the field sweep mode.

Wilmad "Imperial 507-PP" sample tubes were used.

For high temperature studies near the boiling point of the solvent, the tubes were usually sealed at atmospheric pressure.

The concentration of the samples was never noted but was always adjusted to give a reasonable signal to noise ratio. No special care was taken with respect to the amount of liquid in the sample tube except that it was always greater than the minimum height of about 30 mm.

The lock signals were either provided by tetramethylsilane or by hexamethyldisilane. The latter was used in high temperature studies.

In no case was an attempt made to adjust the calibration of the instrument to coincide precisely with the calibration of the chart paper during the course of recording a 1000 Hz spectrum. In consequence, it is not possible to determine the chemical shifts by studying the 1000 Hz spectra shown in this thesis. Their inclusion only serves qualitative purposes. It may not be obvious to the reader that the numbers at the top of the spectra would be those used for a 500 Hz scan. Accurate chemical shifts are given following an account of the synthesis of each compound. The line positions, accurate to ± 0.1 Hz, were measured directly from the recorded peak maxima using the internal frequency counter.

The temperatures of the samples were measured after the spectra had been recorded. This was done by measuring the peak separation of the Varian standard sample

of ethylene glycol. The separation was determined by locking on the C-H peak and measuring the position of the O-H peak. A Varian temperature/peak separation calibration chart was then employed to determine the temperature. The method is probably accurate to within a degree. The principal disadvantage with the method is that it may not be used to measure temperatures above about 175° because of the small separation of the C-H and O-H peaks. Where temperatures above 175° are given, they have been estimated by extrapolation. An error of $\pm 5^\circ$ is probably over-cautious.

The possibility of lineshape distortion, caused by either saturation or over filtering, was excluded by frequent checking.

(4) Elemental analyses.

The analyses were either performed by Galbraith Laboratories, Knoxville, Tennessee, U.S.A., or by Alfred Bernhardt, Mikroanalytisches Laboratorium, West Germany.

(5) Curve Resolving.

The technique allows the determination of areas under overlapping n.m.r. peaks. A Dupont 310 curve resolver was employed.

The large size chart paper on which the n.m.r. spectra were usually recorded precluded the generation of "resolved" peaks on a permanent record.

The method involves:

- (a) Selection of the type of curve to be used.
- (b) Generation of each curve.
- (c) Fitting the curves by adjusting the base line, height and width of each curve.
- (d) Reading off the areas under each curve.

There are problems involved in each manipulation:

- (a) The n.m.r. signal shape lies somewhere between Gaussian and Lorentzian shapes; exactly where is difficult to decide. Furthermore, the signal shape changes with the variable homogeneity of the spectrometer. The best fits were obtained using Lorentzian curves.
- (b) Each curve is generated independently of the others and consists of several segments that may be adjusted more or less independently to give the desired curve. Clearly, it is not possible to generate the same shape in every curve, although every effort was made to minimise errors in this respect.
- (c) It was not possible to obtain perfect fits to any of the spectra because of noise on the spectra and the problems associated with (a) and (b) above.
- (d) The manufacturers have placed the area read out galvanometer in a position where it is difficult to read without parallax errors. This poses problems in adjusting the galvanometer for 100% with all peaks on, and for 0% with all peaks off. Furthermore, it is difficult to read the areas

accurately. The area of a peak is expressed as a percentage of the sum of all peaks. The error in the area of a peak is probably 0.5%, i.e., a peak of 11.2% could be reported as $11.2 \pm 0.5\%$ but see below.

The overall reproducibility in the determination of the area of a peak is about $\pm 3\%$ depending on the nature of the spectrum. The precision of the method was never evaluated.

The advantage of the method is its reproducibility and the lack of very arbitrary decisions that are present in the integration method.

(6) Mass spectra.

The spectra were recorded on a Hitachi Perkin-Elmer RMU 6E spectrometer by Dr. R. T. Rye.

(7) Computer simulation of n.m.r. spectra

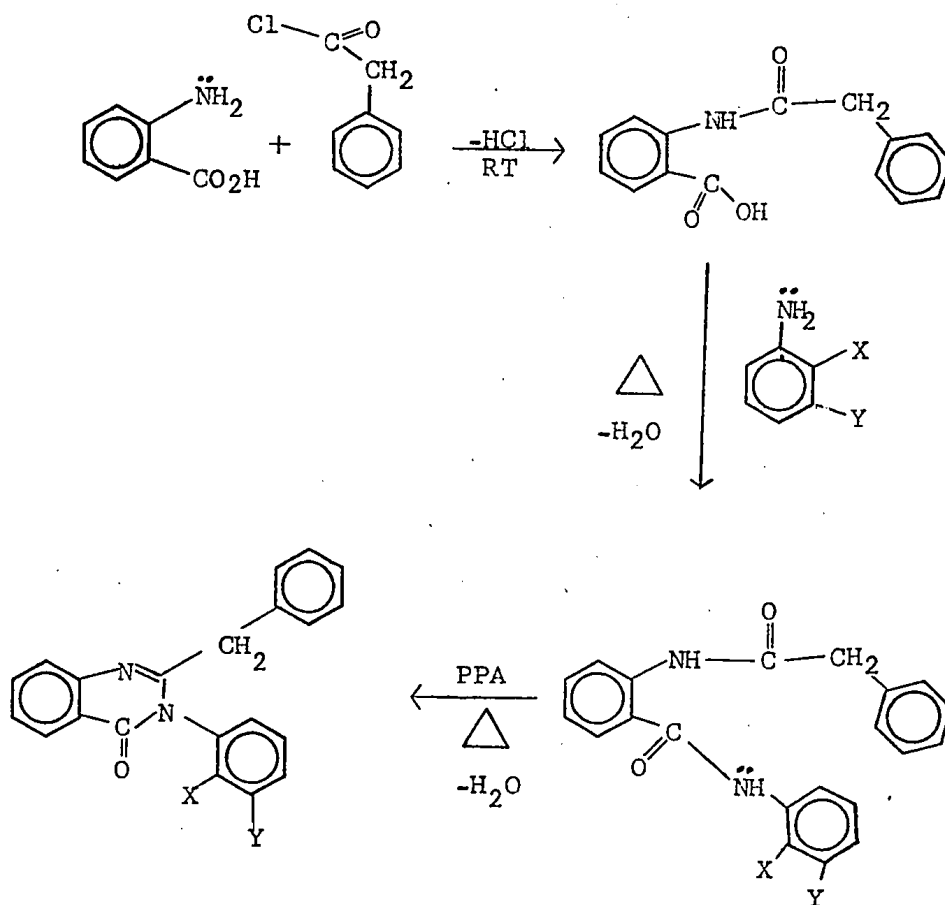
The object was to simulate the experimental spectra in order to determine the rotational lifetimes of the systems under consideration. The appropriate equation (for example, that of an AB system) was fed into a 2114A Hewlett-Packard computer and the parameters necessary to describe the experimental spectrum were punched on the teletype. The six parameters for an AB system are: the mean lifetime, τ , the chemical shift difference, ν_{AB} , the coupling constant, J , the line width, W , and the horizontal and vertical scales.

The calculated spectrum was then plotted on a Houston Instrument "Complot" recorder. After simulating one spectrum well, by varying all the parameters, it was usually found necessary only to vary the lifetime and the scales to match the experimental spectra taken at different temperatures. An example of the method may be found under Calculation of Thermodynamic Parameters.

General Synthetic

Quinazolinones

These novel compounds were synthesised by an adaption of the method of Klosa.³⁵ The precursor, N-phenylacetyl anthranilic acid, was synthesised by an adaption of the method of de Diesbach *et al.*⁵⁵ Following is the synthetic scheme.



The deviation from Fehner's method only involves the amount of time employed in refluxing the isothiocyanate with alanine. Fehner refluxed a mixture of α -naphthyl isothiocyanate and D,L alanine for 3 hours. His experiment was repeated and the reaction was monitored by thin layer chromatography. There was no observable change in the composition of the reaction mixture after 8½ hours although the addition of acid yielded the thiohydantoin. The experiment was repeated without refluxing with precisely the same result. In the syntheses reported in this work, the 3 hour reflux was cut dramatically (see accounts of syntheses).

Also noteworthy is that the chemical shifts of the diastereomeric methyl groups of 3- α -5-methyl-2-thiohydantoin have been reported¹ incorrectly. In pyridine the following were observed: δ_A 1.475, J 7.1 Hz; δ_B 1.546, J 7.1 Hz.

One observation made during the synthesis of the thiohydantoin is difficult to explain. In all cases, the addition of hydrochloric acid was accompanied by the evolution of a gas that smelled like hydrogen sulphide. This probably arises from some side reaction.

Preparation of Quinazolinones and Precursor

N-Phenylacetyl anthranilic acid

The compound was prepared on a number of occasions. The synthesis that yielded the purest product, as determined by the melting point, is reported.

Anthranilic acid (J.T. Baker) (39.0g, 0.285 mol) was dissolved in a solution of 500 ml of 90% ether and 10% ethanol. The solution was filtered and phenylacetyl chloride (Anachemia) (44.1g, 0.285 mol) in ether (50 ml) was added with stirring. A white precipitate formed immediately. The crude product was recrystallised from ethanol and was washed with chloroform to yield white needles. This compound was used in syntheses without further purification.

Yield 19.4g, 27%.

Mp 186° (lit.⁵⁵ 188°)

The infrared spectrum is shown in fig. 19.

2-Benzyl-3-(2-chloro-6-methylphenyl)-4(3H)-quinazolinone

The following method proved unsatisfactory.

N-Phenylacetyl anthranilic acid (10.0g, 0.039 mol) and

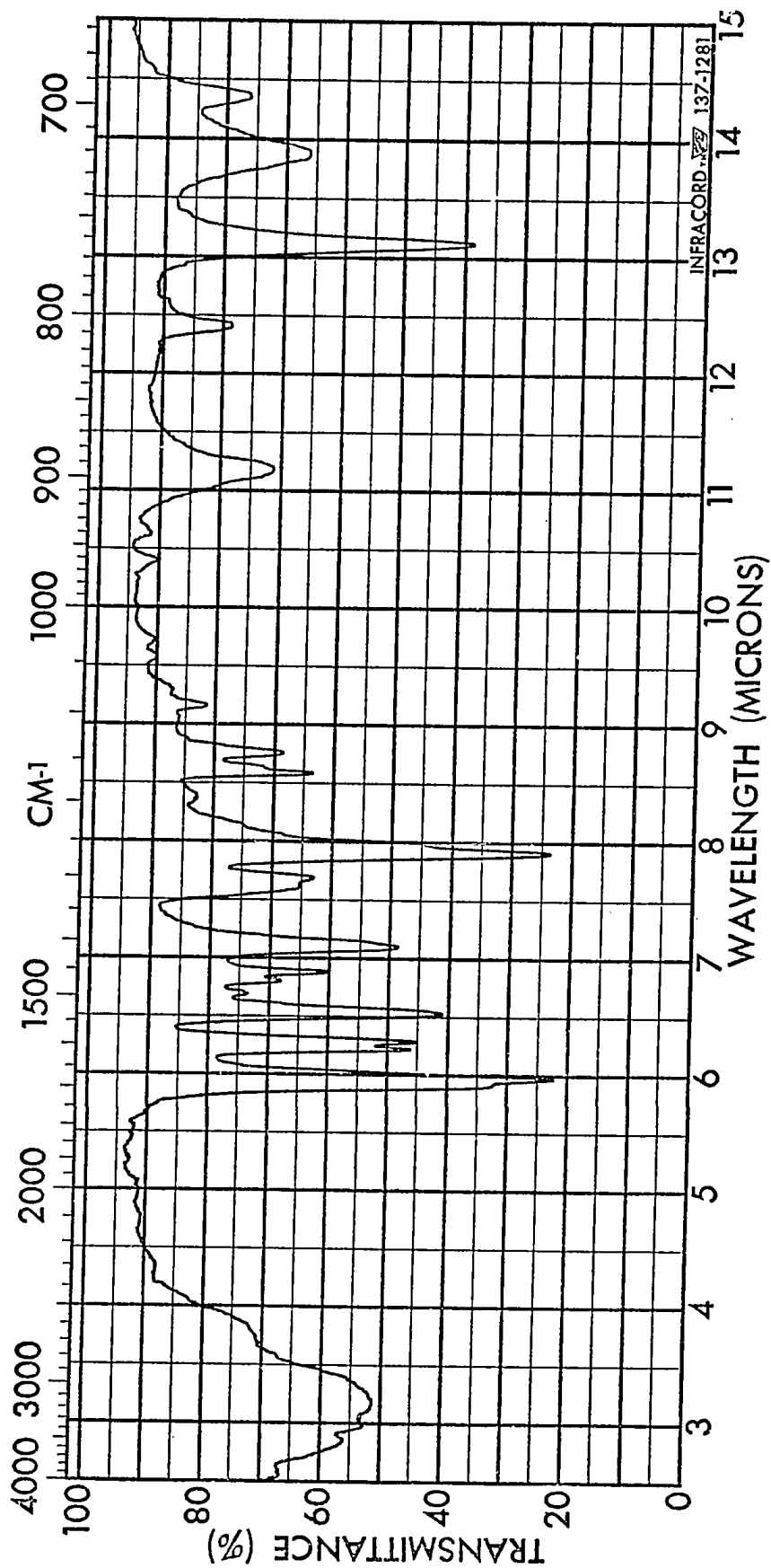


Fig. 19. Infrared spectrum of N-Phenylacetyl anthranilic acid

2-chloro-6-methylaniline (Aldrich) (5.5g, 0.039 mol) were heated to 180° with stirring. A black tar resulted.

An adaptation of the method of Klosa³⁵ was employed successfully.

N-Phenylacetyl anthranilic acid (10.0g, 0.039 mol), 2-chloro-6-methylaniline (5.5g, 0.039 mol) and polyphosphoric acid (35g) were heated to 180° with stirring and kept at that temperature for 20 minutes. After cooling, the solution was poured into water (150 ml), neutralised with sodium carbonate, and the product was extracted with ether. The ether was removed under vacuum and the crude product was recrystallised from methanol to give pale yellow crystals that were dried under vacuum.

Yield 0.82g, 6%.

Mp 152°.

The infrared spectrum is shown in fig. 20.

The nmr spectrum is shown in fig. 21. The solvent was deuteriochloroform but the recorded chemical shifts and coupling constant of the AB quartet are the values found when using nitrobenzene as solvent.

Aromatic, δ 6.70-8.35, multiplet, integration 12.5 H.

Benzyl, δ_A 3.620, δ_B 3.916, J 14.7 Hz, quartet, integration 1.92 H.

Methyl, δ 1.53, singlet, integration 3.0 H.

Elemental analysis; calculated C 73.20, H 4.71, N 7.76; found C 72.97, H 4.15, N 7.69.

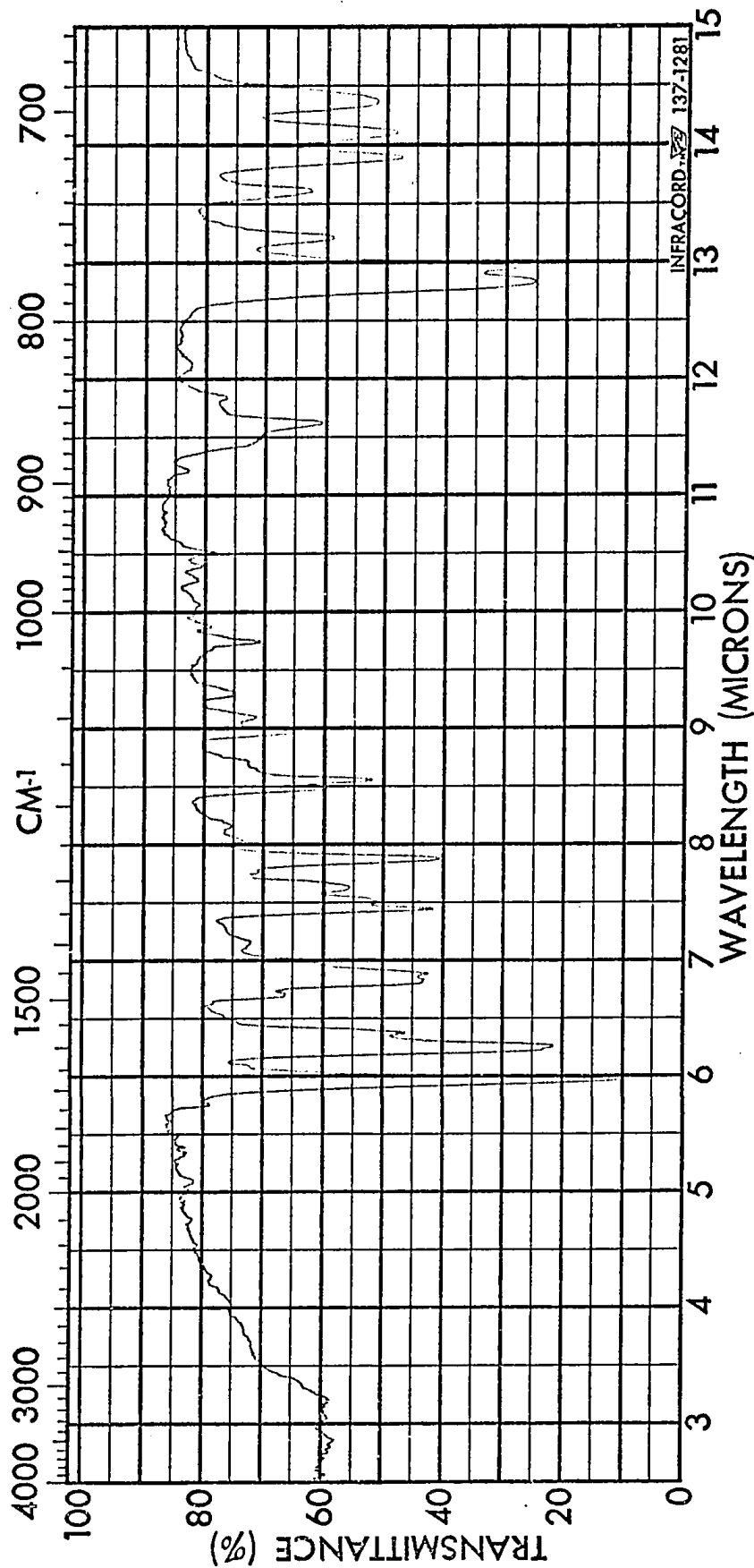


Fig. 20. Infrared spectrum of
2-Benzyl-3-(2-chloro-6-methylphenyl)-4(3H)-quinazolinone

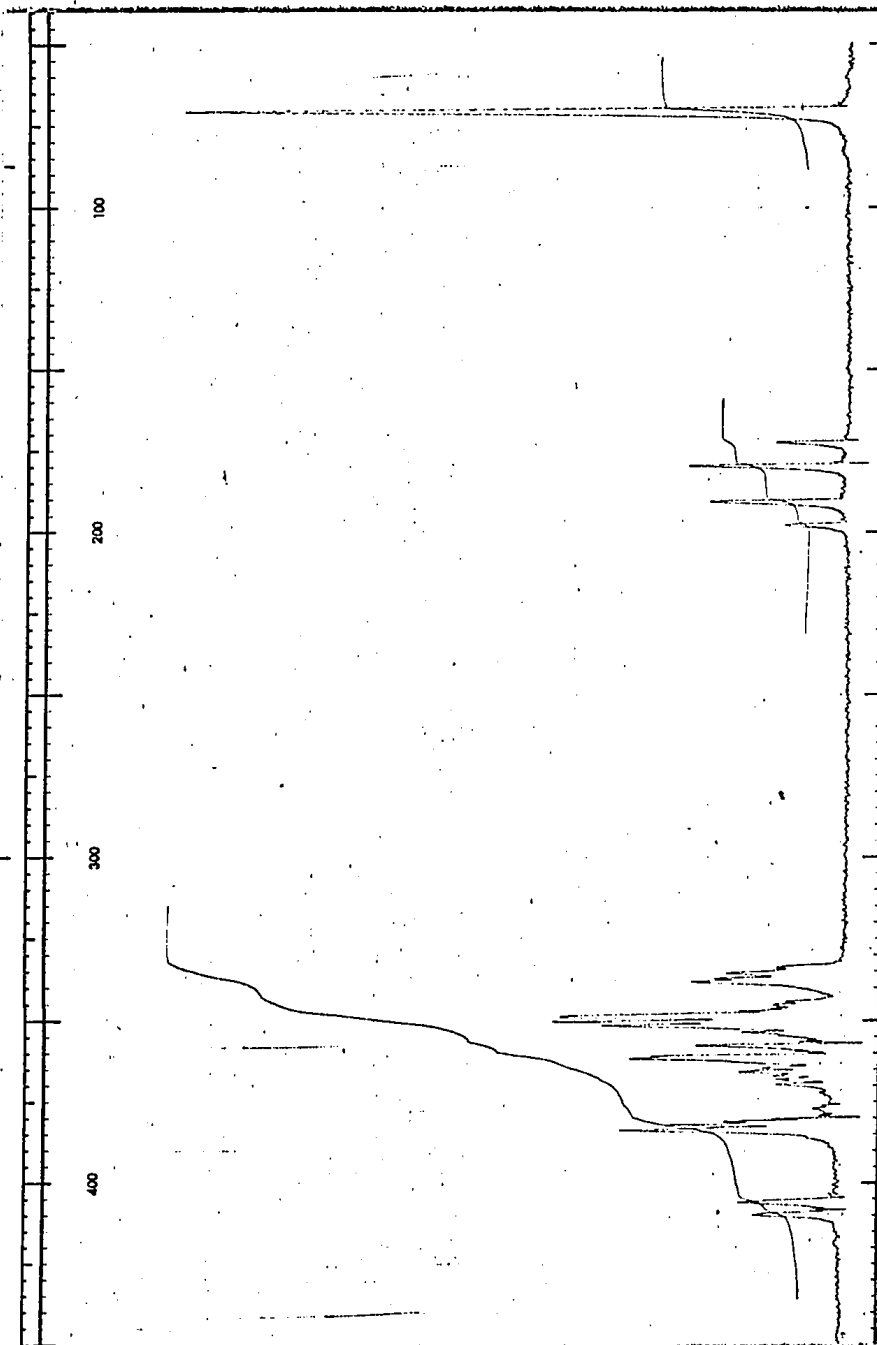


Fig. 21. 100 MHz NMR spectrum of
2-Benzyl-3-(2-chloro-6-methylphenyl)-4(3H)-quinazolinone
in deuteriochloroform solution (1000 Hz scan)

2-Benzyl-3-o-bromophenyl-4(3H)-quinazolinone

N-Phenylacetyl anthranilic acid (10.0g, 0.039 mol), o-bromoaniline (Aldrich) (6.7g, 0.039 mol), and polyphosphoric acid (40g) were heated to 180° with stirring and kept at that temperature for 20 minutes. After cooling, the solution was poured into water (150 ml), neutralised with sodium carbonate and sodium bicarbonate, and the product was extracted with chloroform. The chloroform was removed under vacuum and a brown oil (immiscible with water) resulted. The oil was boiled with methanol but on cooling did not yield crystals. The methanol was removed under vacuum. After standing for 3 hours the oil solidified to yield a brown solid. The product was deemed to be impure since part of it would not dissolve in deuteriochloroform. After filtration, however, no impurities could be detected in the n.m.r. spectrum and in consequence no further purification was performed.

Yield 7.6g, 50%.

Mp 130°

The infrared spectrum is shown in fig. 22.

The n.m.r. spectrum is shown in fig. 23. Deuteriochloroform was used as solvent.

Aromatic, δ 6.7-8.4, multiplet, integration 13.0 H.

Benzyl, δ_A 3.692, δ_B 4.017, J 15.0 Hz, quartet, integration 2.3 H.

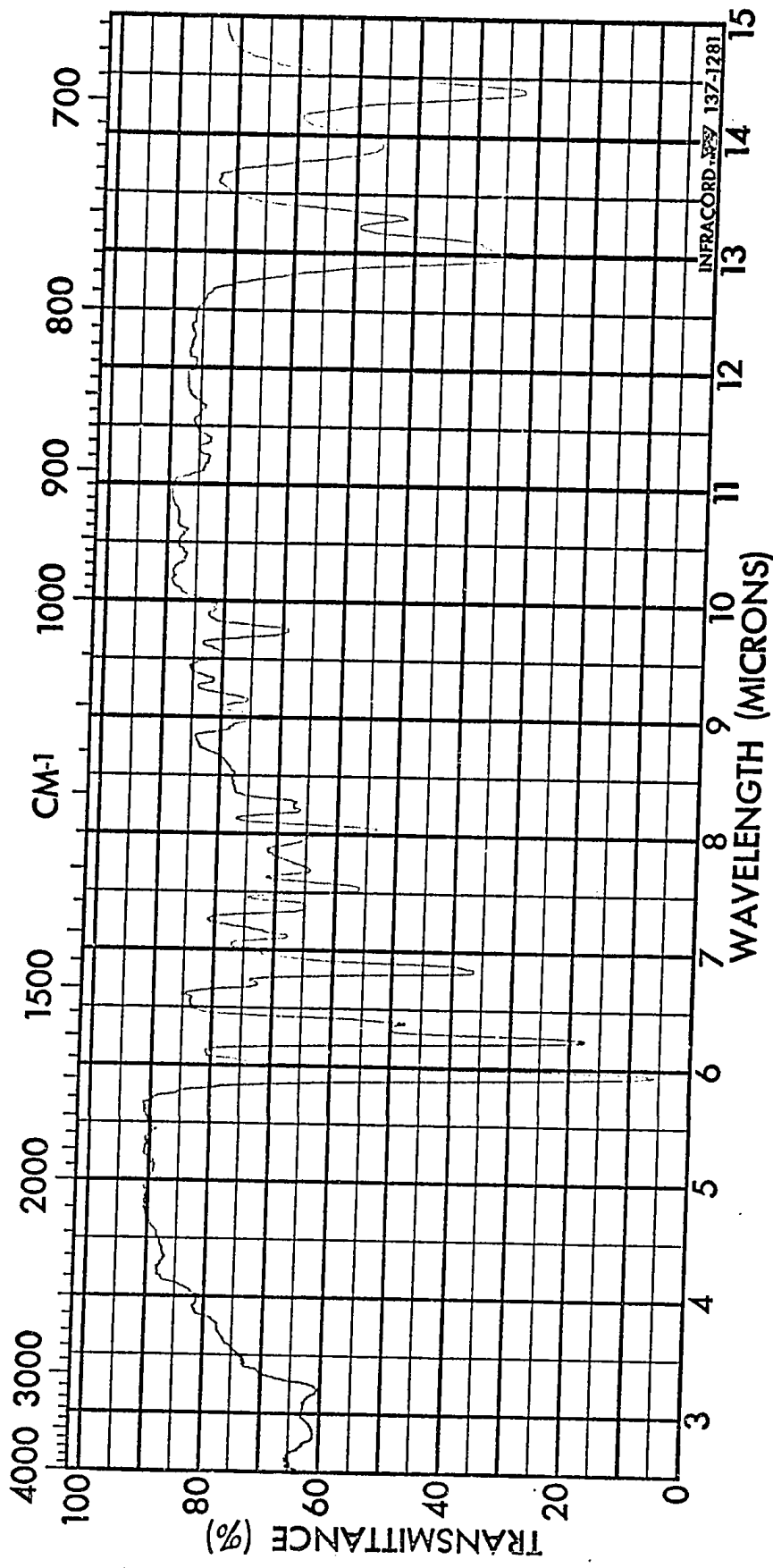


Fig. 22. Infrared spectrum of 2-Benzyl-3-o-bromophenyl-4(3H)-quinazolinone

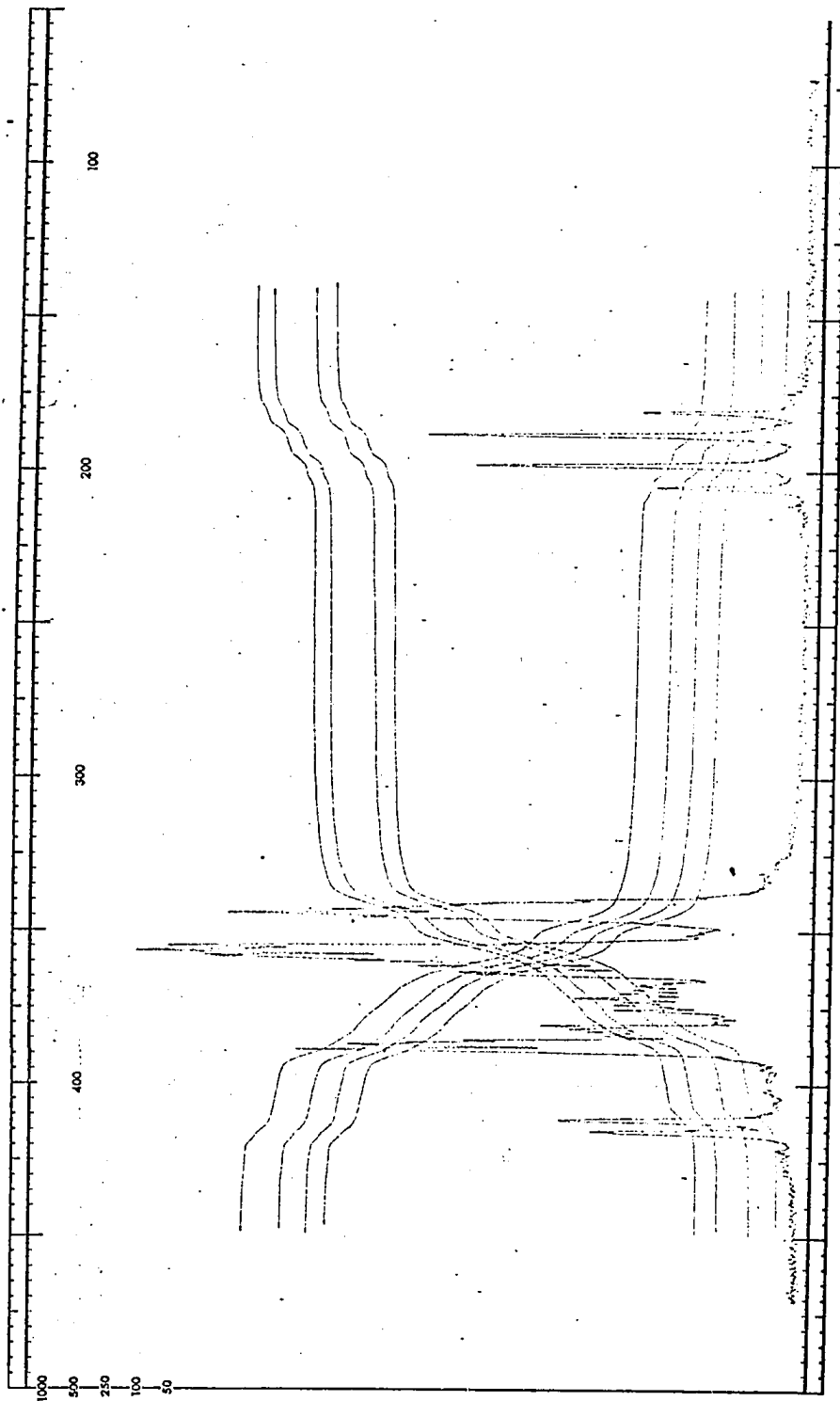


Fig. 23. 100 MHz NMR spectrum of
2-Benzyl-3-o-bromophenyl-4(3H)-quinazolinone
in deuteriochloroform solution (1000 Hz scan)

With nitrobenzene as solvent the benzyl protons gave an AB quartet with δ_A 3.709, δ_B 3.919, J 14.8 Hz. Elemental analysis; calculated C 64.45, H 3.83, N 7.16; found C 64.77, H 3.73, N 6.93.

2-Benzyl-3-o-tolyl-4(3H)-quinazolinone

N-Phenylacetyl anthranilic acid (10.0g, 0.039 mol), *o*-toluidine (Eastman "White label") (3.9g, 0.037 mol), and polyphosphoric acid (41g) were heated to 180° with stirring and kept at that temperature for 25 minutes. After cooling, the solution was poured into a concentrated sodium carbonate solution. When neutralisation was complete the product was extracted with chloroform (150 ml) and washed with hydrochloric acid (50 ml, 6N) to remove any unreacted amine. The chloroform layer was then washed with sodium bicarbonate solution, filtered, and dried over molecular sieves (British Drug Houses, type 4A). The chloroform was removed under vacuum to yield a brown oil that gave a yellow solid after 2 hours.

Yield 3.61g, 30.2%.

Mp 113°.

The infrared spectrum is shown in fig. 24.

The n.m.r. spectrum is shown in fig. 25. Deuteriochloroform was used as solvent.

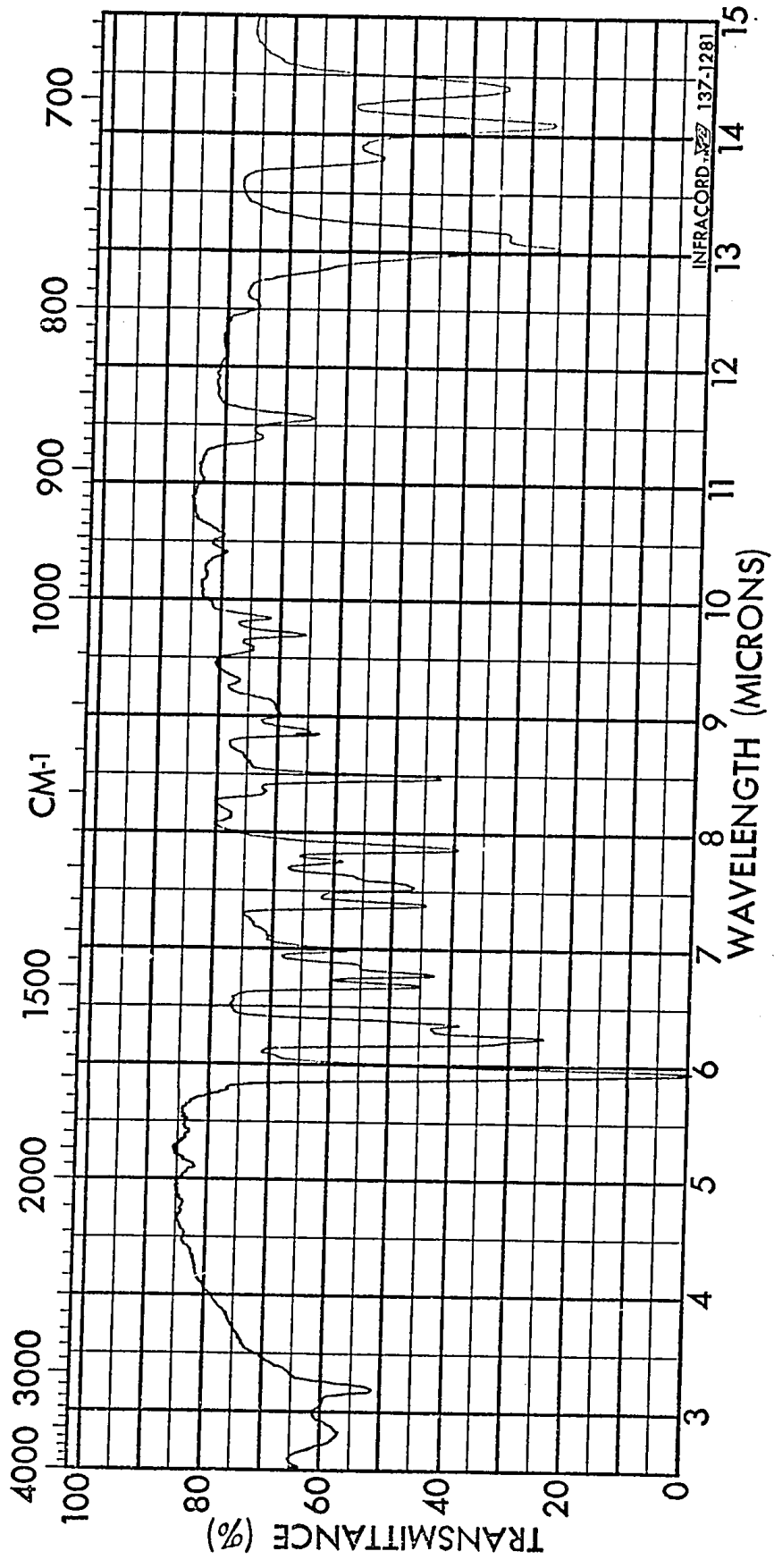


Fig. 24. Infrared spectrum of 2-Benzyl-3-o-tolyl-4(3H)-quinazolinone

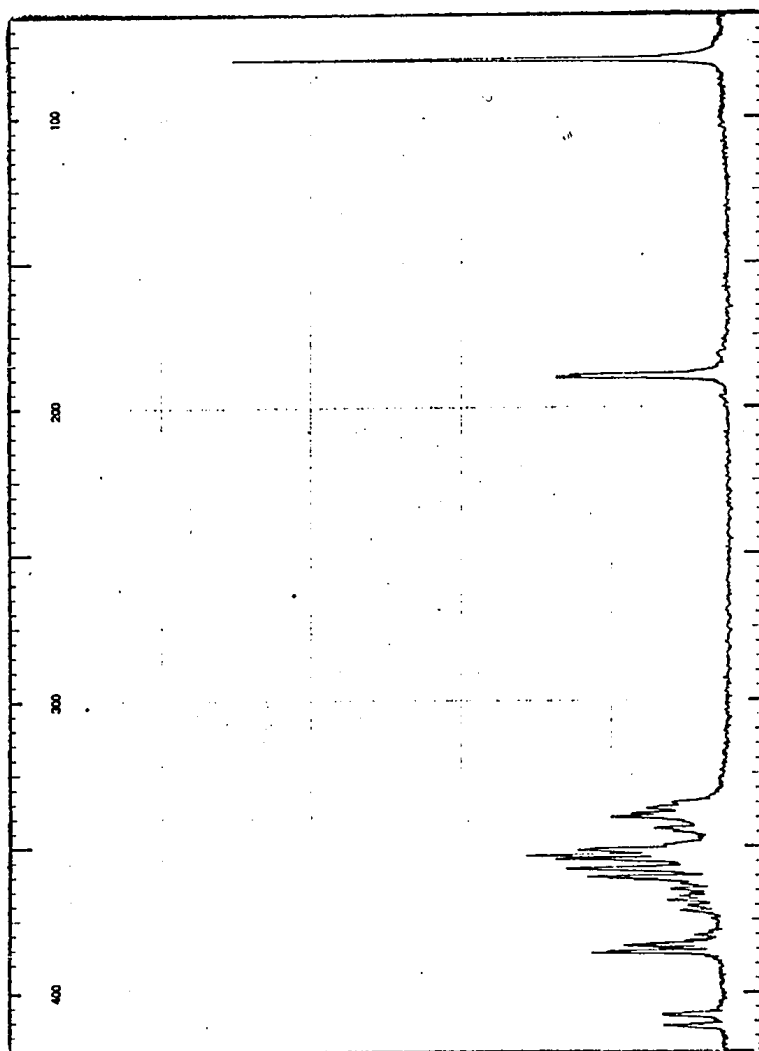


Fig. 25. 100 MHz NMR spectrum of
2-Benzyl-3-o-tolyl-4(3H)-quinazolinone
in deuteriochloroform solution (1000 Hz scan)

Aromatic, δ 6.5-8.4, multiplet, integration 13.2 H.

Benzyl, δ_A 3.810, δ_B 3.873, J 14.6 Hz, quartet, integration 1.9 H.

Methyl, δ 1.66, singlet, integration 2.8 H.

With nitrobenzene as the solvent the benzyl protons showed as a singlet at δ 3.78.

With bromoform as the solvent the benzyl protons gave an AB quartet with δ_A 3.776, δ_B 3.833, J 14.5 Hz.

Elemental analysis; calculated C 80.98, H 5.52, N 8.59; found C 81.05, H 5.37, N 8.58.

2-Benzyl-3-o-chlorophenyl-4(3H)-quinazolinone

N-Phenylacetyl anthranilic acid (8.4g, 0.033 mol), *o*-chloroaniline (Eastman "White label") (4.2g, 0.033 mol), and polyphosphoric acid (40g) were heated to 180° with stirring and kept at that temperature for 20 minutes. After cooling, the solution was poured into a concentrated sodium carbonate solution. When neutralisation was complete, the product was extracted with chloroform, giving a dark green solution. The solution was filtered and dried over molecular sieves (British Drug Houses, type 4A). The chloroform was removed under vacuum and an oil resulted. The oil was dissolved in acetone and poured into water (250 ml). After 12 hours a yellow solid formed. The crude product was recrystallised twice from methanol and washed

with cold acetone (1 ml) to give buff coloured crystals.

Yield 1.33g, 11.6%.

Mp 111°.

The infrared spectrum is shown in fig. 26.

The n.m.r. spectrum is shown in fig. 27. Deuteriochloroform was used as solvent.

Aromatic, δ 6.5-8.3, multiplet, integration 13.0 H.

Benzyl, δ_A 3.713, δ_B 4.004, J 15.1 Hz, quartet, integration 1.8 H.

With nitrobenzene as solvent the benzyl protons gave an AB quartet with δ_A 3.753, δ_B 3.923, J 15.0 Hz.

Elemental analysis; calculated C 72.73, H 4.33, N 8.08; found C 72.45, H 4.42, N 7.97.

2-Benzyl-3-o-biphenyl-4(3H)-quinazolinone

The synthesis of this compound was not successful.

N-Phenylacetyl anthranilic acid (10.0g, 0.0392 mol), *o*-aminobiphenyl (Aldrich) (6.67g, 0.0394 mol), and polyphosphoric acid (40g) were heated to 180° with stirring. A black tar resulted. Purification of the amine may be useful if the synthesis is attempted again.

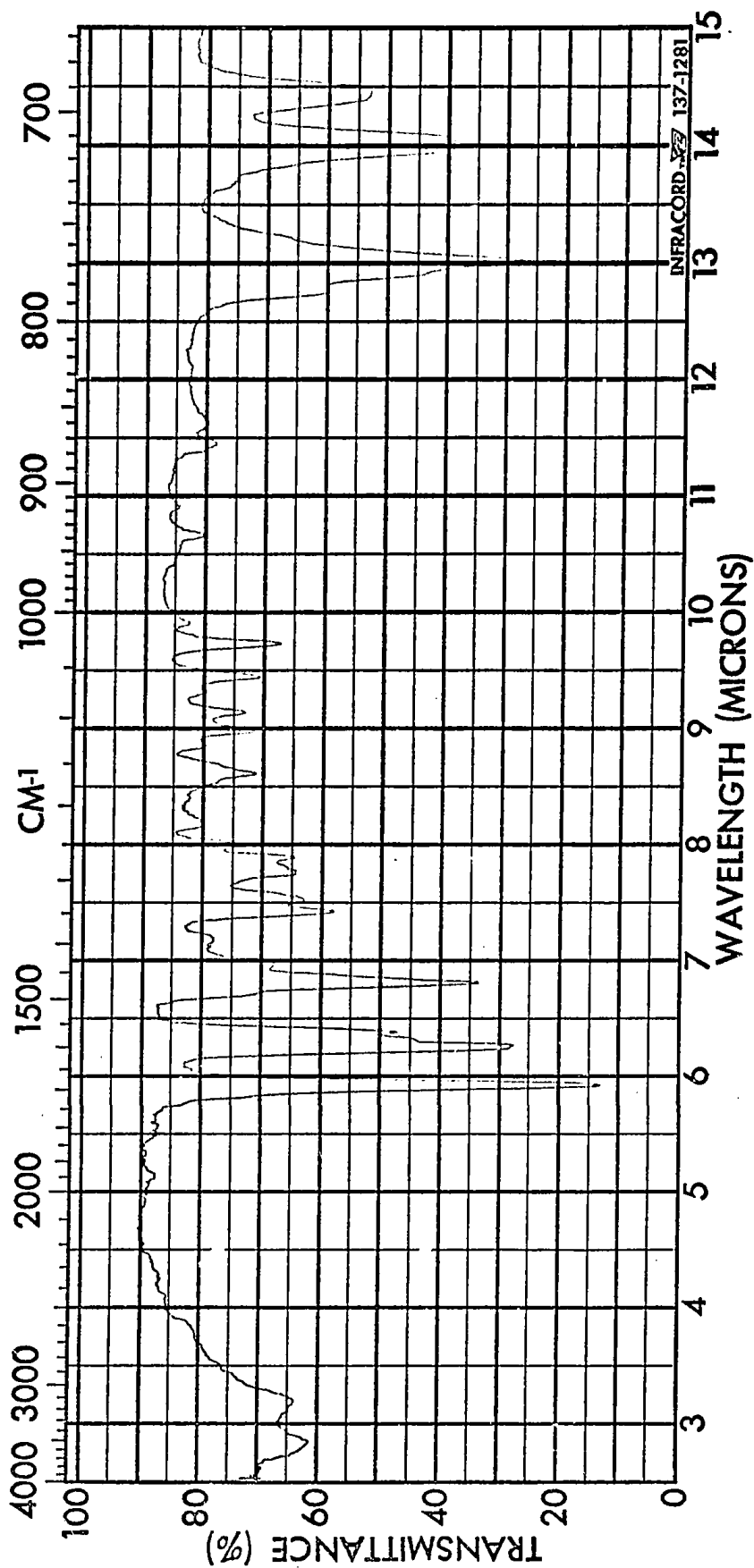


Fig. 26. Infrared spectrum of
2-Benzyl-3-o-chlorophenyl-4(3H)-quinazolinone

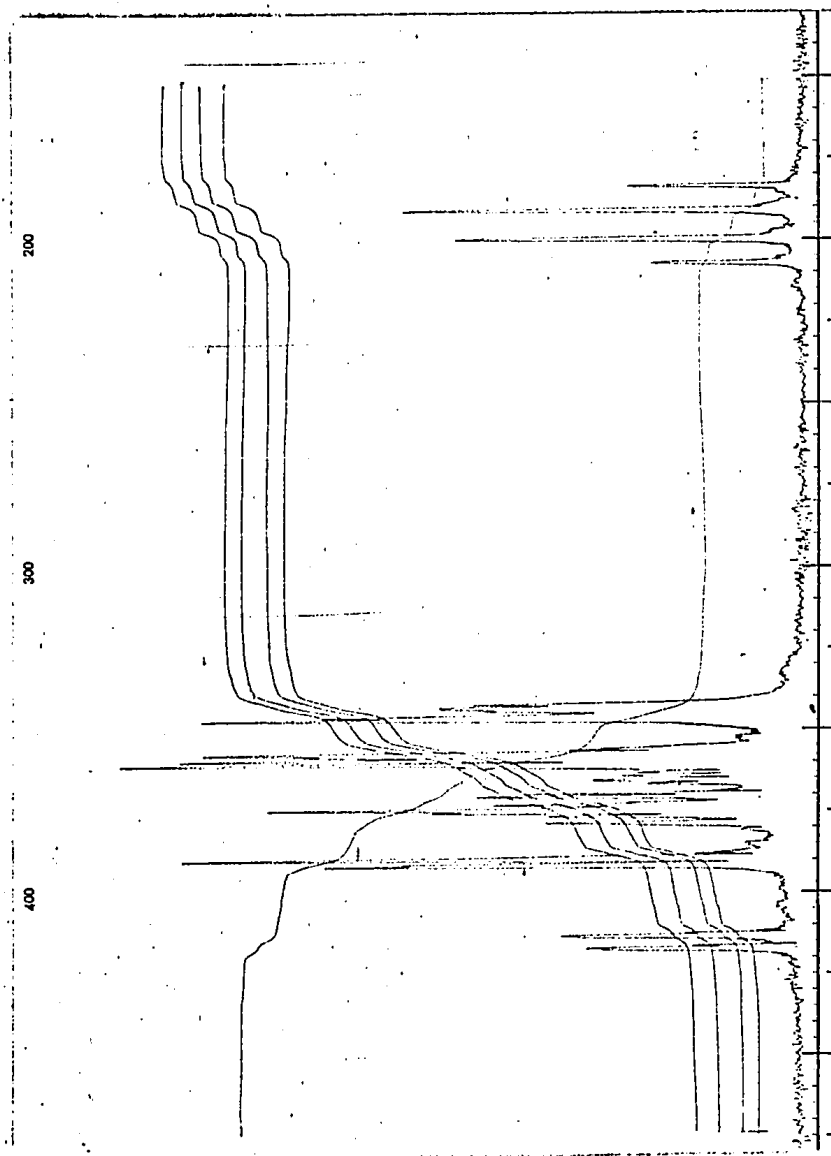


Fig. 27. 100 MHz NMR spectrum of
2-Benzyl-3-o-chlorophenyl-4(3H)-quinazolinone
in deuteriochloroform solution (1000 Hz scan)

2-Benzyl-3-o-fluorophenyl-4(3H)-quinazolinone

N-Phenylacetyl anthranilic acid (10.0g, 0.0392 mol), o-fluoroaniline (Aldrich) (4.35g, 0.0392 mol), and polyphosphoric acid (40g) were heated to 180° with stirring and kept at that temperature for 40 minutes. After cooling, the solution was poured into a concentrated sodium bicarbonate solution. When neutralisation was complete the product was extracted with chloroform. The chloroform was removed under vacuum to yield a brown oil that solidified quickly. The crude product was recrystallised twice from methanol to give white crystals that were dried under vacuum.

Yield 1.9g, 14.7%

Mp 133°

The infrared spectrum is shown in fig. 28.

The n.m.r. spectrum is shown in fig. 29. Deuteriochloroform was used as solvent.

Aromatic, δ 6.6-8.4, multiplet, integration 13.4 H.

Benzyl, δ_A 3.848, δ_B 3.989, J 15.0 Hz, quartet, integration 1.8 H.

With nitrobenzene, DMSO-d₆ and 2-chloropyridine as solvents the benzyl protons appear as a singlet.

With bromoform as the solvent the benzyl protons gave an AB quartet with δ_A 3.823, δ_B 3.966, J 15.1 Hz.

Elemental analysis; calculated C 76.36, H 4.45, N 8.49;

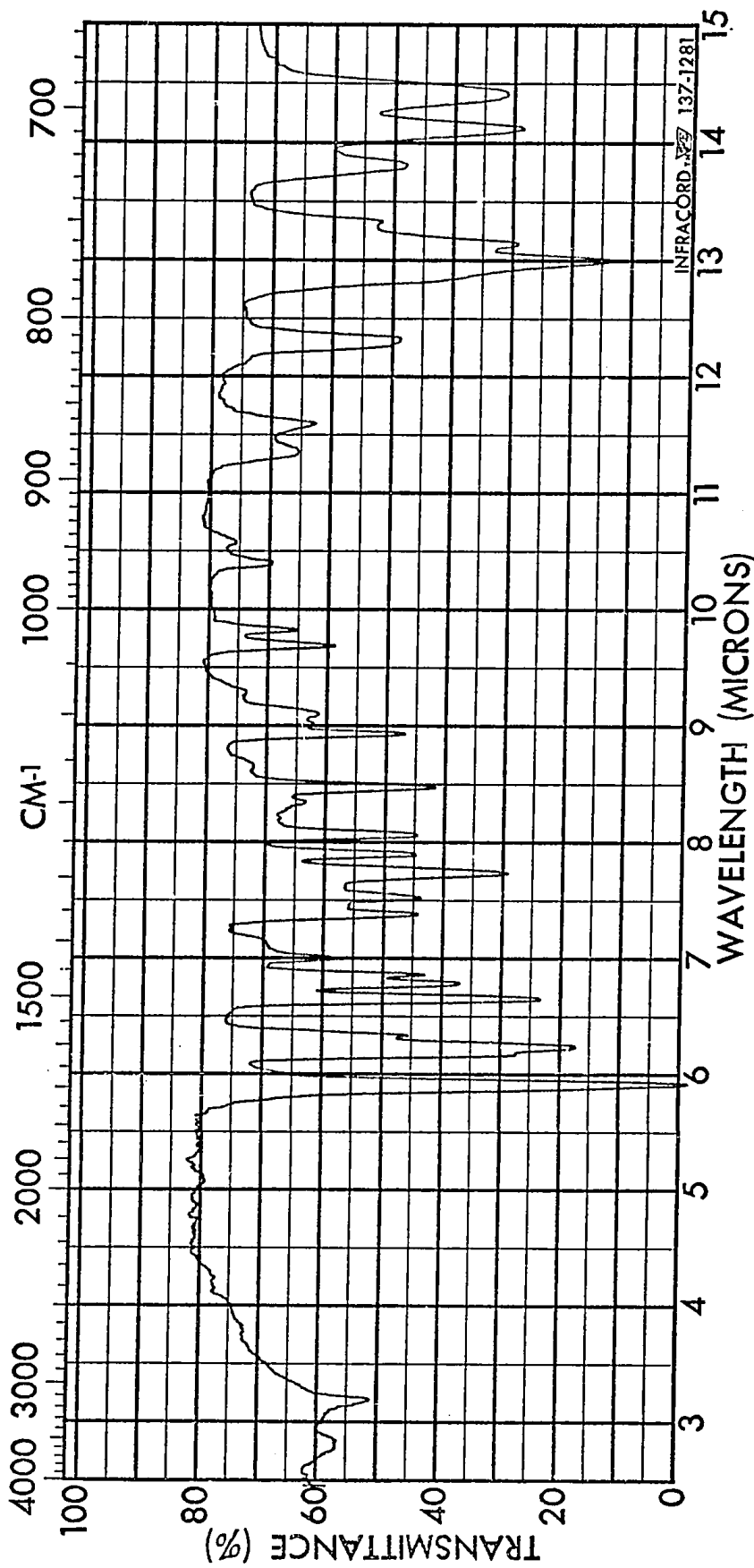


Fig. 28. Infrared spectrum of
2-Benzyl-3-o-fluorophenyl-4(3H)-quinazolinone

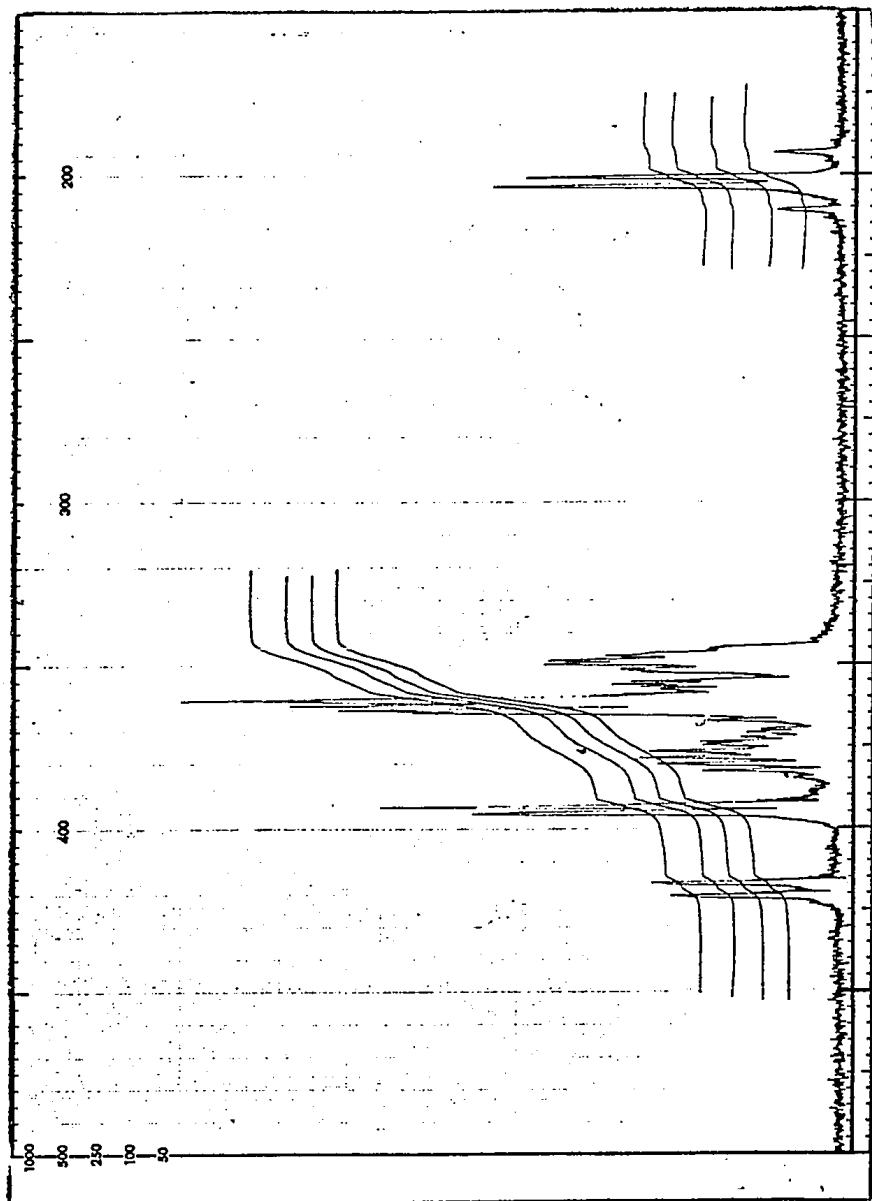


Fig. 29. 100 MHz NMR spectrum of
2-Benzyl-3-o-fluorophenyl-4 (3H)-quinazolinone
in deuteriochloroform solution (1000 Hz scan)

found C 76.46, H 4.73, N 8.60.

2-Benzyl-3-o-hydroxyphenyl-4(3H)-quinazolinone

The synthesis of this compound was not successful.

N-Phenylacetyl anthranilic acid (10.0g, 0.0392 mol), o-aminophenol (K and K) (4.38g, 0.0403 mol), and polyphosphoric acid (40g) were heated to 180° with stirring and kept at that temperature for 30 minutes. After cooling, the solution was poured into a concentrated sodium carbonate solution. When neutralisation was complete the product was extracted with chloroform. The chloroform was removed under vacuum to yield a black oil that did not solidify after 12 hours refrigeration. The oil was dissolved in acetone and poured into water. After 12 hours a yellow solid formed. Infrared analysis showed that the solid was not the desired product nor was it anthranilic acid or either of the starting materials. The solvent (water and acetone) was removed under vacuum to yield a black polymeric material.

2-Benzyl-3- β -naphthyl-4(3H)-quinazolinone

N-Phenylacetyl anthranilic acid (10.0g, 0.0392 mol), 2-naphthylamine (Eastman) (3.62g, 0.0228 mol), and polyphosphoric acid (40g) were heated to 180° with stirring and kept at that temperature for 30 minutes. After cooling,

the solution was poured into a concentrated sodium carbonate solution. When neutralisation was complete the product was extracted with chloroform. On washing the solution with hydrochloric acid (6N) a white precipitate (probably the amine salt) formed in the organic layer. The precipitate was removed by filtration. The process of washing with hydrochloric acid was repeated until no more precipitate formed. The chloroform layer was neutralised with sodium bicarbonate solution. When neutralisation was complete the chloroform layer was dried over molecular sieves and the chloroform was removed under vacuum to give an oil that solidified after standing for 30 minutes. The crude product was recrystallised three times from methanol to give pale yellow needles that were dried under vacuum.

Yield 1.62g, 20%.

Mp 136°.

The infrared spectrum is shown in fig. 30.

The n.m.r. spectrum is shown in fig. 31. Deuteriochloroform was used as solvent.

Aromatic, δ 6.4-8.4, multiplet, integration 15.0 H.

Benzyl, δ_A 3.824, δ_B 3.982, J 14.9 Hz, quartet, integration 1.7 H.

With nitrobenzene as the solvent the benzyl protons gave an AB quartet with δ_A 3.826, δ_B 3.958, J 15.1 Hz.

Elemental analysis; calculated C 83.10, H 4.71, N 7.76; found C 83.11, H 4.81, N 7.69.

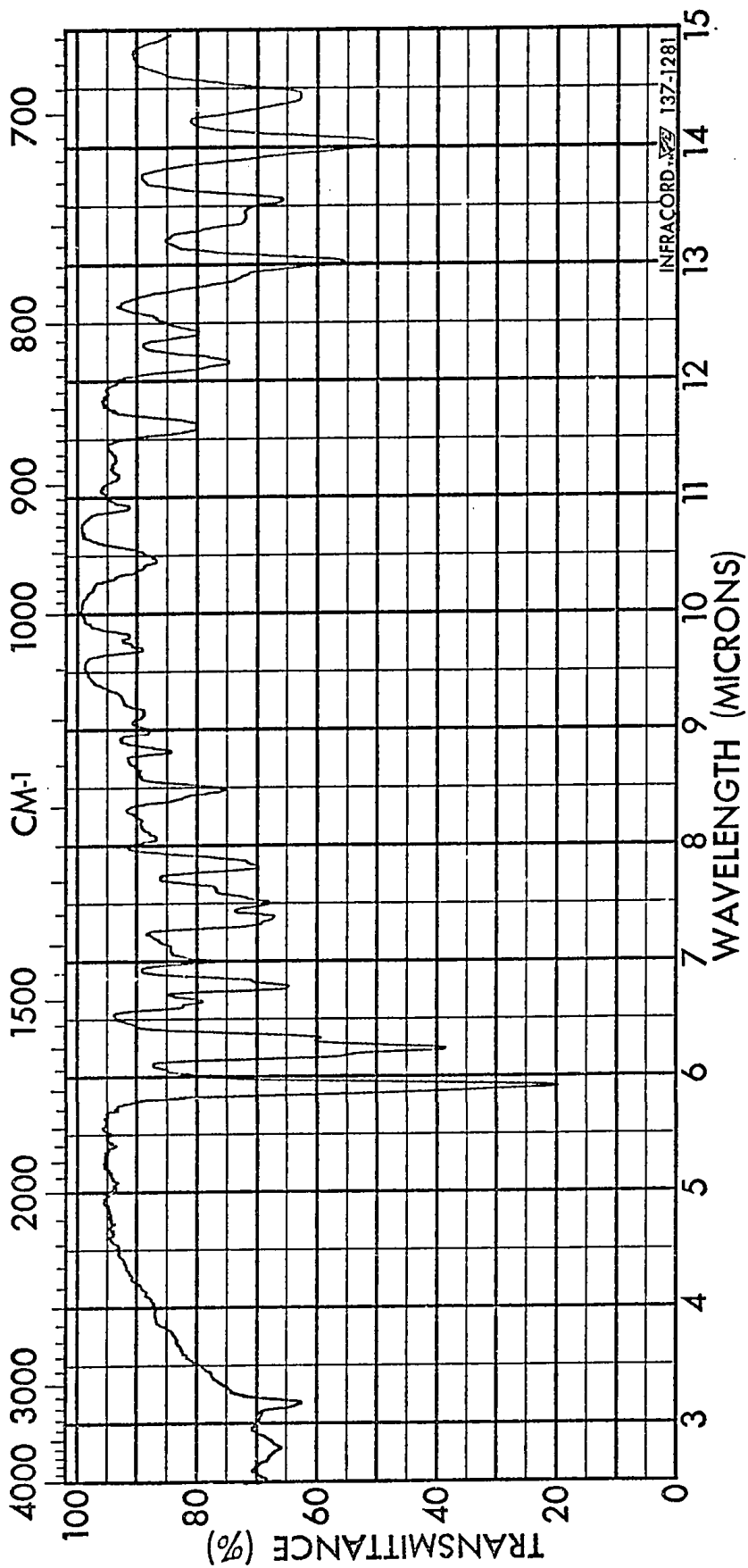


Fig. 30. Infrared spectrum of 2-Benzyl-3- β -naphthyl-4-(3H)-quinazolinone

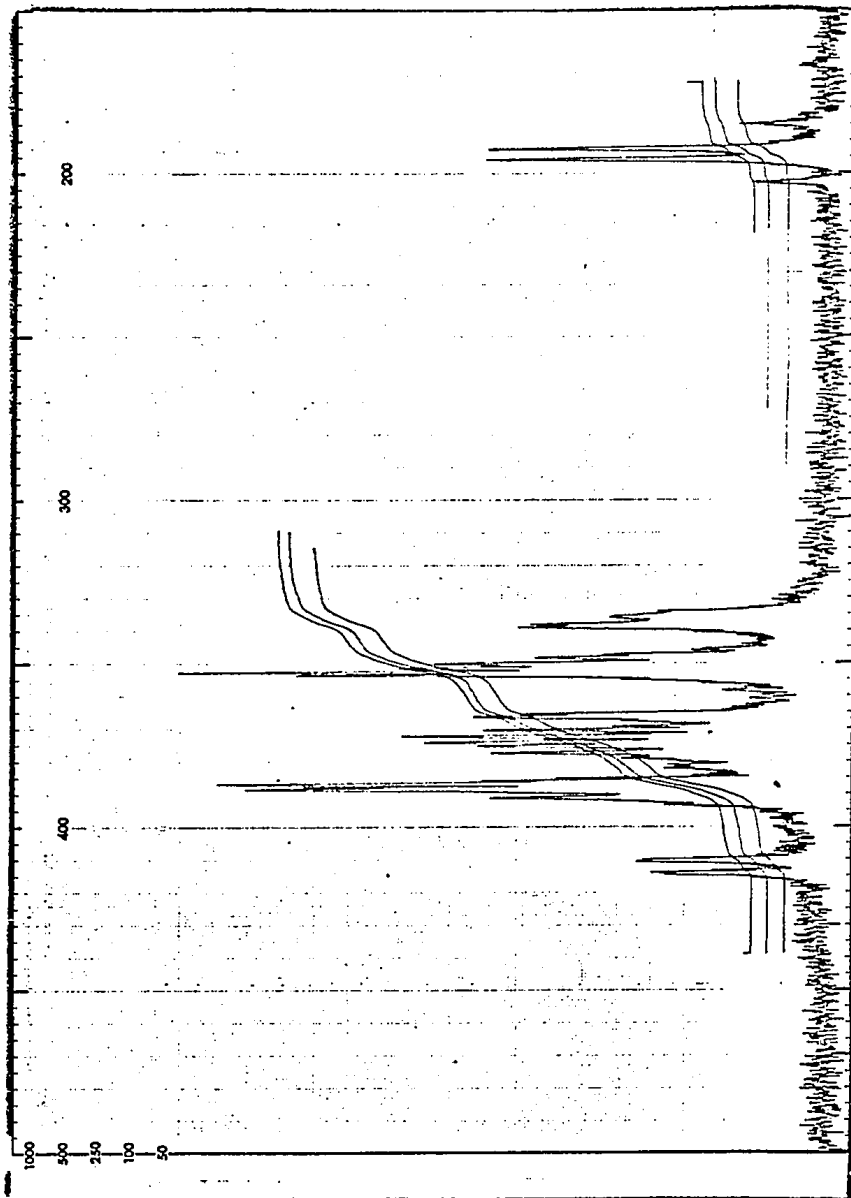


Fig. 31. 100 MHz NMR spectrum of
2-Benzyl-3- β -naphthyl-4-(3H)-quinazolinone
in deuteriochloroform solution (1000 Hz scan)

2-Benzyl-3-m-acetylphenyl-4(3H)-quinazolinone

N-Phenylacetyl anthranilic acid (10.0g, 0.0392 mol), m-aminoacetophenone (K and K) (5.29g, 0.0392 mol), and polyphosphoric acid (44g) were heated to 180° with stirring and kept at that temperature for 25 minutes. After cooling, the solution was poured into a concentrated sodium carbonate solution. When neutralisation was complete the product was extracted with chloroform and washed with hydrochloric acid (6N) to remove any unreacted amine and then washed with sodium bicarbonate. The organic layer was separated and the chloroform was removed under vacuum. A brown oil resulted. The oil was dissolved in ether/ethanol (50:50) and chromatographed on silica gel (100g, 60-120 mesh, British Drug Houses). The column was first eluted with ether (fraction 1, 120 ml, orange; fraction 2, 80 ml, black; fraction 3, 130 ml, orange) then ethanol (fraction 4, 60 ml, yellow; fraction 5, 120 ml, orange) and finally chloroform (fraction 6, 500 ml, yellow). The solvent was evaporated from fraction 2 to give a red oil. The oil was dissolved in acetone and poured into water giving a yellow suspension. After 2 days a yellow solid was filtered off and dried under vacuum.

Yield 0.78g, 5.6%.

Mp 128-130°.

The infrared spectrum is shown in fig. 32.

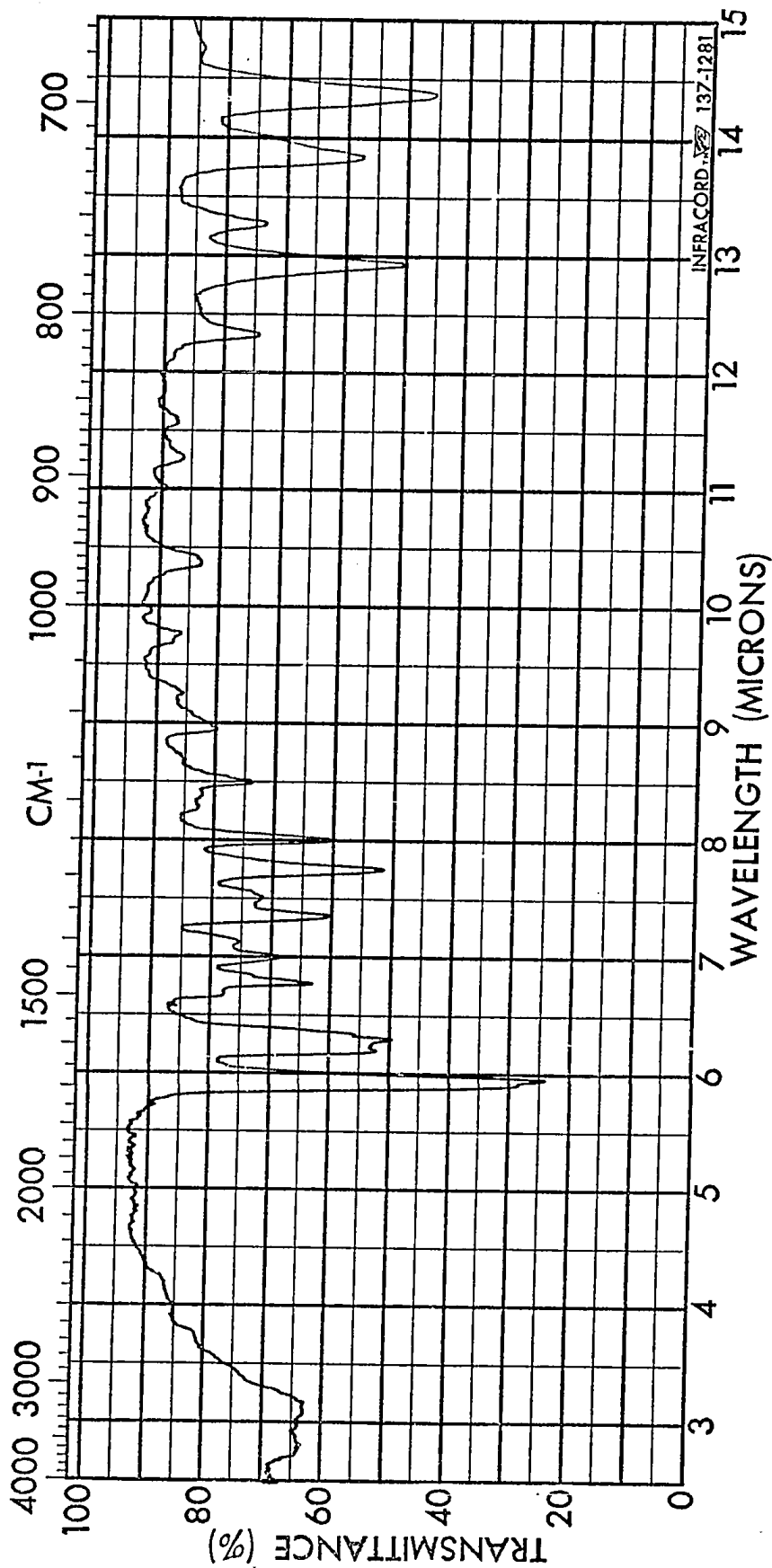


Fig. 32. Infrared spectrum of
2-Benzyl-3-m-acetylphenyl-4(3H)-quinazolinone

The n.m.r. spectrum is shown in fig. 33. Deuteriochloroform was used as solvent.

Aromatic, δ 6.5-8.4, multiplet, integration 13.1 H.

Benzyl, δ_A 3.833, δ_B 3.966, J 14.8 Hz, quartet, integration 1.8 H.

Methyl, δ 2.33, singlet, integration 2.6 H.

With nitrobenzene as the solvent the benzyl protons gave an AB quartet with δ_A 3.861, δ_B 3.966, J 15.0 Hz.

Elemental analysis; calculated C 77.96, H 5.09, N 7.91;

found C 78.10, H 5.17, N 7.80.

2-Benzyl-3-m-bromophenyl-4(3H)-quinazolinone

N-Phenylacetyl anthranilic acid (7.0g, 0.0275 mol), m-bromoaniline (J.T. Baker) (4.7g, 0.0275 mol), and polyphosphoric acid (41g) were heated to 180° with stirring and kept at that temperature for 30 minutes. After cooling, the solution was poured into a concentrated sodium carbonate solution. When neutralisation was complete the product was extracted with chloroform. The organic layer was washed with hydrochloric acid (150 ml, 6N) to remove any unreacted amine. The addition of hydrochloric acid was accompanied by the formation of a large amount of solid material that was removed by filtration. The chloroform layer was washed with sodium bicarbonate solution, separated and dried over molecular sieves. The chloroform was removed under vacuum to yield a brown oil, which yielded a yellow solid on

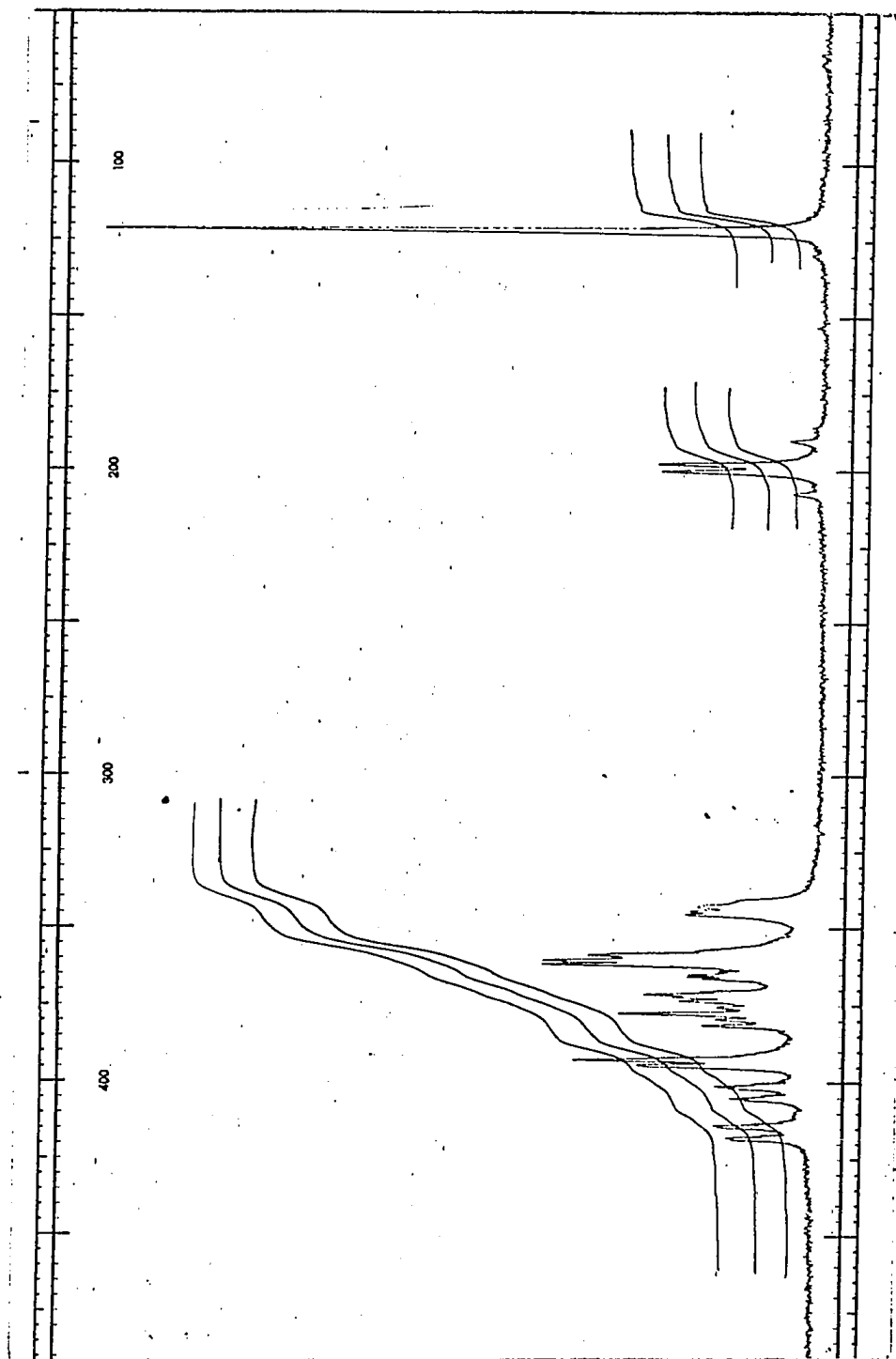


Fig. 33. 100 MHz NMR spectrum of
2-Benzyl-3-m-acetylphenyl-4 (3H)-quinazolinone
in deuteriochloroform solution (1000 Hz scan)

standing for 1½ hours. The crude product was recrystallised from methanol.

Yield 0.87g, 8.1%.

Mp 109-111°.

The infrared spectrum is shown in fig. 34.

The n.m.r. spectrum is shown in fig. 35. Deuteriochloroform was used as solvent.

Aromatic, δ 6.4-8.4, multiplet, integration 13.0 H.

Benzyl, δ_A 3.824, δ_B 3.899, J 14.9 Hz, quartet, integration 1.7 H.

With bromoform as solvent the benzyl protons appeared as a singlet at δ 3.85.

With nitrobenzene as the solvent the benzyl protons gave an AB quartet with δ_A 3.766, δ_B 3.854, J 15.1 Hz.

Elemental analysis; calculated C 64.45, H 3.83, N 7.16; found C 64.28, H 3.66, N 7.15.

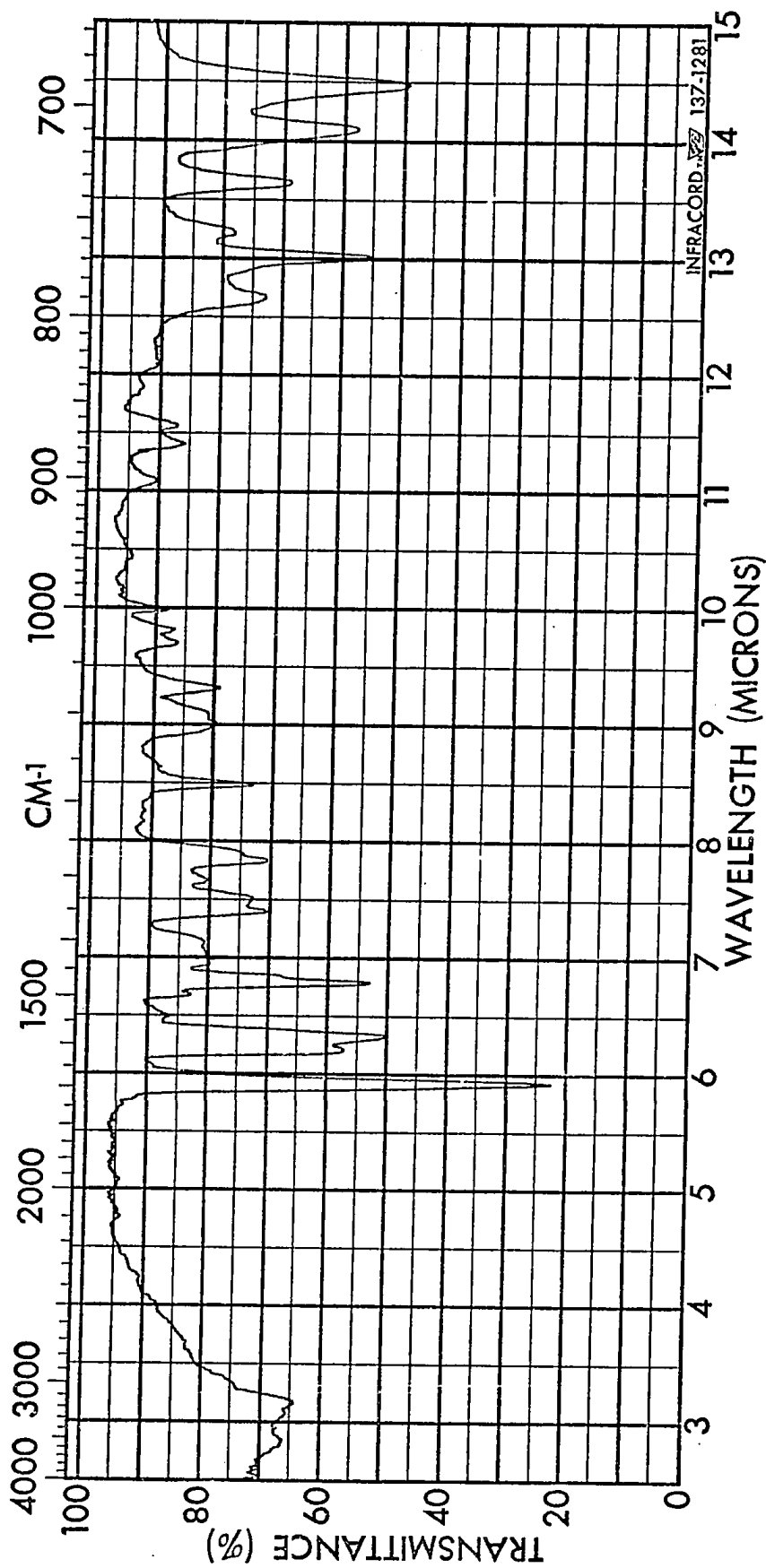


Fig. 34. Infrared spectrum of 2-Benzyl-3-m-bromophenyl-4(3H)-quinazolinone

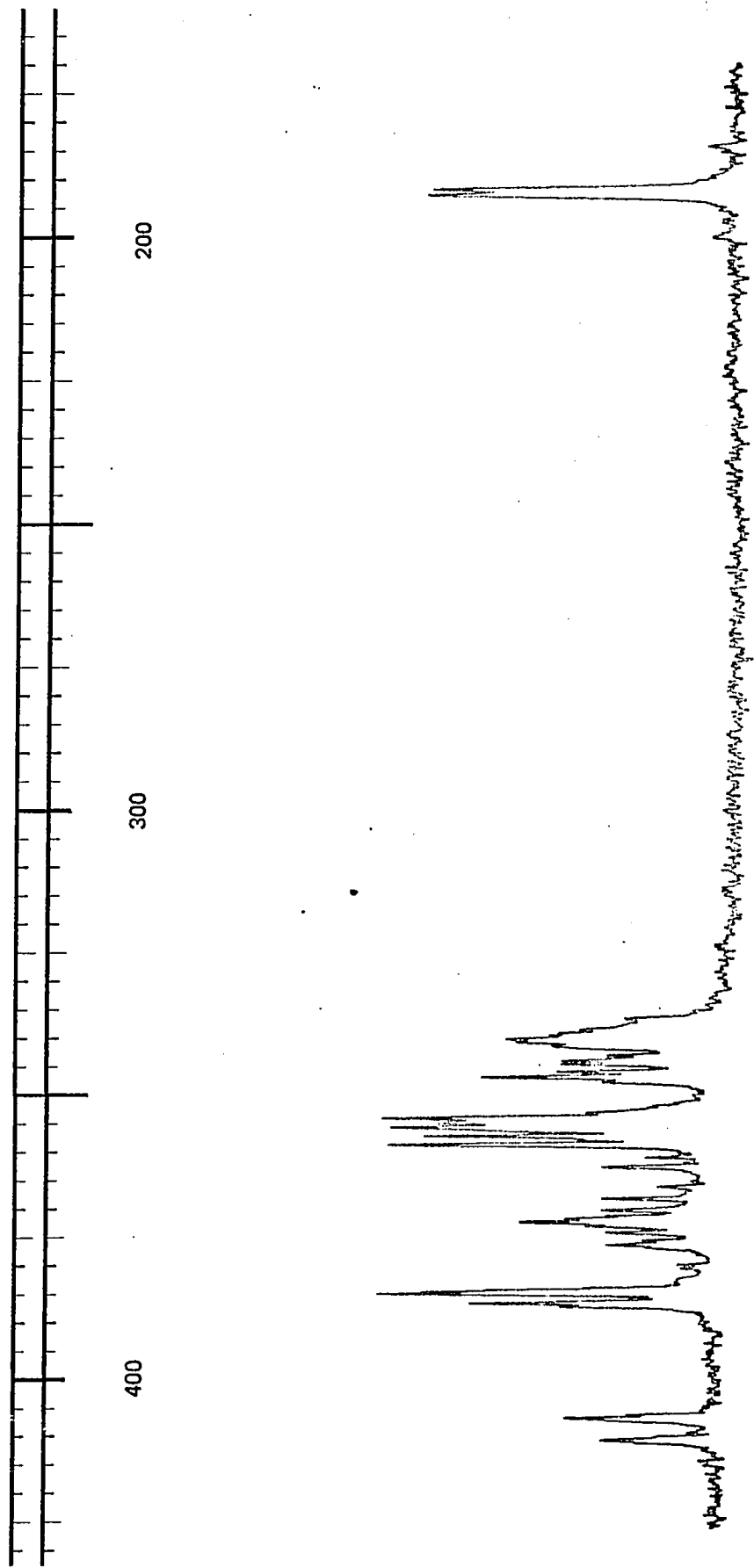


Fig. 35. 100 MHz NMR spectrum of 2-Benzyl-3-m-bromophenyl-4(3H)-quinazolinone in deuteriochloroform solution (1000 Hz scan)

Preparation of Thiohydantoins and Precursors

o-Bromophenyl isothiocyanate

o-Bromoaniline (J.T. Baker) (39.9g, 0.232 mol) in 5 vols of chloroform and thiophosgene (Anachemia) (27.1g, 0.236 mol) in 10 vols of water were stirred together for 30 minutes. The chloroform layer was separated and the chloroform distilled off. The crude isothiocyanate was fractionated through a 4 in. vacuum jacketed Vigreux column under reduced pressure at 104°. The fractions that had essentially superimposable infrared spectra were combined to give a pale yellow liquid. The purity of the product was not determined.

Yield 36.3g, 73%.

Bp 244° dec. (lit.⁵⁶ 257°/770 mm).

The infrared spectrum is shown in fig. 36.

The n.m.r. spectrum, in deuteriochloroform with 2 drops of DMSO-d₆, showed a multiplet at δ 6.9-7.6.

The molecular weight of the product was found to be correct, 214, by a study of its mass spectrum. An inlet temperature of about 100° and an ionisation voltage of 70 eV were employed. Approximately equal intensity parent peaks were found at m/e values of 213 and 215. Prominent peaks corresponding to loss of Br and NCS were also noted.

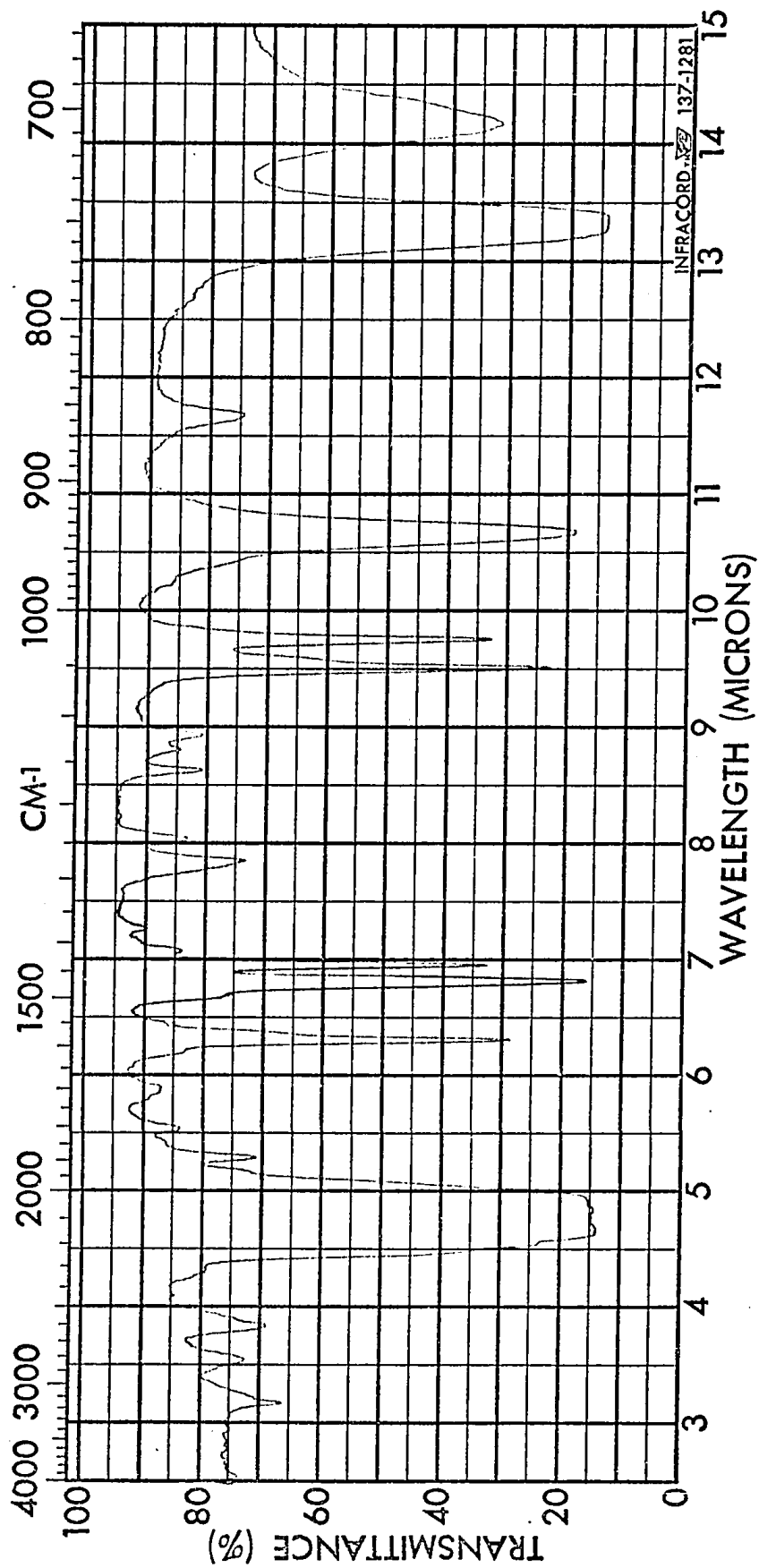


Fig. 36. Infrared spectrum of *o*-Bromophenyl isothiocyanate.

o-Chlorophenyl isothiocyanate

o-Chloroaniline (British Drug Houses) (11.2g, 0.0878 mol) in 5 vols of chloroform and thiophosgene (K and K) (10.3g, 0.0895 mol) in 10 vols of water were stirred together for 30 minutes. The chloroform layer was separated and a white solid that had formed in the chloroform layer was removed by filtration. The chloroform was distilled off and the crude isothiocyanate was fractionated through a 4 in. vacuum jacketed Vigreux column under reduced pressure at 98°. The middle fractions were combined to give a pale yellow liquid. The purity of the product was not determined.

Yield 8.4g, 56%.

The infrared spectrum is shown in fig. 37.

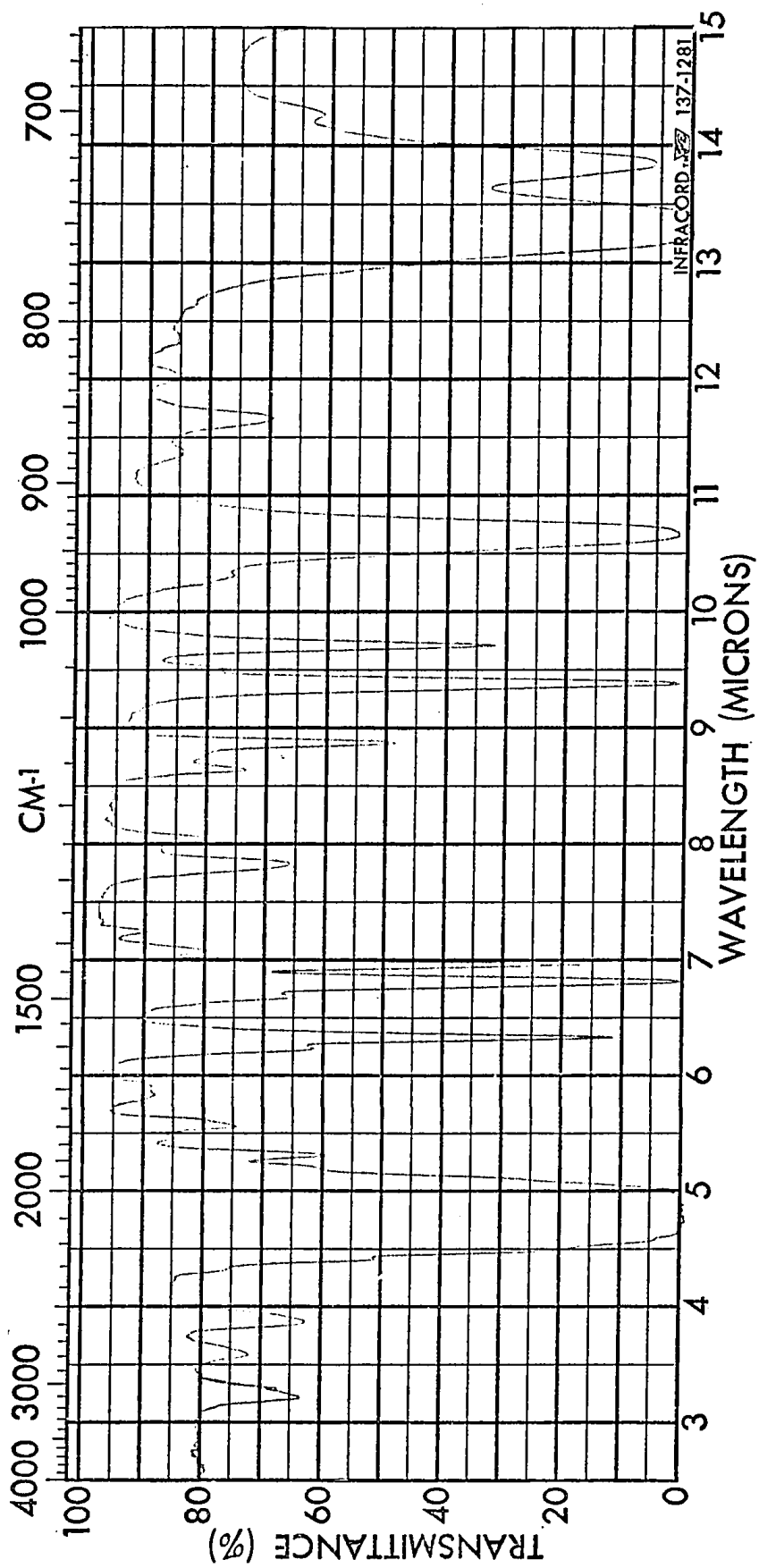


Fig. 37. Infrared spectrum of o-Chlorophenyl isothiocyanate.

o-Methoxyphenyl isothiocyanate

o-Methoxyaniline (Aldrich) (10.7g, 0.0869 mol) in 5 vols of chloroform and thiophosgene (K and K) (10.5g, 0.0913 mol) in 10 vols of water were stirred together for 30 minutes. The chloroform layer was separated and dried over molecular sieves. The volatile components were removed by simple distillation under reduced pressure at 96°. All but the centre fraction was discarded. The product was a dark brown oil of unknown purity.

Yield 6.0g, 42%.

The infrared spectrum is shown in fig. 38.

3-o-Bromophenyl-5-methyl-2-thiohydantoin

D,L-Alanine (Eastman) (13.7g, 0.154 mol) was dissolved in a solution of water (20 ml) and sodium hydroxide (10.1g). o-Bromophenyl isothiocyanate (33.0g, 0.154 mol) was dissolved in ethanol (100 ml) and this solution was added to the alanine solution. The reaction mixture was refluxed for 30 minutes and then

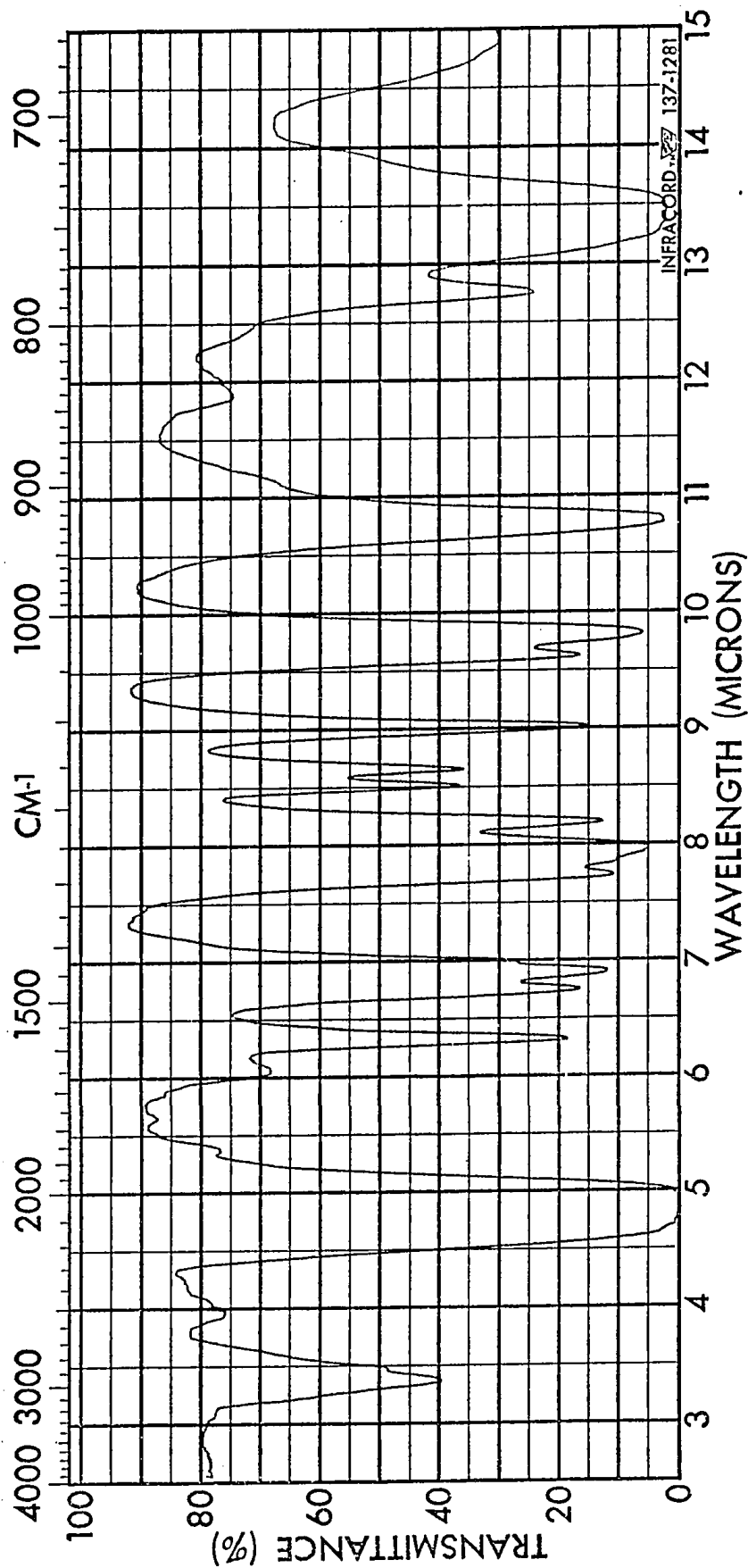


Fig. 38. Infrared spectrum of *o*-Methoxyphenyl isothiocyanate.

allowed to cool to room temperature. The addition of hydrochloric acid (6N, 140 ml) was accompanied by the evolution of a gas smelling like hydrogen sulphide and the formation of a dark brown oil. The oil was removed from the mixture as quickly as was possible using a disposable pipette. It solidified on standing for 5 minutes. The crude product was recrystallised from ethanol (3 times) and from methanol (twice) to give white crystals. The product was a ca. 2:1 mixture of the thermodynamically preferred (low field methyl n.m.r. signal) diastereomer.

Yield 3.1g, 7.1%.

Mp 216-218°.

The infrared spectrum is shown in fig. 39.

The n.m.r. spectrum is shown in fig. 40. DMSO-d₆ was used as solvent.

Aromatic, δ 7.2-7.9, multiplet, integration 3.8 H.

Methine, diastereomer A, δ 4.487, J 7.1 Hz, quartet.

Methine, diastereomer B, δ 4.572, J 7.2 Hz, quartet.

Integration of methine protons 0.9 H.

Methyl, diastereomer A, δ 1.423, J 7.0 Hz, doublet.

Methyl, diastereomer B, δ 1.437, J 7.0 Hz, doublet.

Integration of methyl protons 3.0 H.

With pyridine as solvent the methyl group of diastereomer A shows a doublet at δ 1.431, J 7.1 Hz and the methine

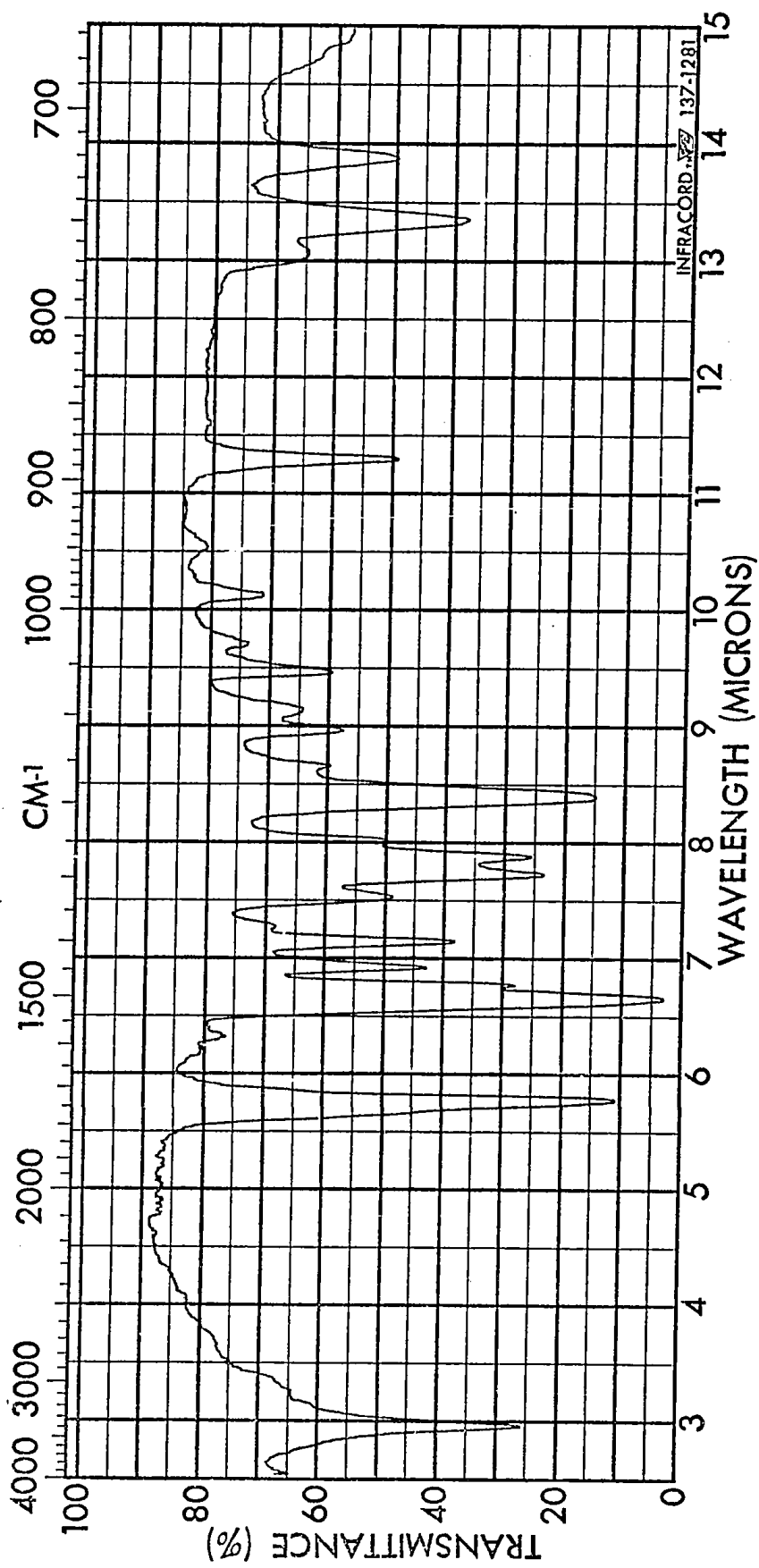


Fig. 39 Infrared spectrum of
3-o-Bromophenyl-5-methyl-2-thiohydantoin.

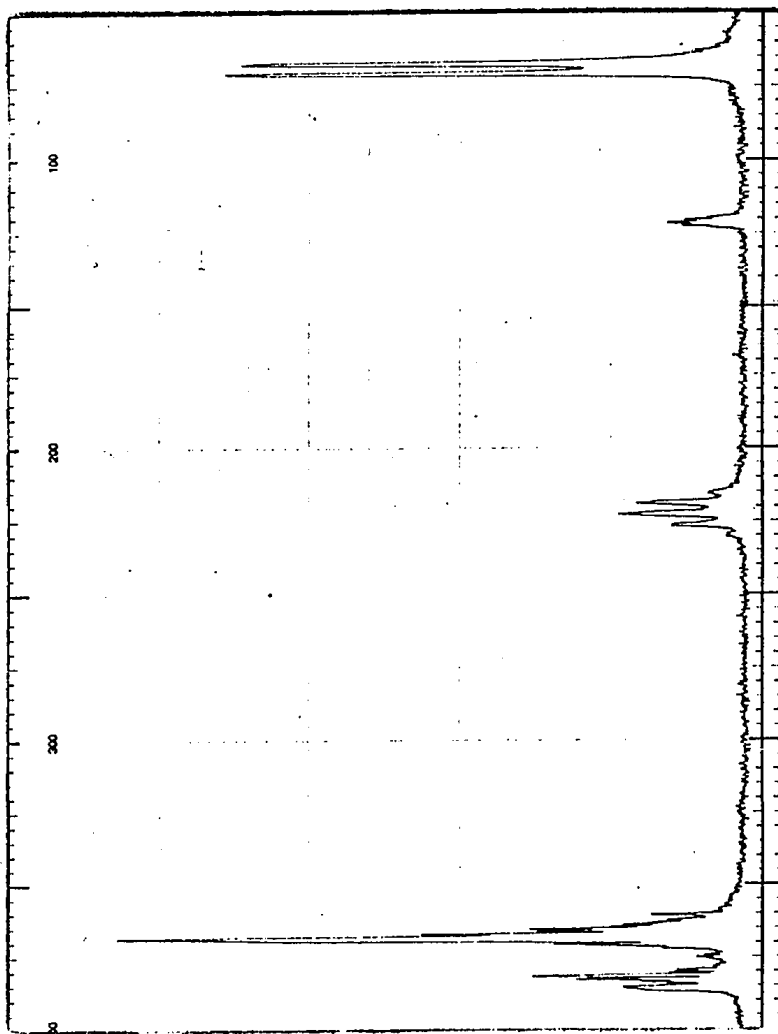


Fig. 40. 100 MHz NMR spectrum of
3-p-Bromophenyl-5-methyl-2-thiohydantoin
in DMSO-d₆ solution (1000 Hz scan)

shows as a quartet at δ 4.459, J 7.1 Hz. Diastereomer B gives a doublet at δ 1.502, J 7.1 Hz and the methine shows as a quartet at δ 4.631, J 7.1 Hz.

In pyridine, with both diastereomers present, the methyl region shows a triplet since there is overlap of two peaks.

Elemental analysis; calculated C 42.10, H 3.15, N 9.82; found C 42.22, H 3.33, N 9.76.

The isolation of the thermodynamically less stable diastereomer was achieved by slow recrystallisation from methanol. The process took several days. A ratio of about 100 ml of solvent per gram of material was employed.

3-o-Tolyl-5-methyl-2-thiohydantoin

D,L-Alanine (Eastman) (3.00g, 0.0337 mol) was dissolved in a solution of water (6 ml) and sodium hydroxide (2.4g). *o*-Tolyl isothiocyanate (K and K) (5.00g, 0.0335 mol) was dissolved in ethanol (30 ml) and this solution was added to the alanine solution. The reaction mixture was refluxed for 10 minutes and then allowed to cool to room temperature. The addition of hydrochloric acid (6N, 39 ml) was accompanied by the evolution of a gas smelling like hydrogen sulphide and

the formation of a yellow oil. The oil was removed from the reaction mixture as quickly as was possible using a disposable pipette. It solidified on standing for 2 minutes. The crude product was recrystallised from ethanol 3 times to give white crystals. The product contained at least 95% of the thermodynamically less stable (high field methyl n.m.r. signal) diastereomer.

Yield 0.67g, 9.1%.

Mp 205-207°.

The infrared spectrum is shown in fig. 41.

The n.m.r. spectrum is shown in fig. 42. DMSO-d₆ was used as solvent.

Aromatic, δ 6.8-7.6, multiplet, integration 3.8 H.

Methine, diastereomer A, δ 4.546, J 7.0 Hz, quartet.

Methine, diastereomer B, δ 4.558, J 7.0 Hz, quartet.

Integration of methine protons 0.9 H.

Tolyl methyl, δ 2.103, singlet, integration 3.0 H.

Methyl, the diastereomers have the same chemical shift in the methyl region, δ 1.412, J 7.0 Hz, doublet, integration 2.9 H.

In pyridine at 57.5° there is a chemical shift difference between the two methyl signals of the diastereomers.

Diastereomer A shows a doublet at δ 1.413, J 7.0 Hz.

Diastereomer B shows a doublet at δ 1.429, J 7.1 Hz.

Elemental analysis; calculated C 60.00, H 5.46, N 12.73;

found C 59.83, H 5.36, N 12.77.

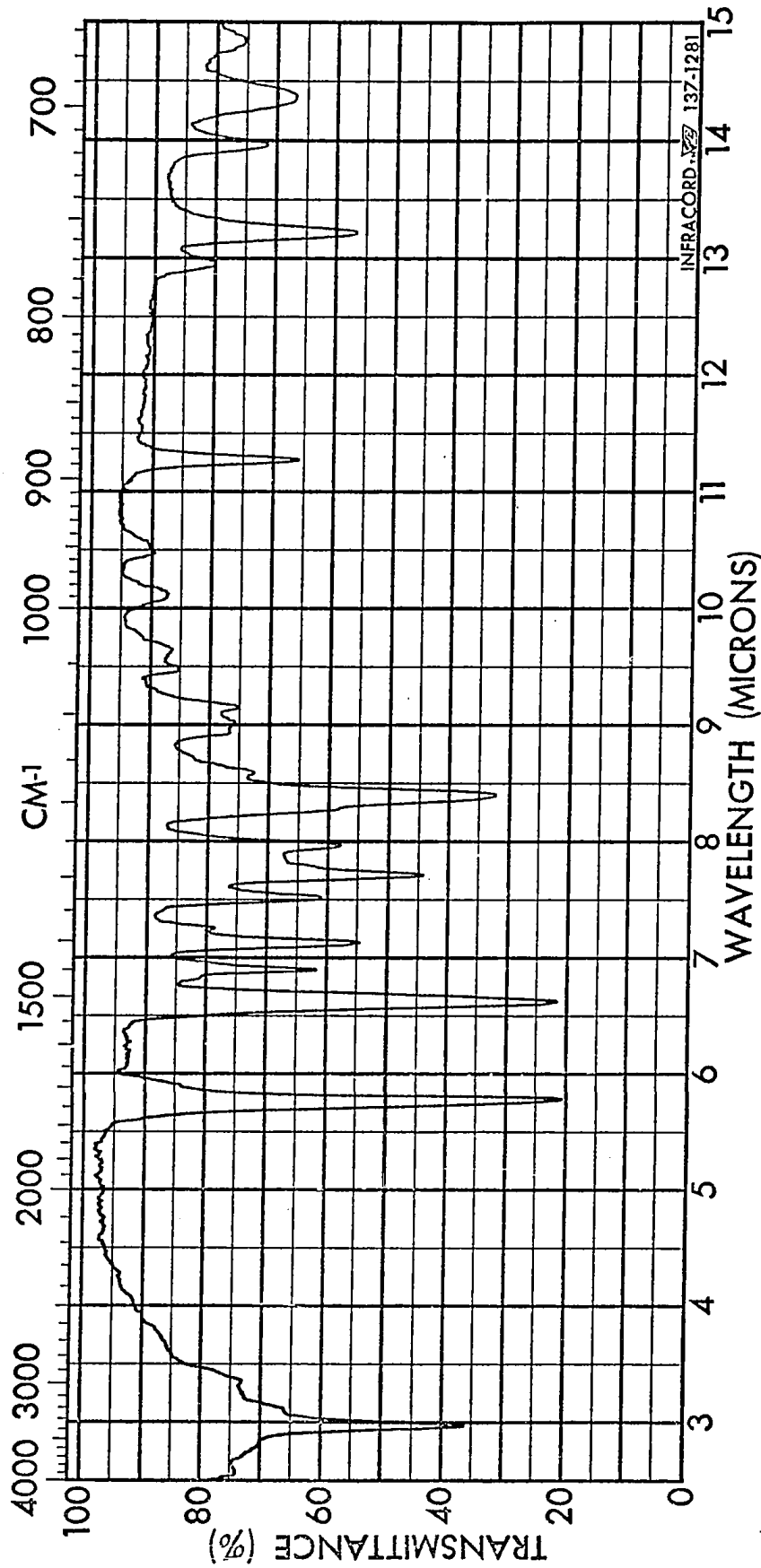


Fig. 41. Infrared spectrum of 3-o-Tolyl-5-methyl-2-thiohydantoin

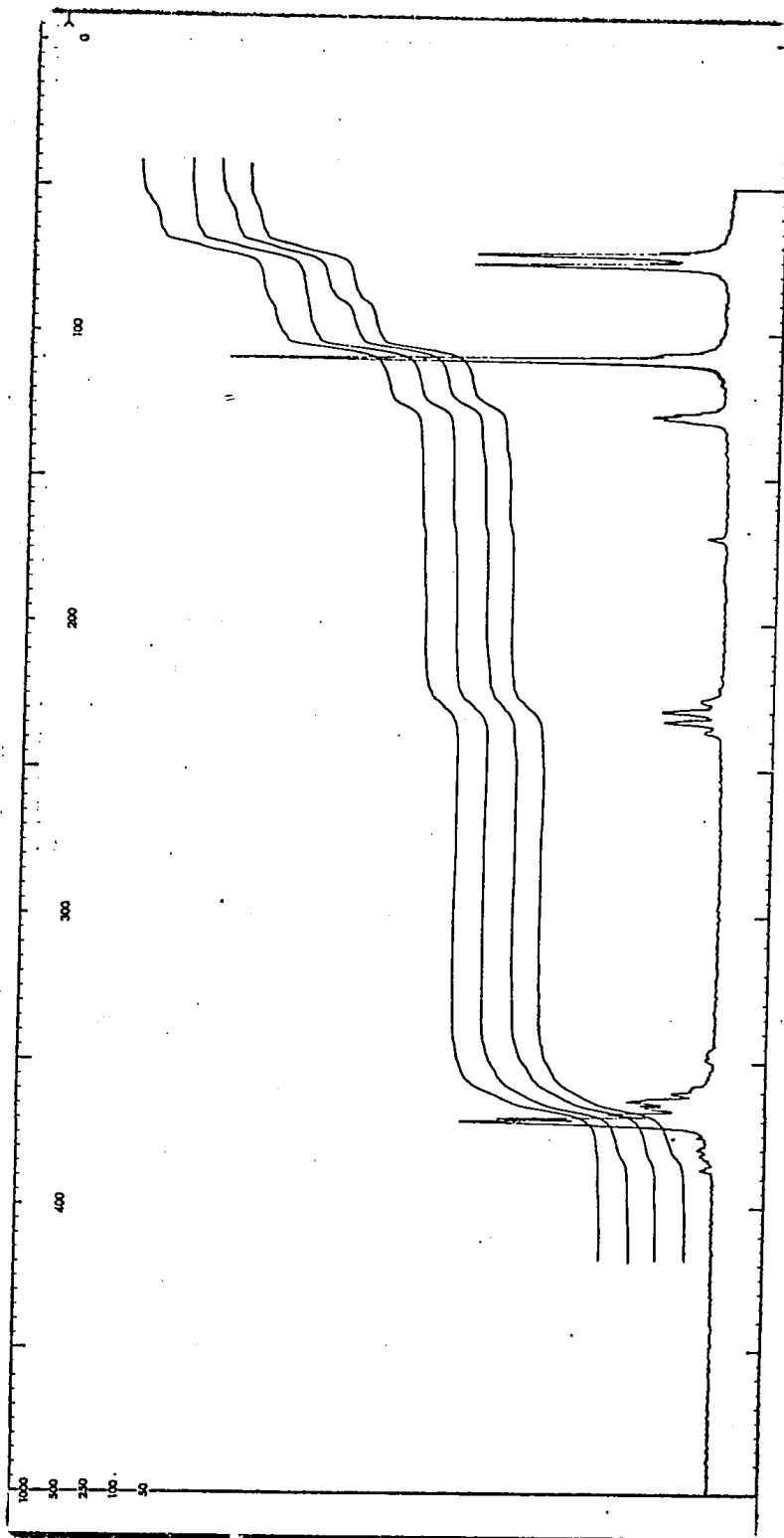


Fig. 42. 100 MHz NMR spectrum of 3-o-Tolyl-5-methyl-2-thiohydantoin in DMSO-d₆ solution (1000 Hz scan)

3-o-Chlorophenyl-5-methyl-2-thiohydantoin

D,L-Alanine (Eastman) (1.33g, 0.0150 mol) was dissolved in a solution of water (2 ml) and sodium hydroxide (1.0g). *o*-Chlorophenyl isothiocyanate (2.55g, 0.0150 mol) was dissolved in ethanol (10 ml) and this solution was added to the alanine solution, giving a black solution. The reaction mixture was refluxed for 10 minutes and then allowed to cool to room temperature. The addition of hydrochloric acid (6N, 19 ml) was accompanied by the evolution of a gas smelling like hydrogen sulphide and the formation of a brown oil that solidified very quickly. The solid was removed from the reaction mixture as quickly as was possible. The crude product was recrystallised twice from ethanol to yield a product that contained at least 95% of the thermodynamically less stable (high field methyl n.m.r. signal) diastereomer.

Yield 0.3g, 8.3%.

Mp 193-195°.

The infrared spectrum is shown in fig. 43.

In pyridine the n.m.r. spectrum shows:

Methine, diastereomer A, δ 4.624, J 7.1 Hz, quartet.

Methine, diastereomer B, δ 4.454, J 7.1 Hz, quartet.

Methyl, diastereomer A, δ 1.423, J 7.0 Hz, doublet.

Methyl, diastereomer B, δ 1.469, J 7.0 Hz, doublet.

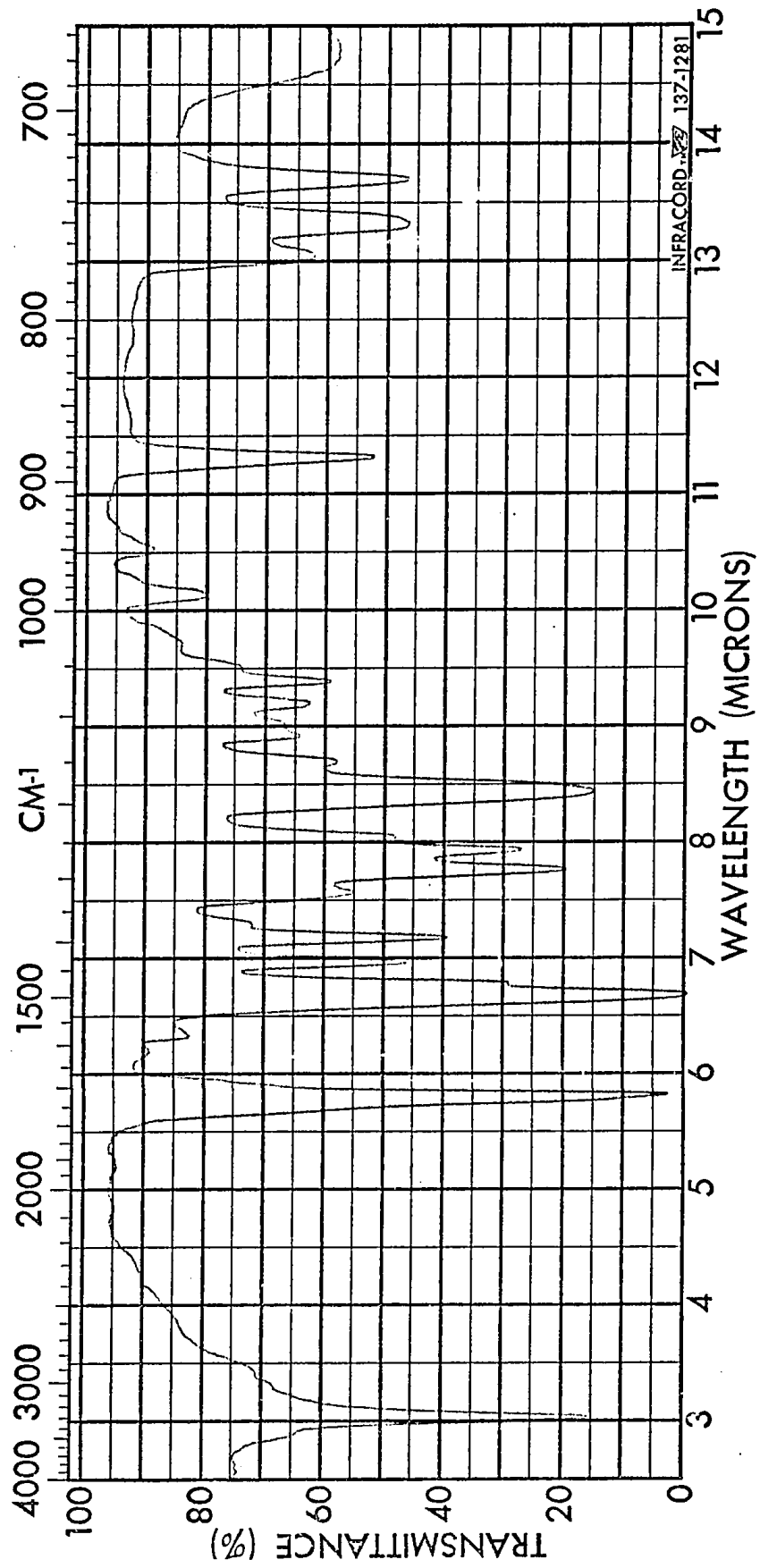


Fig. 43. Infrared spectrum of 3-o-chlorophenyl-5-methyl-2-thiohydantoin

Elemental analysis; calculated C 49.79, H 3.73, N 11.62;
found C 49.77, H 3.76, N 11.69.

3-o-Methoxyphenyl-5-methyl-2-thiohydantoin

D,L-Alanine (Eastman) (2.90g, 0.0326 mol) was dissolved in a solution of water (6ml) and sodium hydroxide (3.05g). *o*-Methoxyphenyl isothiocyanate (3.4g, 0.0228 mol) was dissolved in methanol (30 ml) and this solution was added to the alanine solution. The reaction mixture was refluxed for 30 minutes during which time some solid material came out of solution. The mixture was allowed to cool to room temperature and the solid material was removed by filtration. The addition of hydrochloric acid (6N, 25 ml) to the reaction mixture was accompanied by the evolution of a gas smelling like hydrogen sulphide and the formation of a brown oil which solidified quickly to give a brown solid. Infrared analysis showed that the thiohydantoin was not a major constituent of the brown solid. After standing for 2 hours the reaction mixture yielded a yellow solid. The solid was recrystallised from methanol to yield buff coloured crystals of the desired product. The product contained at least 95% of the thermodynamically less stable (high field methyl n.m.r. signal in pyridine) diastereomer.

Yield 0.84g, 15.6%.

Mp 156-158°.

The infrared spectrum is shown in fig. 44.

The n.m.r. spectrum is shown in fig. 45. DMSO-d₆ was used as solvent.

Aromatic, δ 6.8-7.5, multiplet, integration 3.8 H.

Methine, less stable diastereomer, δ 4.430, quartet, J 7.0 Hz.

Integration of methine protons 1.1 H.

Methoxy methyl, δ 3.671, singlet, integration 2.7 H.

Methyl, less stable diastereomer, δ 1.329, doublet, J 7.0 Hz.

Integration of methyl signals 3.0 H.

In pyridine the methyl signal of the more stable diastereomer shows as a doublet at δ 1.433, J 7.0 Hz, while the methyl signal of the less stable diastereomer shows as a doublet at δ 1.394, J 7.0 Hz.

Elemental analysis; calculated C 55.93, H 5.09, N 11.86;
found C 55.89, H 5.02, N 11.90.

3-o-Fluorophenyl-5-methyl-2-thiohydantoin

D,L-Alanine (Eastman) (2.40g, 0.027 mol) was dissolved in a solution of water (4 ml) and sodium hydroxide (2.0g). 2-Fluorophenyl isothiocyanate (Pfaltz and Bauer) (3.00g, 0.021 mol) was dissolved in ethanol (20 ml) and this solution was added to the alanine solution. The reaction mixture was refluxed for 10 minutes and then

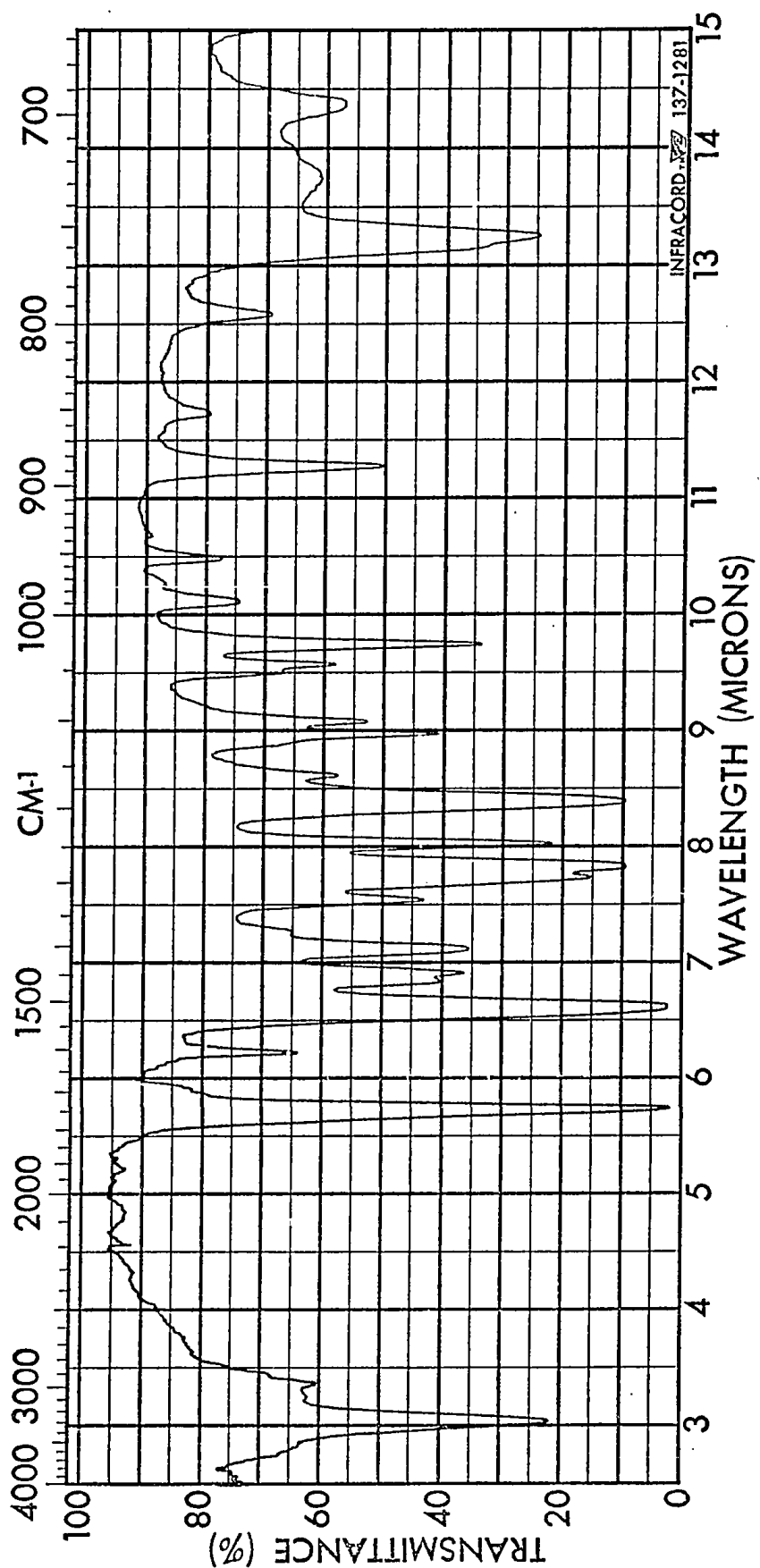


Fig. 44. Infrared spectrum of 3-o-Methoxyphenyl-5-methyl-2-thiohydantoin

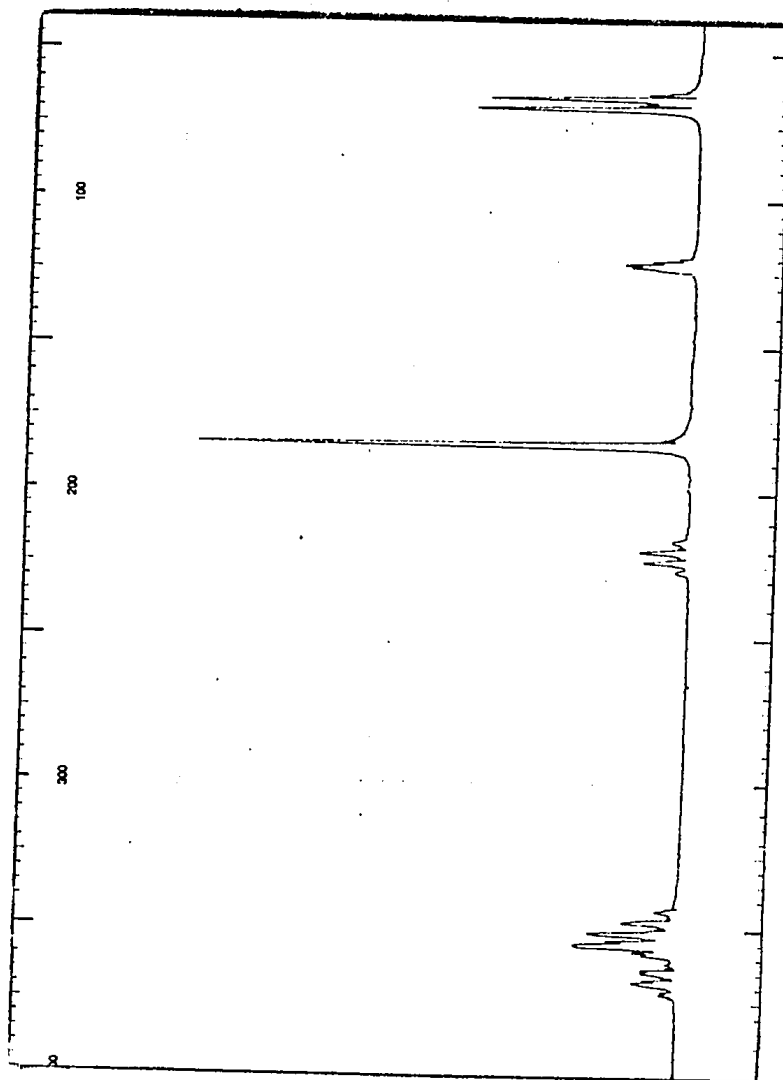


Fig. 45. 100 MHz NMR spectrum of
3-O-Methoxyphenyl-5-methyl-2-thiohydantoin
in DMSO- d_6 solution (1000 Hz scan)

allowed to cool to room temperature. The addition of hydrochloric acid (6N, 29 ml) was accompanied by the evolution of a gas smelling like hydrogen sulphide and the formation of a colourless oil. The oil was quickly removed from the reaction mixture using a disposable pipette, and on standing for 5 minutes yielded a white solid. The crude product was recrystallised twice from ethanol.

Yield 0.32g, 7.2%.

Mp 165-167°.

The infrared spectrum is shown in fig. 46.

The n.m.r. spectrum is shown in fig. 47. DMSO-d₆ was used as solvent.

Aromatic, 7.1-7.7, multiplet, integration 4.2 H.

Methine, 16 peak multiplet*, integration 0.9 H.

One quartet is centred at 4.469 while the other is centred at 4.569. Both quartets have coupling constants of 7.1 Hz.

No experiment was carried out to determine which methine signal corresponds with which methyl signal.

Methyl, diastereomer A, 1.353, J 7.1 Hz, doublet.

Methyl, diastereomer B, 1.386, J 7.0 Hz, doublet.

It was not determined which methyl signal came from the

* The 16 peaks are due to the proton on nitrogen splitting each of the two quartet peaks. The coupling constant for this splitting is 1.3 Hz. This was proven by replacing the hydrogen on nitrogen with deuterium⁵⁷. To the solution in the n.m.r. tube, was added 3 drops of D₂O and 2 drops of triethylamine. The solution was shaken for 5 minutes and then allowed to stand over molecular sieves for 6 days. The n.m.r. spectrum then showed an 8 peak multiplet in the methine region.

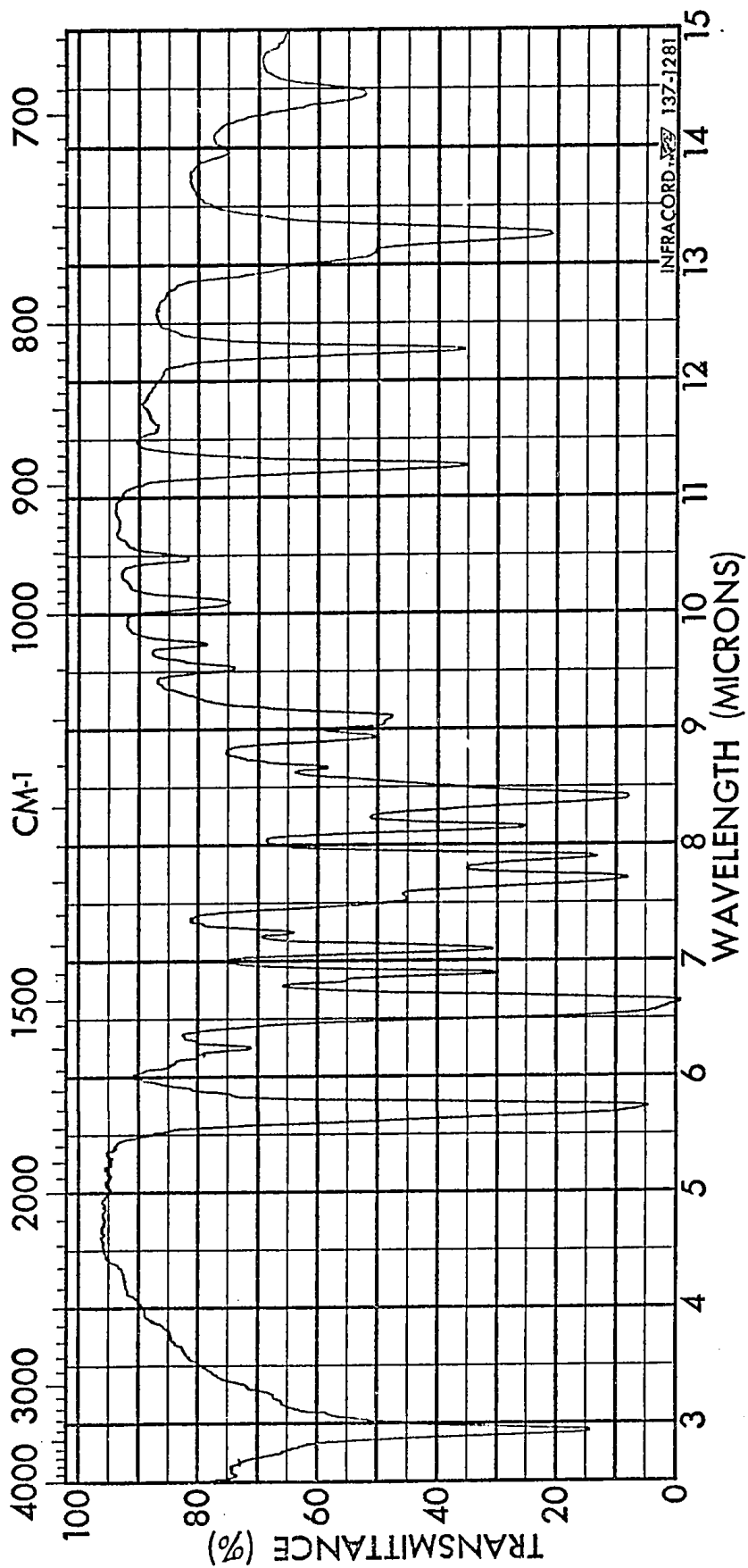


Fig. 46. Infrared spectrum of 3-o-Fluorophenyl-5-methyl-2-thiohydantoin

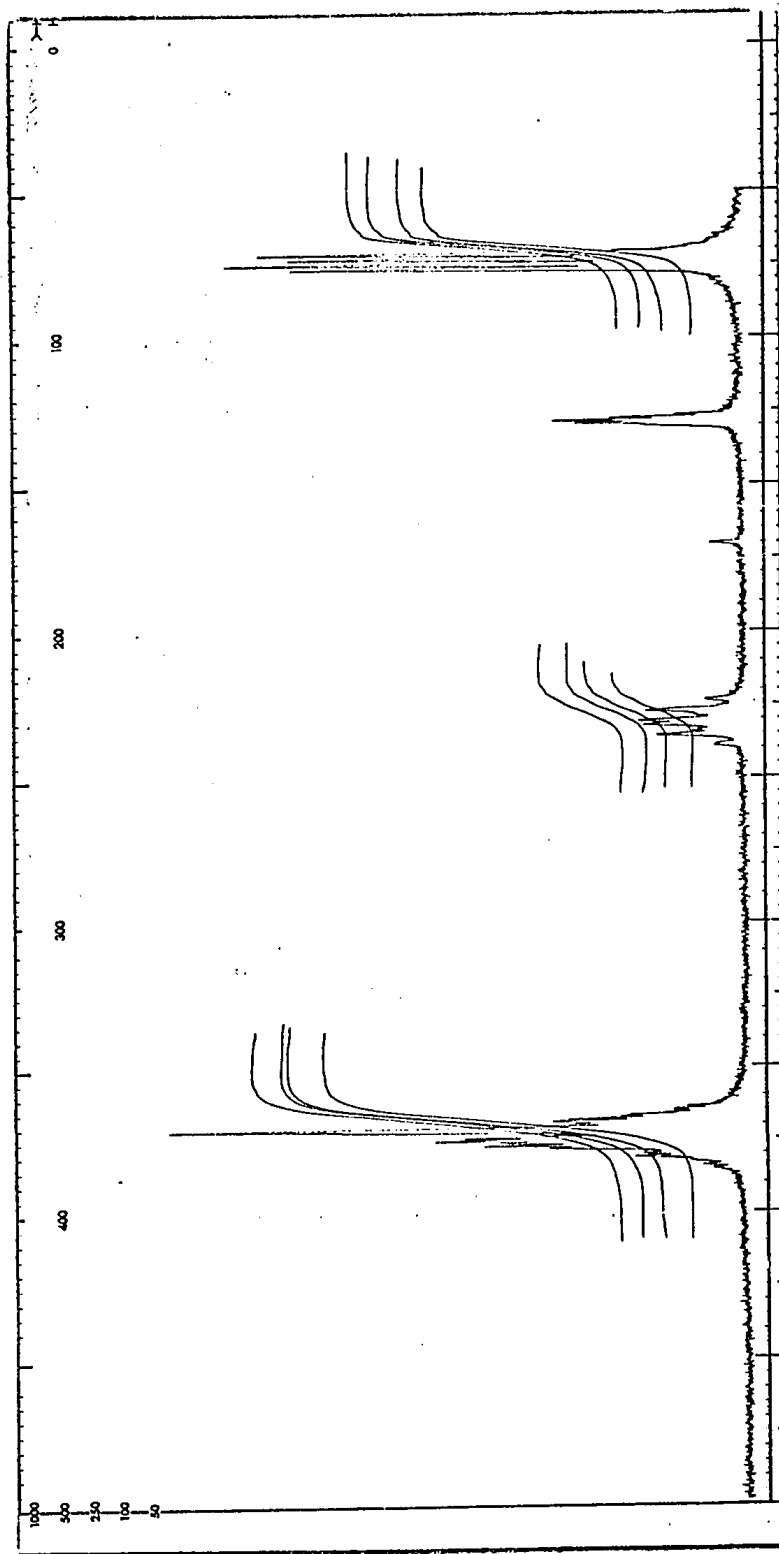


Fig. 47. 100 MHz NMR spectrum of 3-o-Fluorophenyl-5-methyl-2-thiohydantoin in DMSO-d₆ solution (1000 Hz scan)

thermodynamically more stable diastereomer.

Integration of methyl signals 3.0 H.

Elemental analysis; calculated C 53.57, H 4.02, N 12.50;

found C 53.42, H 4.18, N 12.41.

3- β -Naphthyl-5-methyl-2-thiohydantoin

D,L-Alanine (Eastman) (2.40g, 0.027 mol) was dissolved in a solution of water (4 ml) and sodium hydroxide (2.05g). β -Naphthyl isothiocyanate (Pfaltz and Bauer) (5.00g, 0.027 mol) was dissolved in ethanol (20 ml) and this solution was added to the alanine solution. A cloudy suspension resulted. The reaction mixture was refluxed for 30 minutes during which time the suspension disappeared. The mixture was then allowed to cool to room temperature. The addition of hydrochloric acid (6N, 26 ml) was accompanied by the evolution of a gas smelling like hydrogen sulphide and the formation of brown and white precipitates. The white precipitate would not dissolve in cold pyridine and was discarded. The brown precipitate was recrystallised twice from ethanol to give a fluffy white solid.

Yield 1.30g, 18.5%.

Mp 213-215°.

The infrared spectrum is shown in fig. 48

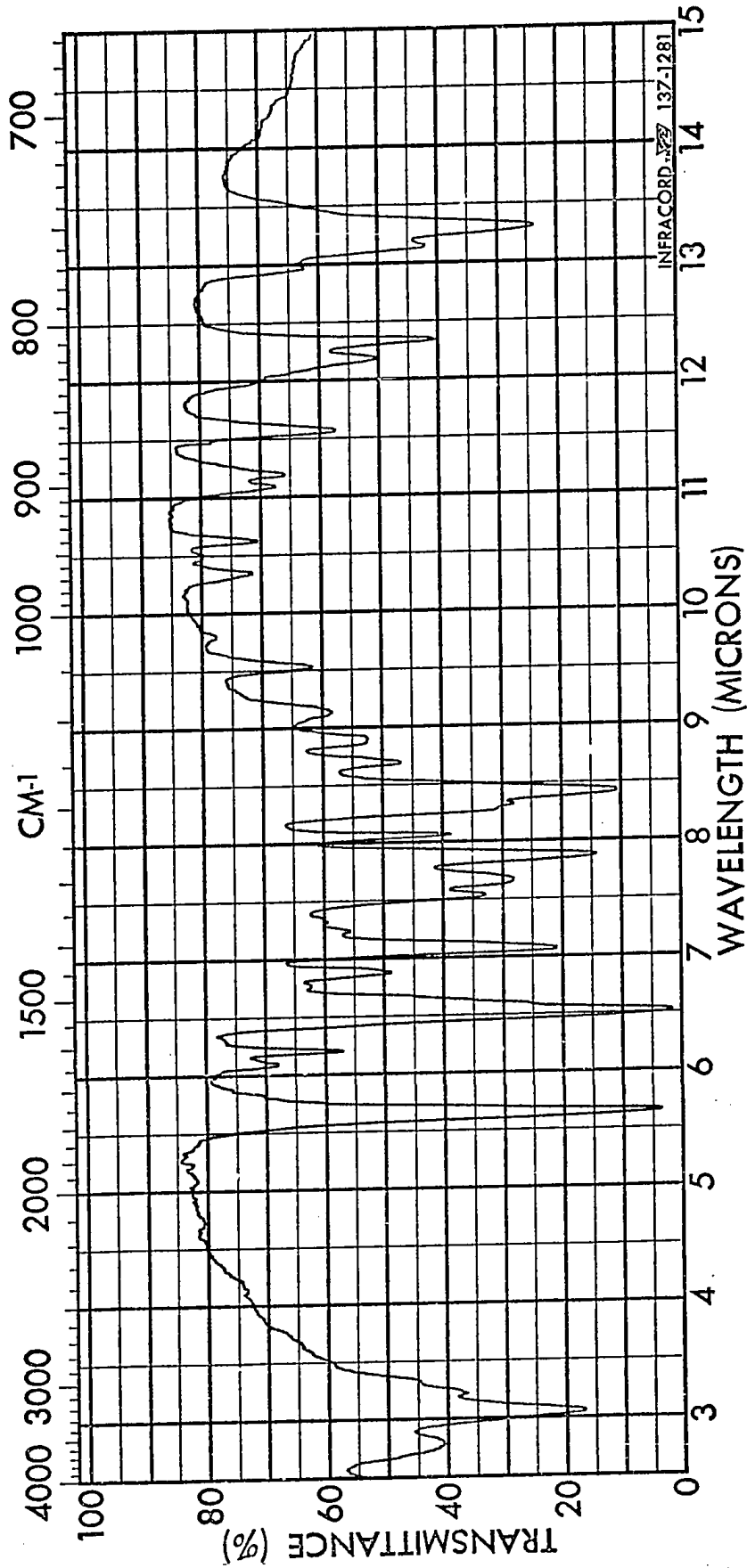


Fig. 48. Infrared spectrum of
3-β-Naphthyl-5-methyl-2-thiopyridone

The n.m.r. spectrum is shown in fig. 49. DMSO-d₆ was used as solvent.

Aromatic, δ 7.2-8.1, multiplet, integration 7.1 H.

Methine, diastereomer A, δ 4.532, J 7.2 Hz, quartet.

Methine, diastereomer B, δ 4.543, J 7.2 Hz, quartet.

Integration of methine signals 0.98 H.

The diastereomers have the same chemical shift in the methyl region, δ 1.460, J 7.1 Hz, integration 3.0 H.

For reasons of insolubility of the compound or small chemical shift difference between the signals of the diastereomers, the following solvents were found to be unsuitable for n.m.r. studies: methyl cyanide, ethylene dichloride, ethyl acetate, acetone, ethanol and nitromethane.

Elemental analysis; calculated C 65.63, H 4.69, N 10.94;
found C 65.83, H 4.41, N 10.81.

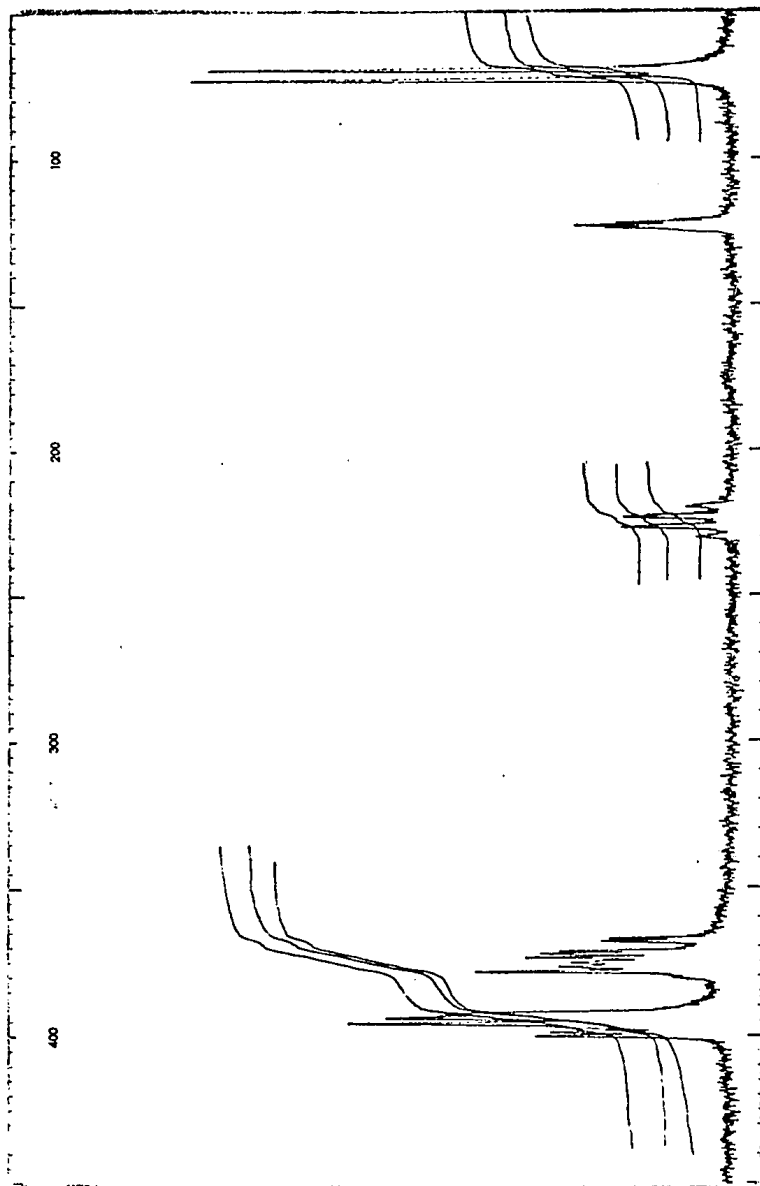


Fig. 49. 100 MHz NMR spectrum of
3- β -Naphthyl-5-methyl-2-thiohydantoin
in DMSO- d_6 solution (1000 Hz scan)

REFERENCES

1. W. E. Bentz, L. D. Colebrook, and J. R. Fehlner, Chem. Commun., 974 (1970).
2. L. D. Colebrook, H. G. Giles, and A. Rosowsky, Tetrahedron Lett., 5239 (1972).
3. L. D. Colebrook, H. G. Giles, A. Granata, S. Icli, and J. R. Fehlner, Can. J. Chem., In press.
4. J. R. Fehlner, Ph.D. Thesis, University of Rochester, 1970.
5. W. E. Bentz, Ph.D. Thesis, University of Rochester, 1971.
6. F. Hund, Ph.D. Thesis, University of Rochester, 1971.
7. D. F. Williams, M.Sc. Thesis, Sir George Williams University, 1972.
8. A. Granata, M.Sc. Thesis, Sir George Williams University, 1972.
9. S. Icli, Personal Communication.
10. D. J. Millen, in "Progress in Stereochemistry", Vol 3, P. B. D. de la Mare and W. Klyne, Eds., Butterworths, London, 1962, p 138.
11. D. M. Hall and M. M. Harris, J. Chem. Soc., 490 (1960).
12. A. S. Cooke and M. M. Harris, ibid., 2365 (1963).

13. C. C. K. Ling and M. M. Harris, ibid., 1825 (1964).
14. Y. Badar, A. S. Cooke, and M. M. Harris, ibid., 1412 (1965).
15. A. S. Cooke and M. M. Harris, J. Chem. Soc., C, 988 (1967).
16. R. Adams, Rec. Chem. Progr., 10, 91 (1949).
17. G. Binsch, in "Topics in Stereochemistry", Vol. 3, E. L. Eliel and N. L. Allinger, Eds., Interscience Publishers, New York, 1968, p 97.
18. R. J. Gillespie and R. F. M. White, in "Progress in Stereochemistry", P. B. D. de la Mare and W. Klyne, Eds., Butterworths, London, 1962, p 53.
19. Y. Shvo, E. C. Taylor, K. Mislow, and M. Raban, J. Amer. Chem. Soc., 89, 4910 (1967).
20. L. Pauling, "The Nature of the Chemical Bond", 3rd ed., Cornell University Press, Ithaca, New York, p 260.
21. United States Patent Office, No. 3,452,019, June 24, 1969.
22. Ibid., No. 3,452,020, June 24, 1969.
23. A. Rosowsky, G. E. Foley, and E. J. Modest, Personal Communication.
24. Imperial Chemical Industries Ltd., Belgian Patent 629-79 (1963); Chem. Abstr., 60, 14512 f (1965).
25. "The Merck Index", Merck and Co., Inc., Rahway, New

Jersey, 1968.

26. R. J. Kurland, M. B. Rubin, and W. B. Wise, J. Chem. Phys., 40, 2426 (1964).
27. W. J. Moore, "Physical Chemistry", Prentice Hall, Englewood Cliffs, New Jersey, 1964, Chapter 8.
28. J. A. Pople, W. G. Schneider, and H. J. Bernstein, "High Resolution Nuclear Magnetic Resonance", McGraw-Hill, New York, 1959, p 223.
29. E. L. Eliel, "Stereochemistry of Carbon Compounds", McGraw-Hill, New York, 1962, Chapter 4.
30. W. J. Moore, "Physical Chemistry", Prentice Hall, Englewood Cliffs, New Jersey, 1964, p 264.
31. S. Glasstone and D. Lewis, "Elements of Physical Chemistry", MacMillan and Co., London, 1965, p 627.
32. C. H. Bamford and C. F. H. Tipper, "Comprehensive Chemical Kinetics", Vol. 1, Elsevier, Amsterdam, 1969, p 404.
33. Idem, ibid., p 374.
34. "Handbook of Chemistry and Physics", The Chemical Rubber Co., Cleveland, Ohio, 1968, p A-161.
35. J. Klosa, J. prakt. Chem., 20, 283 (1963).

36. K. Mislow and M. Raban, in "Topics in Stereochemistry", Vol. 1, N. L. Allinger and E. L. Eliel, Eds., Interscience Publishers, New York, 1967, p 1.
37. F. A. Bovey, "Nuclear Magnetic Resonance Spectroscopy", Academic Press, New York, 1969, p 129.
38. M. Stiles, J. Amer. Chem. Soc., 81, 2598 (1959).
39. H. K. Pujari and M. K. Rout, J. Indian Chem. Soc., 31, 937 (1954).
40. P. D. Lark, B. R. Craven, and R. C. L. Bosworth, "Handling of Chemical Data", Pergamon Press, Oxford, 1968, p 53.
41. G. H. Stout and L. H. Jensen, "X-Ray Structure Determination", MacMillan and Co., New York, 1968.
42. A. D. Adley, P. H. Bird, A. R. Fraser, and M. Onyszchuk, Inorg. Chem., 11, 1402 (1972).
43. T. C. Farrar and E. D. Becker, "Pulse and Fourier Transform NMR", Academic Press, New York, 1971.
44. R. M. Silverstein and G. C. Bassler, "Spectrometric Identification of Organic Compounds", John Wiley and Sons, New York, 1968, p 116.
45. B. H. Mahan, "University Chemistry", Addison-Wesley, Reading, Massachusetts, 1966, p 296.

46. L. A. Walker, K. Folting, and L. L. Merritt,
Acta Crystalogr., B 25, 88 (1969).
47. A. Camerman and N. Camerman, Acta Crystalogr., B 27,
2205 (1971).
48. "Tables of Interatomic Distances and Configurations
in Molecules and Ions", Special Publication No. 11,
The Chemical Society, London, Section A.
49. E. L. Eliel, "Stereochemistry of Carbon Compounds",
McGraw-Hill, New York, 1962, pp. 156-164.
50. E. L. Eliel, N. L. Allinger, S. L. Angyal, and G. A.
Morrison, "Conformational Analysis", New York, 1965,
Ch. 7.
51. T. H. Elliot and P. N. Natarajan, J. Pharm. Pharmac.,
19, 209 (1967).
52. H. S. Kimmel and A. Saifer, Anal. Biochem., 9, 316 (1964).
53. T. Tadatoshi and H. Sakurai, Chem. Commun., 362 (1972).
54. R. N. Haszeldine, J. Chem. Soc., 3423 (1952).
55. H. de Diesbach, J. Gross, and W. Tschannen,
Helv. Chim. Acta, 34, 1050 (1951).
56. G. M. Dyson, H. J. George, and R. F. Hunter,
J. Chem. Soc., 436 (1927).

57. L. M. Jackman and S. Sternhell, "Applications of Nuclear Magnetic Resonance Spectroscopy in Organic Chemistry", Pergamon Press, Oxford, 1969, p 360.
58. H. S. Gutowsky and C. H. Holm, J. Chem. Phys., 25, 1228 (1956).
59. J. A. Pople, W. G. Schneider, and H. J. Bernstein, "High Resolution Nuclear Magnetic Resonance", McGraw-Hill, New York, 1959, pp. 218-224.

APPENDIX

PROGRAMME WAYTPA

This programme calculates Arrhenius and Eyring activation parameters at 90% confidence limits from inputted temperatures, lifetimes and errors in lifetimes. It uses a weighted least squares analysis to fit the Arrhenius equation (in logarithmic form) to the input data. It is assumed that there are no errors in the temperatures.

The equation is

$$\ln(1/\tau) = \ln(A) - E_a/RT$$

Error analysis is given at each stage of the calculation, i.e. following the regression calculations, following the Arrhenius calculations and following the Eyring calculations. The Eyring parameters are calculated at a temperature specified by the user.

Data cards are prepared as follows:

Item 1	Format(I3, 7A10)
NRUN	Run number. Any non-zero number will do. A zero value for NRUN terminates the job.
IDEN	Alphanumeric identification.

- Item 2 Format(F10.0)
TEMP Temperature (°K) at which the Eyring parameters
 are to be calculated.
- Item 3 Format(3F10.0)
TC(I) Temperature of measurement in °C.
TAU(I) Mean lifetime in seconds.
ROR(I) Error in lifetime in seconds.
- Item 4 Blank card.
 Note: WAYTPA does its own counting of data cards.
 This card signals the end of the experimental
 data set.

Data sets (Items 1 - 4) may be stacked one after another. The run is terminated by an additional blank card. Note: This means that there will be two blank cards at the end of the complete data deck.

There is no mathematical justification for using an unweighted least squares treatment when dealing with log functions, however, if it is desired to make a comparison with the results of a non-weighted least squares analysis a card should be inserted after the card reading:

7 CONTINUE

The card should read (starting in column 7):

$Z(1)=Z(2)=Z(3)=\dots\dots\dots Z(n)=1.0$

Where n is the number of data points..

C PROGRAM WAYTPA (INPUT, OUTPUT, TAPE5=INPUT, TAPE6=OUTPUT)

C SIR GEORGE WILLIAMS UNIVERSITY. JUNE 1972.
C FCRTRAN IV FOR CDC 6400.

C CALCULATION OF ARRHENIUS AND EYRING ACTIVATION PARAMETERS
C USING LINEAR REGRESSION ANALYSIS

C OPTIONS ALLOW FOR EQUAL WEIGHTING OF ALL POINTS OR WEIGHTING
C EACH POINT INVERSELY BY ITS VARIANCE

C THE OPTIONS ARE AUTOMATICALLY SELECTED BY THE PROGRAMME

C BASED ON

C C.H. BAMFORD AND C.F.H. TIPPER

C COMPREHENSIVE CHEMICAL KINETICS, VOL1

C ELSEVIER, AMSTERDAM, 1969, P404

C NOTE THAT THE WEIGHTING FACTORS ARE NOT BASED ON THE
C SQUARE OF THE RECIPROCAL OF THE ERROR, SEE P374

C DEDICATED TO THE 1971 BRITISH LIONS

C CONFIDENCE LIMITS ARE BASED ON SLOPE

C AND INTERCEPT OF ARRHENIUS LINE

C $K = A \cdot \exp(-EACT/RT)$

C DIMENSION IDEN(7), IAU(50), IC(50), IK(50), IR(50), REXP(50), REIT(50),
1HEXP(50), SEXP(50), SFIT(50), GEXP(50), GFIT(50)

C DIMENSION ALKE(50), ALKR(50), ROR(50), XOR(50), Z(50), DELTA(50)

C DIMENSION PCE(50)

C GK=1.98646E-3

C BK=1.38049E-16

C PK=6.6254E-27

C RKH=BK/PK

```

ALNR=ALCG(RKH)
1 READ(5,100)NRUN, IDEN
100 FORMAT(I3,7A10)
IF (NRUN.EQ.0) STOP 1
WRITE(6,101)
101 FORMAT(15H1PROGRAM WAYTPA,///1X,21(1H*),* ARRHENIUS AND EYRING ACT
IVATION PARAMETERS AND 90 PERCENT CONFIDENCE INTERVALS *,21(1H*)//
2/)
READ(5,102)TEMP
102 FORMAT(F10.0)
I=1
2 READ(5,103)T(I),TAU(I),ROR(I)
103 FORMAT(3F10.0)
ERFLAG=ROR(I)
IF (TAU(I).EQ.0.0.AND.TC(I).EQ.0.0) GO TO 3
I=I+1
GO TO 2
3 NCATA=I-1
C
C WRITE OUT EXPERIMENTAL DATA
WRITE(6,105)NRUN, IDEN
105 FCRMAT(* CASE NUMBER *,I3,10X,7A10,///)
IF(ERFLAG.NE.0.0) WRITE(6,104)
104 FORMAT(* EACH EXPERIMENTAL POINT IS INVERSELY WEIGHTED BY ITS VARI
1ANCE*,//)
IF(ERFLAG.EQ.0.0) WRITE(6,108)
108 FORMAT(* ALL EXPERIMENTAL POINTS HAVE EQUAL WEIGHTS*,///)
WRITE(6,106)
106 FORMAT(//1X,20(1H*),* EXPERIMENTAL LIFETIMES, RATE CONSTANTS, TEMP
ERATURES, ERRORS, AND WEIGHTING FACTORS *,20(1H*)//)
WRITE(6,110)
110 FORMAT(5X,*POINT*,5X,*LIFETIME*,5X,*RATE CONST
1ANT*,5X,*DEGRFES C.*),

```

```

15X,*DEGREES K.*,5X,*ERROR IN*,8X,*ERROR IN*,7X,*PERCENT*,5X,
2*WEIGHT
3T*/15X,*{SECONDS}*5X,*{(1/SECONDS)*,37X,*LIFETIME*,7X,*RATE
4CCNST.*
56X,*ERROR*,6X,*FACTOR*/)
SUMZ=0.0
DC 4 I=1,NDATA
TK(I)=TC(I)+273.16
TR(I)=1000.0/TK(I)
REXP(I)=1.0/TAU(I)
XCR(I)=0.5*(1.0/(TAU(I)-ROR(I))-1.0/(TAU(I)+ROR(I)))
PCE(I)=100.0*ROR(I)/TAU(I)
IF (ERFLAG.EQ.0.0) GO TO 4
SUMZ=SUMZ+TAU(I)/ROR(I)
4 CCNTINUE
IF (ERFLAG.EQ.0.0) GO TO 5
O=NDATA/SUMZ
DC 6 I=1,NDATA
IF (ERFLAG.EQ.0.0) Z(I)=1.0
IF (ERFLAG.EQ.0.0) GO TO 7
Z(I)=O*(TAU(I)/ROR(I))
7 CCNTINUE
WRITE(6,111)I,TAU(I),REXP(I),TC(I),TK(I),ROR(I),XCR(I),PCE(I),Z(I)
111 FORMAT(6X,I2,5X,E10.4,5X,F10.4,9X,F6.1,9X,F6.1,7X,E10.4,6X,E10.4,5
1X,F6.2,6X,F6.2)
6 CCNTINUE
C
C
REGRESSION CALCULATIONS
WRITE(6,120)
120 FORMAT(////1X,21(1H*)) * LINEAR REGRESSION TO ARRHENIUS EQUATION *,
120(1H*)//)
SUMZX=SUMZY=SUMZXY=SUMZXX=SUMXX=SUMX=0.0

```

```

DC 8 I=1,NDATA
ALKE(I)=ALOG(REXP(I))
SUMZX=SUMZX+Z(I)/TK(I)
SUMZY=SUMZY+Z(I)*ALOG(REXP(I))
SUMZXY=SUMZXY+(Z(I)/TK(I))*ALCG(REXP(I))
SUMZXX=SUMZXX+Z(I)*(1.0/TK(I))**2
SUMXX=SUMXX+(1.0/TK(I))**2
SUMY=SUMY+1.0/TK(I)
8 CONTINUE
NF=NDATA-2
FN=NF
PN=NDATA
D=(PN*SUMZXX)-(SUMZX)**2
SLOPE=-((SUMZX*SUMZY-PN*SUMZXY)/D
YINT=((SUMZY*SUMZXX)-(SUMZX*SUMZXY))/D
EACT=-GK*SLOPE
A=EXP(YINT)
XAV=SUMX/PN
CSUMXX=SUMXX-PN*(XAV**2)
DO 9 I=1,NDATA
DELTA(I)=ALKE(I)-(ALOG(A)-(EACT/GK)*1.0/TK(I))
9 CONTINUE
SUMDE=0.0
DO 13 I=1,NDATA
SUMDE=SUMDE+Z(I)*DELTA(I)**2
13 CONTINUE
ERSLOPE=SQRT(SUMDE*PN/(FN*D))
ERINT=SQRT(SUMDE*SUMZXX/(FN*D))
EACTER=GK*ERSLOPE
SUMY=0.0
DC 12 I=1,NDATA
SUMYY=SUMYY+(Z(I)*ALKE(I))**2
12 CONTINUE

```

```

STERR2=(SUMJE**2)/FN
SIERR=SQRI(SIERR2)
W1=SUMXX/(PN*CSUMXX)

C
WRITE(6,121)
121 FORMAT(// * COMPARISON OF EXPERIMENTAL AND REGRESSION VALUES OF LN(
1 RATE CONSTANT) * // 5X, * POINT * , 5X, * LN(KEXP) * , 5X, * LN(KFIT) * , 5X, * DIFFER
2 ENCE * , 5X, * DIFF/SIERROR * , 5X, * DEGREES C. * //)
DO 20 I=1,NDATA
ALKR(I)=YINT+SLOPE/TK(I)
DY=ALKE(I)-ALKR(I)
RY=DY/STERR
WRITE(6,122)I,ALKE(I),ALKR(I),DY,RY,TC(I)
122 FORMAI(6X,I2,5X,F8.3,5X,F8.3,6X,F8.3,8X,F8.2,7X,F8.1)
20 CCNTINUE
WRITE(6,123)
123 FORMAT(///1X,4(1H*) * STANDARD LINEAR REGRESSION ERRORS * ,5(1H*) /
1//)
WRITE(6,124)STERR
124 FCRMAI(5X, * STANDARD ERROR IN REGRESSION = * ,F8.3//)
WRITE(6,125)ERINT
125 FCRMAT(5X, * STANDARD ERROR IN INTERCEPT = * ,F8.3//)
WRITE(6,126)ERSLOPE
126 FORMAT(10X, * STANDARD ERROR IN SLOPE = * ,F8.3//)
ST=0.0
CALL STUDENI(NE,SI)
C
90 PERCENT CONFIDENCE INTERVAL IN LN(K) AT A CHOSEN
C
TEMPERATURE
W2=1.0/PN+((1.0/TEMP-XAV)**2)/CSUMXX
ERRY=STERR*SQRT(W2)
CIY=ST*ERRY
C
90 PERCENT CONFIDENCE INTERVAL IN SLOPE
CISLOPE=ST*ERSLOPE

```

```

C          90 PERCENT CONFIDENCE INTERVAL IN INTERCEPT
          CIYINT=SI*ERINT
          CLOGA=YINT/2.303
          CLOGIA=CIYINT/2.303
C          90 PERCENT CONFIDENCE INTERVAL IN ACTIVATION ENERGY
          CIE=GK*CISLOPE
          ELO=EACT-CIE
          EHI=EACT+CIE
          YINTHI=YINT+CIYINT
          YINTLO=YINT-CIYINT
          ALC=EXP(YINTLC)
          AHI=EXP(YINTHI)
          WRITE(6,130)
130 FORMAT(//1X,38(1H*),* ARRHENIUS ACTIVATION PARAMETERS *,38(1H*)//
1* ACTIVATION PARAMETERS AND STANDARD ERRORS*/
          WRITE(6,134)EACT,EACTER
134 FORMAT(/5X,*ACTIVATION ENERGY = *,F7.3,5X,*STANDARD ERROR = *,
1F6.3)
          WRITE(6,135)YINT,ERINT
135 FORMAT(/8X,*NATURAL LOG(A) = *,F7.3,5X,*STANDARD ERROR = *,F6.3/)
          WRITE(6,136)
136 FORMAT(//* ACTIVATION PARAMETERS AND CONFIDENCE LIMITS*/
          WRITE(6,131)EACT,CIE,ELO,EHI
131 FORMAT(/5X,*ACTIVATION ENERGY = *,F7.3,3X,*(+OR-)*,F6.3,5X,
1*LOWER LIMIT = *,F7.3,3X,*UPPER LIMIT = *,F7.3,2X,*KCAL/MOLE*)
          WRITE(6,132)A,ALO,AHI
132 FORMAT(/6X,*FREQUENCY FACTOR = *,E10.4,5X,*LOWER LIMIT = *,E10.4,
13X,* UPPER LIMIT = *,E10.4)
          WRITE(6,137)YINT,CIYINT
137 FORMAT(/8X,*NATURAL LOG(A) = *,F7.3,3X,*(+OR-)*,F6.3)
          WRITE(6,133)CLOGA,CLOGIA
133 FCRMAI(/9X,*COMMON LOG(A) = *,F7.3,3X,*(+OR-)*,F6.3)
C

```

```

C      CALCULATE EYRING PARAMETERS
      WRITE(6,140)
140  FORMAT(///1X,31(1H*), * EYRING ACTIVATION PARAMETERS *,31(1H*)//)
      WRITE(6,142)
142  FORMAT(5X,*POINT*,8X,*ENTHALPY*,10X,*-----ENTROPY (E.U.) -----*,
110X,*FREE ENERGY (KCAL/MOLE)*,17X,*(KCAL/MOLE)*,9X,*EXP.*,6X,
2*FIT*,5X,*DIFF.*,11X,*EXP.*,5X,*FIT*,5X,*DIFF.*//)
DC 14  I=1,NDATA
      HEXP(I)=EACT-GK*TK(I)
      GEXP(I)=(GK*TK(I))*(ALNR+ALOG(TK(I))-ALCG(REXP(I)))
      SEXP(I)=1000.0*(HEXP(I)-GEXP(I))/TK(I)
      RFIT(I)=A*EXP(SLOPE/TK(I))
      GFIT(I)=(GK*TK(I))*(ALNR+ALOG(TK(I))-ALCG(RFIT(I)))
      SEII(I)=1000.0*GK*(YINT-ALNR-ALOG(TK(I))-1.0)
      DIFFS=SEXP(I)-SFIT(I)
      DIFFG=GEXP(I)-GFIT(I)
      WRITE(6,141)I,HEXP(I),SEXP(I),DIFFS,GEXP(I),GFIT(I),DIFFG
141  FORMAT(6X,I2,10X,F7.3,10X,F7.2,3X,F7.2,F7.2,9X,F8.3,F9.3,F8.3)
14  CCNTINUE

```

```

C
C      CALCULATE EYRING PARAMETERS FOR A SPECIFIC TEMPERATURE
      WRITE(6,150)TEMP
150  FORMAT(///* EYRING ACTIVATION PARAMETERS CALCULATED FOR *,F5.1,
1 * DEG. K.*//34X,*(+OR-)*,6X,*INTERVAL*,6X,*LOWER*,8X,*UPPER*//)
      YTEMP=YINT+SLOPE/TEMP
      YLO=YIEMP-GIY
      YHI=YTEMP+GIY

```

```

C
C      90 PERCENT CONFIDENCE INTERVAL IN FREE ENERGY
      RTEMP=A*EXP(SLOPE/TEMP)
      GT=(GK*TEMP)*(ALNR+ALOG(TEMP)-ALOG(RTEMP))
      GLO=(GK*TEMP)*(ALNR+ALOG(TEMP)-YHI)
      GHI=(GK*TEMP)*(ALNR+ALOG(TEMP)-YLO)
      GERR=GHI-GLC

```

```

GERR2=GERR/2.0
C 90 PERCENT CONFIDENCE INTERVAL IN ENTHALPY
HT=EACT-GK*TEMP
HLC=ELO-GK*TEMP
HHI=EHI-GK*TEMP
HERR=HHI-HLO
HERR2=HERR/2.0

C 90 PERCENT CONFIDENCE INTERVAL IN ENTROPY
STO=1000.0*GK*(YINT-ALNR-ALOG(TEMP))-1.0)
SLO=1000.0*GK*(YINTLO-ALNR-ALOG(TEMP))-1.0)
SHI=1000.0*GK*(YINTHI-ALNR-ALOG(TEMP))-1.0)
SERR=SHI-SLO
SERR2=SERR/2.0
WRITE(6,151)HT,HERR2,HERR,HLO,HHI
151 FORMAT(8X,'ENTHALPY = ',F7.3,4(6X,F7.3),2X,'KCAL/MOLE*')
WRITE(6,152)STO,SERR2,SERR,SLO,SHI
152 FORMAT(9X,'ENTROPY = ',F6.2,4(7X,F6.2),3X,'E.U.*')
WRITE(6,153)GT,GERR2,GERR,GLO,GHI
153 FORMAT(5X,'FREE ENERGY = ',F7.3,4(6X,F7.3),2X,'KCAL/MOLE*')
WRITE(6,154)RTMP,TEMP
154 FORMAT(7X,'RATE CONSTANT =',E10.4,' (1/SEC.) AT ',F5.1,
1* DEGREES K.*')
CLT=1.0/RTMP
WRITE(6,155)CLT,TEMP
155 FORMAT(8X,'LIFETIME =',E10.4,' ( SEC. ) AT ',F5.1,
1* DEGREES K.*')

C CALCULATE DATA FOR PLOTTING
WRITE(6,160)
160 FORMAT(///4(1H*),* DATA FOR PREPARATION OF ARRHENIUS PLOT *,4(1H*)
1//5X,*PCINT*,5X,*LN(KEXP)*,5X,*LN(KFIT)*,5X,*1000/T*')
DC 60 I=1,NDATA
WRITE(6,161)I,ALKE(I),ALKR(I),TR(I)

```


161 FORMAT(6X,I2,5X,F8.3,5X,F8.3,4X,F8.3)

60 CCNTINUE

WRITE(6,199)

159 FORMAT(////2(1X,110(1H*))//)

C

START NEXT CASE

GC TO 1

END

C SUBROUTINE STUDENT(NF,VAL)

STUDENTS T VALUES FOR 90 PERCENT CONFIDENCE LIMITS

DIMENSION T(48)

T(1)=6.314

T(2)=2.920

T(3)=2.353

T(4)=2.132

T(5)=2.015

T(6)=1.943

T(7)=1.895

T(8)=1.860

T(9)=1.833

T(10)=1.812

T(11)=1.796

T(12)=1.782

T(13)=1.771

T(14)=1.761

T(15)=1.753

T(16)=1.746

T(17)=1.740

T(18)=1.734

T(19)=1.729

T(20)=1.725

T(21)=1.721

T(22)=1.717

```
T(23)=1.714  
T(24)=1.711  
T(25)=1.708  
T(26)=1.706  
T(27)=1.703  
T(28)=1.701  
T(29)=1.70  
T(30)=1.70  
DC 1 I=31,35  
T(I)=1.69  
1 CONTINUE  
DC 2 I=36,40  
T(I)=1.68  
2 CONTINUE  
VAL=T(NF)  
RETURN  
END
```

Programme QQPLOT

This programme is used to simulate the collapse of two quartets to one quartet. It is based on a modified Gutowsky and Holm^{58,59} formulation and is valid only for first order, or nearly first order, spectra.

The equations, derived by Gutowsky and Holm from the Bloch equations, are as follows

The intensity, I, at any point, w, is given by

$$I = K \left[\frac{(1 + \tau/T_2) P + QR}{P^2 + R^2} \right]$$

where $\tau = \frac{\tau_A \tau_B}{\tau_A + \tau_B}$

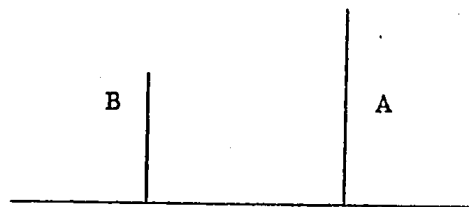
$$P = \tau \left[(1/T_2)^2 - \left[\frac{1}{2}(w_A + w_B) - w \right]^2 + (w_A - w_B)^2 \frac{1}{4} \right] + 1/T_2$$

$$Q = \tau \left[\frac{1}{2}(w_A + w_B) - w - \frac{1}{2}(P_A - P_B)(w_A - w_B) \right]$$

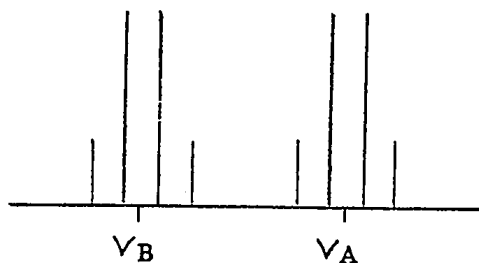
and $R = \left[\frac{1}{2}(w_A + w_B) - w \right] (1 + 2\tau/T_2) + \frac{1}{2}(P_A - P_B)(w_A - w_B)$

P_A and P_B are the populations of the two rotamers and are equal to $\tau_A/(\tau_A + \tau_B)$ and $\tau_B/(\tau_A + \tau_B)$, respectively. τ_A and τ_B are the lifetimes of the two rotamers, while w_A and w_B are the chemical shifts in radians/sec. K and T_2 are the scaling factor and transverse relaxation time, respectively.

These equations have previously been applied to two signals - two sites cases of exchange



In the case under consideration, however, eight signals (i.e., four pairs of signals) need to be generated. The centre of each quartet is placed in the chemical shift position, γ , and each line of the quartet is generated at



a position displaced from the adjacent line by an amount equal to the coupling constant. Collapse of the spectra is observed as the lifetimes are decreased (see Results section on 3- β -naphthyl-5-methyl-2-thiohydantoin)

The input cards are prepared as follows:

- Item 1. NSPEC, IDEN Format (I3, 18A4)
- NSPEC is the spectrum number and is printed on the plot output. Any non-zero number may be used. A zero number for NSPEC will terminate the run.
- IDEN is the alphanumeric identification and is

printed on the plot output.

Item 2. TAUA, TAUB, ANU, BNU, AJ, BJ, WIDTH, FAC

Format (8F10.0)

TAUA = lifetime in seconds on site A

TAUB = lifetime in seconds on site B

ANU = chemical shift in Hz on site A

BNU = chemical shift in Hz on site B

AJ = coupling constant in Hz on site A

BJ = coupling constant in Hz on site B

WIDTH = natural line width in Hz at half height

FAC = ratio of intensities of outer peaks of quartets.

Item 3. FR1, FR2, SCALE, HEIGHT

Format (4F10.0)

FR1 = low frequency limit of plot

FR2 = high frequency limit of plot

SCALE = plot scale in mm/Hz

HEIGHT = plot height in mm (less or equal to 250.0 mm)

Notes: Any number of runs may be stacked one after another.

The run is terminated by a blank card.

The plot has the low frequency limit on the left hand side.

PROGRAM QOPL0T(INPUT,OUTPUT,TAPE1,TAPE60=INPUT,TAPE61=OUTPUT)
WRITTEN JULY 1971. MODIFIED FOR CDC 6400 MARCH, 1972.
DEPARTMENT OF CHEMISTRY. SIR GEORGE WILLIAMS UNIVERSITY

NUCLEAR MAGNETIC RESONANCE LINE SHAPE CALCULATION

THIS PROGRAM CALCULATES AND PLOTS THE LINE SHAPE OF TWO
QUARTETS EXCHANGING OVER TWO SITES

IT IS ASSUMED THAT THE SPECTRUM IS VERY CLOSE TO FIRST ORDER

LINE SHAPE PARAMETERS-

TAUA = LIFETIME IN SECONDS ON SITE A

TAUB = LIFETIME IN SECONDS ON SITE B

ANU = CHEMICAL SHIFT IN HZ ON SITE A

BNU = CHEMICAL SHIFT IN HZ ON SITE B

AJ = COUPLING CONSTANT IN HZ ON SITE A

BJ = COUPLING CONSTANT IN HZ ON SITE B

WIDTH = NATURAL LINE WIDTH IN HZ AT HALF HEIGHT

FAC = RATIO OF INTENSITIES OF OUTER PEAKS OF THE QUARTETS

DIMENSION IDEN(7),Y(3000),KRAY(14),PU(4),GU(4),RU(4),FU(4)

WRITE(61,200)

200 FORMAT(15H PROGRAM QOPL0T//)

NPLOT = 0

1 READ(60,201)NSPEC,IDEN

201 FORMAT(I3,7A10)

IF (NSPEC.EQ.0) GO TO 900

NPLOT=NPLOT +1

READ(60,202)TAUA,TAUB,ANU,BNU,AJ,BJ,WIDTH,FAC

202 FORMAT(8F10.0)

READ(60,203)FR1,FR2,SCALE,HEIGHT

203 FORMAT(4F10.0)

IF (HEIGHT.GT.250.0) HEIGHT=250.0

```

WRITE(61,204) NSPEC, IDEN
204 EORMAT(10H SPECIRUM ,I3,10X,7A10//)
WRITE(61,205)
205 FCRMAT(19H SITE A PARAMETERS-/)
WRITE(61,207) TAU A, ANU, AJ, WIDTH, FAC
WRITE(61,206)
206 FCRMAT(19H SITE B PARAMETERS-/)
WRITE(61,207) IAU B, BNU, BJ, WIDTH, FAC
207 FCRMAT(5X,23H MEAN LIFETIME (SEC) = ,F8.4,/5X,23H CHEMICAL SHIFT (
1HZ) = ,F8.2,/2X,26H COUPLING CONSTANT (HZ) = ,F8.2,/9X,19H LINE WI
20TH (HZ) = ,F8.2,/5X,23H RELATIONSHIP FACTOR = ,F8.2//)
WRITE(61,208) FR1, FR2, SCALE, HEIGHT
208 FCRMAT(20H PLOTTING PARAMETERS//5X,18HFREQUENCY RANGE = ,F8.2,4H T
10 ,F8.2,3H HZ/5X,9H SCALE = ,E6.2,6H MM/HZ,5X,10H HEIGHT = ,E6.2,3
2H MM//)
DENS=100.0
XMAX=SCALE*(FR2-FR1)/25.4
NPOINT=DENS*XMAX+0.5
IF (NPOINT.GT.3000) NPOINT=3000
STEP=(FR2-FR1)/FLOAT(NPOINT)

C
C CALCULATE THEORETICAL SPECTRUM
PI=3.1415927
TPI=6.2831853
TPISQ=39.4784
RIT=PI*WIDTH
RITSO=RIT*RIT
TCR=(TAUA*TAUB)/(TAUA+TAUB)
TCRIT=TOR*RIT
DELP=(TAUA-TAUB)/(TAUA+TAUB)
SNU=0.5*(ANU+BNU)
DNU=0.5*(ANU-PAU)
SJ=0.25*(AJ+BJ)

```

```

DJ=0.25*(AJ-BJ)
FREQ=FR1-STEP
DC 20 I=1,NPOINT
FREQ=FREQ+STEP
SNO=SNO-5.0*SJ
DNO=DNO-5.0*DJ
DC 16 J=1,4
SNO=SNO+2.0*SJ
DNO=DNO+2.0*DJ
DLGNO=SNO-FREQ
DLPNU=DELP*DNO
PL(J)=TOR*(RITSQ-TPISQ*(DLGNO*DLGNO-DNO*DNO))+RIT
QU(J)=TOR*TPI*(DLGNO-DLPNU)
RU(J)=TPI*(DLGNO*(1.0+2.0*TORIT)+DLPNU)
FU(J)=(PU(J)*(1.0+TORIT)+QU(J)*RU(J))/(PU(J)*FU(J)+RU(J)*RU(J))
16 CONTINUE
Y(I)=FU(1)+(2.0+FAC)*FU(2)+(1.0+2.0*FAC)*FU(3)+FAC*FU(4)
20 CCNTINUE
C
C SCALE SPECTRUM TO DESIRED HEIGHT
YMAX=Y(1)
DO 21 I=2,NPOINT
IF (YMAX.GT.Y(I)) GO TO 21
YMAX=Y(I)
21 CCNTINUE
FACTOR=HEIGHT/(25.4*YMAX)
DC 28 I=1,NPOINT
Y(I)=Y(I)*FACTOR
C
C DRAW AXES AND TICK MARKS
LY=XMAX+1.0
YL=(FR2-FR1)*FLOAT(LY)/XMAX
YLOW=FR1

```



```

CALL AXISXY(1,10,LY,1.0,10.0,YL,0.0,YL0h,0.0,YLOW)
YI=YLOW
CALL PLOTXY(10.0,YT,0,0)
30 YI=YI+5.0
YIIM=YLCW+YL
IF (YI.GT.YLIM) GO TO 35
CALL PLOTXY(10.0,YT,1,0)
CALL PLOTXY(9.95,YI,1,0)
CALL PLOTXY(10.0,YT,1,0)
YI=YI+5.0
IF (YI.GT.YLIM) GO TO 35
CALL PLOTXY(10.0,YT,1,0)
CALL PLOTXY(9.90,YT,1,0)
CALL PLOTXY(10.0,YI,1,0)
GO TO 30
35 CALL PLOTXY(10.0,YLIM,1,0)
CALL PLOTXY(0.0,YLIM,1,0)
C
C PLOT THE SPECTRUM
X=FR1
YYY=9.85-Y(I)
CALL PLOTXY(YYY,X,0,0)
DC 24 I=2,NPOINT
X=X+STEP
YYY=9.85-Y(I)
24 CALL PLOTXY(YYY,X,1,0)
ENCODE(56,110,KRAY(1))NSPEC,TAUA,TAUB
110 FORMAT(9HSPECTRUM,I3,4X,17HMEAN LIFETIMES = ,F9.4,5H AND ,F9.4)
YI=YLOW+YL*(FLGAT(LY)-0.2)/FLOAT(LY)
CALL PLOTXY(1.0,YI,0,0)
CALL LABEL(56,1,4,KRAY(1))
IFR1=FR1
IFR2=FR2

```

```

IRF=0
ILF=0
ENCODE(4,111,ILF)IFR1
ENCODE(4,111,IRF)IFR2
111 FCRMAT(I4)
Y2=YLOW+YL*(FLOAT(LY)-0.6)/FLOAT(LY)
CALL PLCTXY(0.15,Y2,0,0)
CALL LABEL(4,1,3,IRF)
Y3=YLOW+0.1*YL/FLOAT(LY)
CALL PLCTXY(0.15,Y3,0,0)
CALL LABEL(4,1,3,ILF)
CALL PLCTXY(1.0,Y3,0,0)
CALL LABEL(72,1,4>IDEN(1))
CALL PLCTXY(0.0,YLOW,0,0)
WRITE(61,100)NFPLOT
100 FORMAT(41H SUMMARY OF CALCULATIONS FOR PLOT NUMBER ,I3,/)
WRITE(61,102)NFOINT
102 FORMAT(9X,28H NUMBER OF POINTS PLOTTED = ,I4)
WRITE(61,105)L
105 FCRMAT(37H LENGTH OF FREQUENCY AXIS (INCHES) = ,I3)
WRITE(61,106)YL
106 FCRMAT(3X,34H LENGTH OF FREQUENCY AXIS IN HZ = ,F7.2)
WRITE(61,107)FR1,X
107 FORMAT(10X,27H FREQUENCY RANGE PLOTTED = ,F7.2,4H TC ,F7.2,3H HZ//
1////)
C
C START NEXT CASE
GO TO 1
900 CCNTINUE
ENDFILE 1
REWIND 1
STOP 1
END

```

Programme PLOTAB

This programme calculates and plots the spectrum of an AB spin system undergoing intramolecular exchange.

Input cards are prepared as follows:

- Card 1. NSPEC, IDEN Format (I3, 18A4)
NSPEC is the spectrum number and is printed on the plot output. Any non-zero number may be used. A zero value for NSPEC will terminate the run. IDEN is the alphanumeric identification and is printed on the plot output.
- Card 2. B(1), B(2), B(3), B(4) Format (4F10.0)
B(1) = mean lifetime in seconds
B(2) = chemical shift difference in Hz
B(3) = coupling constant in Hz
B(4) = natural linewidth in Hz
- Card 3. FR1, FR2, SCALE, HEIGHT Format (4F10.0)
FR1 = low frequency limit of plot
FR2 = high frequency limit of plot
SCALE = plot scale in mm/Hz
HEIGHT = plot height in mm, less than 250.0 mm

Any number of runs may be stacked one after the other. The run is terminated by a blank card.

```

PROGRAM PLOTAB
C THIS PROGRAM PLOTS THE OUTPUT FROM NLINAB
C A PLOT OF THE DIGITIZED SPECTRUM IS SUPERIMPOSED ON THE SPECTRUM
C CALCULATED FROM THE BEST FIT PARAMETERS
C B(1) = MEAN LIFETIME IN SECONDS, B(2) = CHEMICAL SHIFT IN H7
C B(3) = COUPLING CONSTANT IN HZ, B(4) = SCALING FACTOR,
C B(5) = NATURAL LINEWIDTH IN HZ
C
C DIMENSION IDEN(18),SPECX(200),SPECY(200),Y(3000),B(5),KRAY(10)
C NPLOT=0
1 READ(60,200)NSPEC,IDEN
200 FORMAT(13,1A4)
IF (NSPEC.EQ.0) STOP
NPLOT=NPLOT+1
READ(60,201)NDATA,B(1),B(2),B(3),B(4),B(5)
201 FORMAT(13,7X,5F10.0)
READ(60,202)FR1,FR2,SCALE,HEIGHT,XCNTR
202 FORMAT(5F10.0)
READ(60,210)LX,JPRINT,IAX
210 FORMAT(3I2)
IF (LX.GT.10) LX=10
XL=LX
HMAX=XL*25.0
IF (HEIGHT.GT.HMAX) HEIGHT=HMAX
WRITE(61,203)NSPEC,IDEN
203 FORMAT(15H PROGRAM PLOTAB//10H SPECTRUM ,I3,10X,18A4//)
WRITE(61,204)B(1),B(2),B(3),B(5),B(4)
204 FORMAT(23H CALCULATION PARAMETERS//5X,25H MEAN LIFETIME (SEC) =
1,F8.3,/5X,25H CHEMICAL SHIFT (HZ) = ,F8.2,5X,25HCOUPLING CONSTAN
2T (HZ) = ,F8.2/5X,25H LINE WIDTH (HZ) = ,F8.2,/5X,25H
3 SCALING FACTOR = ,F8.3,/)
WRITE(61,205)FR1,FR2,SCALE,HEIGHT
205 FORMAT(20H PLOTTING PARAMETERS//5X,18HFREQUENCY RANGE = ,F8.2,4H T

```

```

10 ,F8.2,3H WZ/5X,9H SCALE = ,F6.2,6H MM/HZ,5X,10H HEIGHT = ,F6.2,3
2H MM//)
DO 10 I=1,NDATA
10 READ(60,206)SPECY(I),SPECX(I)
206 FORMAT(2F10.0)
WRITE(61,207)
207 FORMAT(19H DIGITIZED SPECTRUM//5X,9HINTENSITY,5X,9HFREQUENCY//)
DO 15 I=1,NDATA
15 WRITE(61,208)SPECY(I),SPECX(I)
208 FORMAT(3X,F10.3,4X,F10.3)
IF (XCNTR.EQ.0.0) GO TO 17
DO 16 I=1,NDATA
16 SPECX(I)=SPECX(I)-XCNTR
WRITE(61,209)XCNTR
209 FORMAT(//25H AB CENTRE CORRECTION OF ,F7.2,25H HZ APPLIED TO INPU
1T DATA)
1/ CONTINUE
DENS=100.0
XMAX=SCALE*(FR2-FR1)/25.4
NPOINT=DENS*XMAX
IF (NPOINT.GT.3000) NPOINT=3000
STEP=(FR2-FR1)/NPOINT
C
C CALCULATE THEORETICAL SPECTRUM
PI=3.1415927
TWOPI=6.2831853
TTWO=1.0/(PI*B(5))
FAC1=2.0/B(1)+1.0/TTWO
FAC2=FAC1*FAC1
FAC3=1.0/TTWO
FAC4=FAC3*FAC3
FAC5=(TWOPI*B(2))**2
S=FR1-STEP

```

```

DO 20 I=1,NPOINT
S=S+STEP
FAC6=(TWOPI*S)**2
FAC7=(TWOPI*(S-R(3)))**2
FAC8=(TWOPI*(S+R(3)))**2
FAC9=(FAC6-FAC5/4.0-(TWOPI**2)*B(3)*S)**2
FAC10=(FAC6-FAC5/4.0+(TWOPI**2)*B(3)*S)**2
TOP1=2.0*FAC3*FAC2+0.5*FAC5*FAC1+2.0*FAC3*FAC7
TOP2=2.0*FAC3*FAC2+0.5*FAC5*FAC1+2.0*FAC3*FAC8
DEN1=FAC4*FAC2+0.5*FAC3*FAC5*FAC1+FAC4*FAC7+FAC6*FAC2+FAC9
DEN2=FAC4*FAC2+0.5*FAC3*FAC5*FAC1+FAC4*FAC8+FAC6*FAC2+FAC10
20 Y(I)=H(4)*(TOP1/DEN1+TOP2/DEN2)
C
C SCALE BOTH SPECTRA TO DESIRED HEIGHT
YMAX=Y(1)
DO 21 I=2,NPOINT
IF (YMAX.GT.Y(I)) GO TO 21
YMAX=Y(I)
21 CONTINUE
FACTOR=HEIGHT/(25.4*YMAX)
DO 28 I=1,NPOINT
28 Y(I)=Y(I)*FACTOR
DO 36 I=1,NDATA
36 SPECY(I)=SPFCY(I)*FACTOR
C
C DRAW AXES AND TICK MARKS
XL1=XL-0.05
XL2=XL-0.1
XL3=XL-0.15
LY=XMAX+1.0
YL=(FR2-FR1)*FLOAT(LY)/XMAX
YLOW=FR1
CALL AXISXY(4HTAPE,LX,LY,1.0,10.0,YL,0.0,YLOW,0.0,YLOW)

```

```

IF (IAX.NE.0) CALL LOCATE(3,1,1,6)
YT=YLOW
CALL PLOTXY(XL2,YT,0,0)
CALL PLOTXY(XL,YT,1,0)
30 YT=YT+5.0
YLIM=YLOW+YI
IF (YT.GT.YLIM) GO TO 35
CALL PLOTXY(XL,YT,1,0)
CALL PLOTXY(XL1,YT,1,0)
CALL PLOTXY(XL,YT,1,0)
YT=YT+5.0
IF (YT.GT.YLIM) GO TO 35
CALL PLOTXY(XL,YT,1,0)
CALL PLOTXY(XL2,YT,1,0)
CALL PLOTXY(XL,YT,1,0)
GO TO 30
35 CALL PLOTXY(XL,YLIM,1,0)
C
C PLOT THE TWO SPECTRA
X=FRI
YYY=XL3-Y(I)
CALL PLOTXY(YYY,X,0,0)
DO 24 I=2,NPOINT
X=X+STEP
YYY=XL3-Y(I)
24 CALL PLOTXY(YYY,X,1,0)
IF (IPRINT.EQ.0) GO TO 38
ENCODE(40,110,KRAY(1))NSPEC,B(1)
110 FORMAT(9HSPFCTRIUM ,I3,4X,16HMEAN LIFETIME = ,F8.3)
YI=YLOW+YL*/FLOAT(LY)-0.2)/FLOAT(LY)
CALL PLOTXY(1.0,YI,0,0)
CALL LABEL(40,1.4,KRAY(1))
IFR1=FRI

```



```

IFR2=FR2
IRF=0
ILF=0
ENCODE(4,11,ILF)IFR1
ENCODE(4,11,IRF)IFR2
111 FORMAT(I4)
Y2=YLOW+YL*(FLOAT(LY)-0.6)/FLOAT(LY)
CALL PLOTXY(0.15,Y2,0,0)
CALL LABEL(4,1,3,IRF)
Y3=YLOW+0.1*YL/FLOAT(LY)
CALL PLOTXY(0.15,Y3,0,0)
CALL LABEL(4,1,3,ILF)
CALL PLOTXY(1.0,Y3,0,0)
CALL LABEL(72,1,4>IDEN(1))
38 CONTINUE
DO 40 I=1,NDATA
YSPEC=XL3-SPECY(I)
40 CALL PLOTXY(YSPEC,SPECX(I),0,9)
CALL PLOTXY(0.0,YLOW,0,0)
WRITE(61,100)NPOINT
100 FORMAT(/41H SUMMARY OF CALCULATIONS FOR PLOT NUMBER ,I3,/)
WRITE(61,102)NPOINT
102 FORMAT(9X,24H NUMBER OF POINTS PLOTTED = ,I4)
WRITE(61,105)LY
105 FORMAT(37H LENGTH OF FREQUENCY AXIS (INCHES) = ,I3)
WRITE(61,106)YL
106 FORMAT(3X,34H LENGTH OF FREQUENCY AXIS IN HZ = ,F7.2)
WRITE(61,107)FRI,X
107 FORMAT(10X,27H FREQUENCY RANGE PLOTTED = ,F7.2,4H TO ,F7.2,3H H7//
1//)
ENDFILE 3
GO TO 1
END

```

PROGRAMME GHPLT

This is an interactive programme, written to plot the n.m.r. line shape in the case of exchange between two sites in the absence of spin-spin coupling. It may be considered to be a simpler version of QQPLOT. The computer asks for the following parameters: the chemical shift of moiety A, the chemical shift of moiety B, the lifetime on site A, the lifetime on site B, the line width, and the scale factors.

```
      FTN,B
      PROGRAM GHPLT
      COMMON Y(256)
      WRITE(2,10)
10  FORMAT("NMR LINE SHAPE FOR EXCHANGE BETWEEN TWO SITES")
      WRITE(2,11)
11  FORMAT("WITH ZERO COUPLING, PLOT ONLY"/)
      WRITE(2,20)
20  FORMAT("NOTE:  YES = 1, NO = 0")
      WRITE(2,21)
21  FORMAT("ENTER PARAMETERS IN FREE FIELD FORMAT"/)
      WRITE(2,12)
12  FORMAT("CHEMICAL SHIFT A (HZ) = ")
      READ(1,*)SHFTA
      WRITE(2,13)
13  FORMAT("CHEMICAL SHIFT B (HZ) = ")
      READ(1,*)SHFTB
      WRITE(2,14)
14  FORMAT("LIFETIME ON SITE A (SEC) = ")
      READ(1,*)TAUA
      WRITE(2,16)
16  FORMAT("LIFETIME ON SITE B (SEC) = ")
      READ(1,*)TAUB
      WRITE(2,15)
15  FORMAT("LINE WIDTH (HZ) = ")
      READ(1,*)WIDTH
      WRITE(2,17)
17  FORMAT("FREQUENCY LOWER LIMIT (HZ) = ")
      READ(1,*)FREQL
      WRITE(2,18)
18  FORMAT("FREQUENCY UPPER LIMIT (HZ) = ")
      READ(1,*)FREQH
      WRITE(2,40)

40  FORMAT(//"PARAMETERS:"/)
      WRITE(2,41)SHFTA,SHFTB
41  FORMAT(13H  SHIFT(A) = ,F6.2,14H  SHIFT(B) = ,F6.2)
      WRITE(2,42)TAUA,TAUB
42  FORMAT(13H  TAU(A) = ,F7.4,13H  TAU(B) = ,F7.4)
      WRITE(2,43)WIDTH,FREQL,FREQH
43  FORMAT(10H  WIDTH = ,F5.2,15H  FREQ. RANGE = ,F6.2,4H TO ,F6.2/)
      WRITE(2,44)
44  FORMAT("IS A RE-START REQUIRED?")
      READ(1,*)IR
      IF (IR) 60,45,60
45  CONTINUE
```

```

PI=3.14159
PT=2.0*PI
TAU=TAUA*TAUB/(TAUA+TAUB)
R=1.0/(WIDTH*PI)
PONE=TAU/TAUB
PTWO=TAU/TAUA

SONE=PI*(SHFTA+SHFTB)
STWO=PI*(SHFTA-SHFTB)
DIFFP=(PONE-PTWO)*STWO
FREQI=(FREQH-FREQL)/255.0
FREQD=PT*FREQI
FREQ=FREQL*PT
DO 111 N=1,256
PC=TAU*(1.0/(R*R)-(SONE-FREQ)**2+STWO**2)+1.0/R
Q=TAU*(SONE-FREQ-DIFFP)
RA=(SONE-FREQ)*(1.0+2.0*TAU/R)+DIFFP
Y(N)=1000.0*((1.0+TAU/R)*PC+Q*RA)/(PC**2+RA**2)
FREQ=FREQ+FREQD
111 CONTINUE
115 WRITE(2,50)
50 FORMAT("PREPARE PLOTTER")
PAUSE
NP=256
CALL PLOTT(NP,FREQL,FREQH)
WRITE(2,37)
37 FORMAT("PLOT COMPLETED"//)
WRITE(2,38)
38 FORMAT("RE-PLOT ?")
READ(1,*)JP
IF (JP) 115,58,115
58 PAUSE
60 WRITE(2,61)
61 FORMAT("RE-START: CHANGE PARAMETERS AS NECESSARY"//)
GO TO 1
END
END$

```